

Aus dem Max Delbrück Centrum für Molekulare Medizin (MDC) und der
Klinik für Neurologie der Medizinischen Fakultät Charité –
Universitätsmedizin Berlin

DISSERTATION

**EGCG directly targets intracellular amyloid- β (1-42)
aggregates and promotes their lysosomal degradation**

zur Erlangung des akademischen Grades
Doctor medicinae (Dr. med.)

vorgelegt der Medizinischen Fakultät
Charité – Universitätsmedizin Berlin

von

Christopher Secker

aus Reutlingen

Datum der Promotion: 01.03.2019

Table of Contents

1	Abstract.....	9
1.1	Abstract (English)	9
1.2	Abstract (German).....	11
2	Introduction	13
2.1	Alzheimer's disease: impact & clinical presentation	13
2.2	Epidemiology	13
2.3	Molecular pathophysiology in Alzheimer's disease	14
2.4	Intracellular A β 42 deposition and cellular degradation	16
2.5	Molecular therapeutic strategies in Alzheimer's disease	17
2.6	Aim of the work.....	20
3	Material and Methods.....	21
3.1	A β 42 peptide stock solutions.....	21
3.2	Preparation and fluorescent labeling of A β 42 aggregates	21
3.3	Atomic Force Microscopy (AFM)	21
3.4	Fluorescence polarization-based A β 42 aggregation assay	21
3.5	Neuroblastoma cell culture and treatment with A β 42(-TAMRA) aggregates	22
3.6	Preparation of cell lysates for biochemical analysis	22
3.7	Polyacrylamide gel electrophoresis and Western blotting	22
3.8	Native and denaturing filter retardation assays	23
3.9	Automated fluorescence microscopy and quantification of aggregates in cells	23
3.10	Immunofluorescence microscopy and staining of cells with dyes.....	24
3.11	Confocal microscopy.....	24
3.12	Screening of a polyphenol compound library	25
3.13	Thioflavin T A β 42 aggregate binding and seeding assay	25
3.14	Preparation of neuronal primary cultures from rat hippocampi.....	26
3.15	Mitochondrial metabolic rate assay (MTT)	26
3.16	Mouse embryonal fibroblast (MEF) cell culture	27
3.17	Cathepsin B enzyme activity assay	27
3.18	EGCG derivative library.....	27
3.19	Co-localization studies of EGCG and intracellular A β 42 aggregates	28
3.20	EGCG-mediated remodeling of A β 42 aggregates.....	28
3.21	Transmission electron microscopy (TEM)	28

3.22	Density gradient centrifugation.....	29
3.23	In vitro Cathepsin B activity and cleavage of A β 42 aggregates	29
3.24	Material and equipment.....	30
4	Results.....	40
4.1	Fluorescent labeling and characterization of preformed A β 42 aggregates.....	40
4.2	A β 42 aggregates are rapidly internalized by SH-EP cells and are directed towards the endolysosomal pathway.....	42
4.3	A β 42 aggregates are internalized through actin-dependent, lipid raft-mediated macropinocytosis.....	46
4.4	A cell-based screening assay facilitates the identification of small molecules promoting the clearance of intracellular A β aggregates	48
4.5	EGCG-mediated degradation mitigates A β 42 seeding activity and rescues A β 42-induced toxicity	53
4.6	Intracellular A β 42 aggregates accumulate in lysosomes and the EGCG-mediated effect is dependent on lysosomal enzyme activity	56
4.7	EGCG treatment increases maturation of Cathepsin B and boosts lysosomal enzyme activity.....	59
4.8	In-cell potency of EGCG and structural related derivatives strongly correlates with modulation of A β 42 aggregation in vitro.....	61
4.9	EGCG directly targets intracellular A β 42 aggregates	64
4.10	EGCG-mediated remodeling of A β 42 aggregates facilitates cleavage through the lysosomal enzyme Cathepsin B	67
5	Discussion.....	72
5.1	A cell-based, high-throughput compound screening assay recapitulating intracellular A β 42 aggregate pathology	72
5.2	Direct A β 42 aggregate targeting compounds reduce cellular aggregate load, seeding activity and A β 42-induced toxicity.....	73
5.3	A potential mechanism of the EGCG-induced reduction of intracellular A β 42 aggregates	74
6	References.....	79
7	Addendum.....	97

Figures

Figure 1. Deaths per million persons in 2012 due to dementias including AD	13
Figure 2. Characterization of preformed A β 42 aggregates	40
Figure 3. Biochemical analysis of SH-EP cell lysates after treatment with A β 42 aggregates.....	42
Figure 4. A β 42 aggregate internalization and cellular aggregate formation.....	43
Figure 5. Intracellular A β 42 aggregates accumulate in acidic organelles	45
Figure 6. A β 42 aggregate internalization via lipid-raft mediated macropinocytosis	47
Figure 7. Cell-based screening assays identifies polyphenols increasing A β 42 aggregate degradation	49
Figure 8. Titration experiment with increasing concentrations of EGCG	51
Figure 9. Analysis of the effect of EGCG on TAMRA fluorescence	52
Figure 10. Validation of EGCG-mediated A β 42 aggregate degradation	53
Figure 11. Seeding activity of cell extracts from SH-EP cells with intracellular A β 42 aggregates.....	54
Figure 12. EGCG treatment rescues A β 42-induced toxicity	55
Figure 13. Co-localization of internalized A β 42-TAMRA aggregates with lysosomal markers.....	57
Figure 14. EGCG-mediated promotion of cellular A β 42 degradation is dependent on autophagy and lysosomal enzyme activity	58
Figure 15. EGCG treatment increases CatB maturation.....	59
Figure 16. EGCG treatment increases CatB enzyme activity in SH-EP cells	60
Figure 17. EGCG derivatives' <i>in cell</i> potency correlates with <i>in vitro</i> A β 42 aggregation inhibition	62
Figure 18. EGCG derivatives for cellular co-localization studies in SH-EP cells.....	66
Figure 19. Enzymatic cathepsin B activity <i>in vitro</i> is not modulated by EGCG at assay concentrations	67
Figure 20. EGCG-induced A β 42 aggregate remodeling	68
Figure 21. Quantification of EGCG-mediated structural A β 42 aggregate remodeling using gradient centrifugation.....	69
Figure 22. EGCG-mediated A β 42 aggregate remodeling facilitates lysosomal enzyme cleavage	70
Figure 23. Model of EGCG-mediated reduction of cellular A β 42 aggregates	77

Tables

Table 1. EGCG derivatives	30
Table 2. List of recombinant proteins and peptides	32
Table 3. List of antibodies.....	33
Table 4. List of dyes, fluorophores and substrates	34
Table 5. Laboratory kits, chemicals and stock solutions.....	35
Table 6. List of buffer solutions.....	36
Table 7. Plate types and specifications	38
Table 8. List of laboratory instruments and equipment	38
Table 9. List of Software used	39

Abbreviations

Ab	antibody
AB-AM	antibiotic-antimycotic
abbr.	abbreviation
AD	Alzheimer's disease; Alzheimer-Demenz
ADDLs	amyloid- β derived diffusible ligands
AEBSF	4-(2-Aminoethyl)benzenesulfonyl fluoride
AFM	atomic force microscopy
aggr.	aggregate
ANOVA	analysis of variance
ApoE	apolipoprotein E
ApoE2	apolipoprotein E ϵ 2
ApoE3	apolipoprotein E ϵ 3
ApoE4	apolipoprotein E ϵ 4
APP	amyloid precursor protein
AraC	cytarabin C
AU	artificial units
A β	amyloid- β peptide
A β 40	amyloid- β (1-40) peptide
A β 42	amyloid- β (1-42) peptide
BACE1	β -site amyloid precursor protein cleaving enzyme 1
BSA	bovine serum albumin
C	catechin
CatB	cathepsin B
CG	catechin gallate
CNS	central nervous system
CTB	cholera toxin subunit B
CVCL	Cellosaurus
CytD	cytochalasin D
DHB	dihydroxybenzoate
disaggr.	disaggregation
DMEM	Dulbecco's modified eagle medium

DMSO	dimethyl sulfoxide
DTT	dithiothreitol
EC	epicatechin
ECG	epicatechin gallate
EGC	epigallocatechin
EGCG	epigallocatechin gallate
EIPA	5-(N-ethyl-N-isopropyl) amiloride
Em	emission
EOAD	early-onset Alzheimer's disease
Ex	excitation
FAM	5-Carboxyfluorescein
FB	fluorbenzoate
FCS	fetal calve serum
FITC	fluorescein isothiocyanate
FTD	frontotemporal dementia
g	g-force (m/s ²)
GC	gallocatechin
GCG	gallocatechin gallate
GM1	monosialotetrahexosylganglioside
H + L	heavy and light chain
HB	hydroxybenzoate
HCS	high-content system
HFIP	1,1,1,3,3,3-Hexafluoroisopropanol
HRP	horseradish peroxidase
IC ₅₀	half maximal inhibitory concentration
ICMJE	International Committee of Medical Journal Editors
LAMP2	lysosome-associated membrane protein 2
LBD	Lewy body dementia / disease
LDLR	low-density lipoprotein receptor
LOAD	late-onset Alzheimer's disease
LRP1	low-density receptor-related protein 1
M	molar, molar concentration (mole/liter)
MEF	mouse embryonal fibroblast

MES	2-(N-morpholino)ethanesulfonic acid
monom.	monomer
MTT	3-(4,5-dimethylthiazol-2-yl)-2,5-diphenyltetrazolium bromide
NFT	neurofibrillary tangle
NMR	nuclear magnetic resonance
NP40	Nonidet P-40, 4-Nonylphenyl-polyethylene glycol
LSB	low salt buffer
PAGE	polyacrylamide gel electrophoresis
PBS	phosphate-buffered saline
PBS-T	phosphate buffered saline with tween
PFA	paraformaldehyde
PI	protease inhibitor
PMSF	phenylmethylsulfonyl fluoride
PSEN1	presenilin 1
PSEN2	presenilin 2
QIAD	quantitative determination of interference with amyloid- β aggregate size distribution
ref.	reference
rpm	rounds per minute
RRID	Research Resource Identifiers
RT	room temperature
SDS	sodium dodecyl sulfate
SSS	standard salt solution
TAMRA	5-Carboxytetramethylrhodamine
TB	transfer buffer
TEM	transmission electron microscopy
ThS	Thioflavin S
ThT	Thioflavin T
URM	uniform requirements for manuscripts
v/v	volume per volume
w/	with
w/o	without
w/v	weight per volume

WHO

ZZ-RR-AMC

World Health Organisation

Z-Arg-Arg-7-amido-4-methylcoumarin hydrochloride

1 Abstract

1.1 Abstract (English)

Introduction: Several lines of evidence indicate that aggregation and accumulation of amyloid- β (1-42) (A β 42) causes cellular dysfunction and toxicity. Besides extracellular A β 42 plaque formation and the intraneuronal deposition of hyperphosphorylated tau protein in Alzheimer's disease (AD) patient brains, intracellular A β 42 aggregation plays an important role in AD pathogenesis and even precedes extracellular A β 42 plaque formation. The fact that neuronal cells internalize secreted A β 42 whereby intracellular A β 42 aggregation is induced by a prion-like seeding process, has further highlighted the importance of intraneuronal A β 42 aggregation in disease progression. A potential causal therapy of AD involves slowing disease progression by targeting seeding-competent intracellular A β 42 aggregates and enhancing their degradation in neuronal cells.

Method: Therefore, a cell-based screening assay was established that allows the identification of small molecules effectively promoting the degradation of endocytotically internalized A β 42 aggregates. This cell-based assay was intensively characterized and used in a proof-of-principle approach to screen a focused library of polyphenolic compounds preselected based on their anti-amyloidogenic properties *in vitro*. Further, atomic force, electron and confocal microscopy, biochemical analysis and enzyme activity assays were used and structure-activity relationship studies were performed to elucidate the mechanisms underlying the promotion of cellular aggregate degradation by direct amyloid-targeting compounds.

Results: The polyphenol epigallocatechin gallate (EGCG) most potently promoted the clearance of intracellular A β 42 aggregates in the neuroblastoma cell model. As a consequence of EGCG treatment, intracellular A β 42 aggregate load is reduced, A β 42 seeding-activity of cellular extracts is mitigated and A β 42-induced mitochondrial metabolic impairment is rescued in neuroblastoma cells as well in primary neurons. Mechanistic studies revealed that EGCG directly targets intracellular A β 42 aggregates and that the EGCG-mediated increase in A β 42 degradation is primarily dependent on lysosomal enzyme activity. Furthermore, EGCG-induced structural remodeling of fibrillar A β 42 aggregates into amorphous subspecies showed to enhance lysosomal enzymatic cleavage by the cysteine-protease cathepsin B (CatB), presenting a potential mechanism for the strong increase of cellular A β 42 aggregate degradation.

Take home points: Thus, this study shows that the direct targeting of intracellular A β 42 aggregates with amyloid-remodeling compounds can be a promising approach to promote the degradation of proteotoxic peptide species. This can be an effective strategy to support the endogenous autophago-lysosomal degradation of intracellularly accumulating proteins in neurodegenerative proteinopathies such as amyotrophic lateral sclerosis, Huntington's, Parkinson's and Alzheimer's disease.

1.2 Abstract (German)

Einleitung: Zahlreiche Studien haben gezeigt, dass die Aggregation und Akkumulation von Amyloid- β (1-42) (A β 42) eine zelluläre Dysfunktion und Zelltoxizität zur Folge haben. Neben der Entstehung von extrazellulären A β 42 Plaques und der intrazellulären Ablagerung von hyperphosphorylierten Tau Proteinen im neuronalen Gewebe von Alzheimer Patienten, spielt die intrazelluläre Ablagerung von A β 42 Aggregaten eine zentrale Rolle in der Pathogenese der Alzheimer-Demenz (AD) und geht der extrazellulären Plaque-Bildung sogar voraus. Die Erkenntnis, dass neuronale Zellen sekretiertes A β 42 aufnehmen und dadurch eine intrazelluläre Fehlfaltung in einem Prionen-ähnlichen Seeding-Prozess induziert werden kann, lässt der intraneuronalen A β 42 Ablagerung in der molekularen Pathogenese der Krankheitsprogression eine besondere Wichtigkeit zukommen.

Methodik: Aufgrund dessen haben wir ein zellbasiertes Testverfahren entwickelt, mit dem niedermolekulare Substanzen identifiziert werden können, welche den Abbau von endozytotisch internalisierten, seeding-kompetenten A β 42 Aggregaten fördern. Mittels diesem zellbasierten Screeningverfahren haben wir eine fokussierte Bibliothek aus Polyphenol-Verbindungen getestet, die aufgrund ihrer bekannten, anti-amyloidogenen Wirkung vorselektiert wurden. Darüber hinaus wurden Rasterkraft-, Elektronen- und Konfokalmikroskopie sowie biochemische Proteinanalyse- und Enzymaktivitätsverfahren verwendet, um den zugrundeliegenden Mechanismus der Förderung des Abbaus von intrazellulären Proteinaggregatspezies durch anti-amyloidogene, niedermolekulare Substanzen aufzuklären.

Ergebnisse: Das Polyphenol Epigallocatechingallat (EGCG) zeigte die potenteste Wirkung auf die Reduktion von intrazellulären A β 42 Aggregaten in unserem Modellsystem. Durch die EGCG-Behandlung wird die Menge an intrazellulären A β 42 Aggregaten stark reduziert, die Seeding-Kapazität zellulärer Extrakte abgeschwächt und der durch A β 42 induzierten verminderten mitochondrialen Stoffwechselaktivität sowohl in Neuroblastoma-Zellen als auch in primären Neuronen entgegengewirkt. Mechanistische Untersuchungen offenbarten zudem, dass EGCG direkt an intrazellulären A β 42 Aggregaten ansetzt, dass die Abbau-fördernde Wirkung abhängig von der lysosomalen Enzymaktivität ist und, dass die durch EGCG bewirkte, strukturelle Umlagerung von fibrillären Aggregaten in amorphe Subspezies den A β 42 Abbau durch das lysosomale Enzym

Cathepsin B erleichtert.

Fazit: Diese experimentellen Arbeiten zeigen somit, dass Amyloidstruktur-verändernde, niedermolekulare Substanzen, die direkt an intrazelluläre A β 42 Aggregate binden, einen vielversprechenden Ansatz zur Reduktion der intrazellulären A β 42 Last darstellen. Dieser Ansatz könnte genutzt werden, um bei proteinopathischen neurodegenerativen Erkrankungen wie der amyotrophen Lateralsklerose, Chorea Huntington, Parkinson und der Alzheimer Erkrankung die zelleigene Verstoffwechslung von fehlgefalteten, intrazellulär-akkumulierenden Proteinen im lysosomalen Kompartiment zu stärken.

2 Introduction

2.1 Alzheimer's disease: impact & clinical presentation

Alzheimer's disease (AD) represents the most common type of dementia (Wang et al., 2017). It is an incurable neurodegenerative disease, which is one of the greatest challenges for our health system (Winblad et al., 2016). The typical presentation of an Alzheimer's patient is characterized by cognitive decline such as memory impairment, an executive dysfunction and difficulties in daily life activities. These characteristic symptoms arise usually between the age of 65 and 70, increase in a slow and periodic manner where body functions are gradually lost and ultimately leads to death after seven to ten years (Scheltens et al., 2016).

2.2 Epidemiology

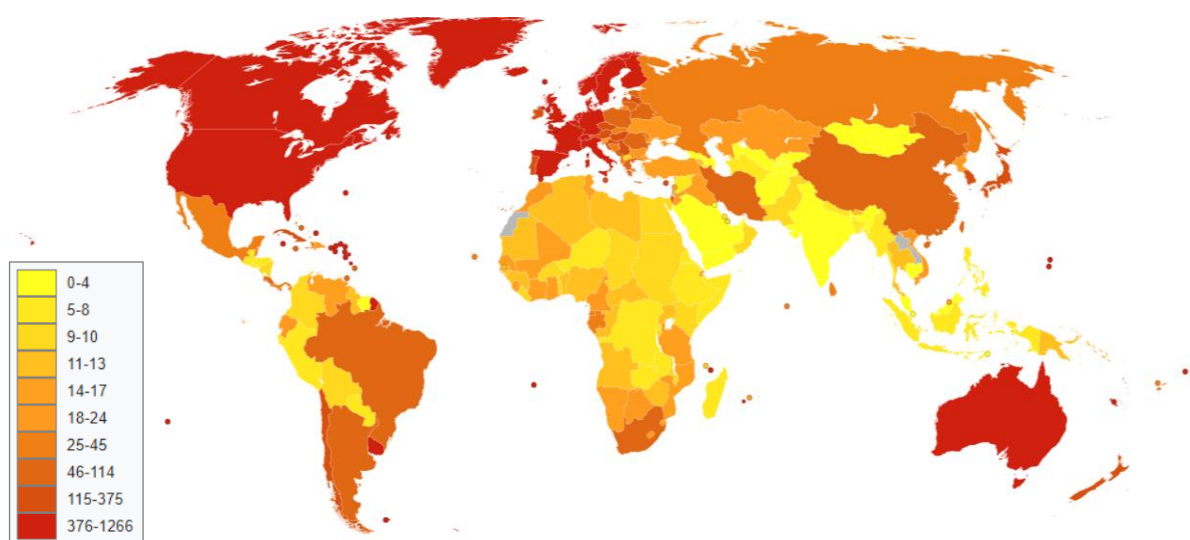


Figure 1. Deaths per million persons in 2012 due to dementias including AD (*WHO 2012 & Canuckguy et al.*) _____

Approximately 40 million people worldwide are affected by dementia. A number, which is expected to double every 20 years until 2050 (Prince et al., 2016). As AD is a disease of the elderly, developing countries – due to their much older population – are projected to have a much higher increase over the coming years compared to Western Europe and the USA. Around 30 to 40 percent of dementia cases are from the Alzheimer subtype. Other common forms of dementia include vascular dementia, dementia with Lewy bodies (LBD) and frontotemporal dementia (FTD). The incidence of AD ranges from 4 to 8 per thousand-person years and doubles with the strongest known risk factor, age, every 5 years from the age of 65. Thus, the prevalence of AD is strongly influenced by the age of

the observed population. (Mercy et al., 2008).

2.3 Molecular pathophysiology in Alzheimer's disease

The cause for Alzheimer's disease is still unknown. However, all forms of AD share common pathological hallmarks in postmortem tissue: intracellular neurofibrillary tangles (NFTs) of phosphorylated tau protein and the extracellular deposition of A β peptides (Masters et al., 2015). These peptides represent fragments of the thereafter-named amyloid precursor protein (APP) and are produced by endoproteolytic cleavage of the full-length transmembrane protein (Gandy and DeKosky, 2013).

The strongest evidence pointing towards A β aggregate formation as a causal process in AD pathogenesis comes from inherited, familial cases. Here, dominant mutations in the catalytic subunits of the APP cleaving enzyme complex – presenilin 1 (PSEN1) and presenilin 2 (PSEN2) – lead to an increased production of the longer amyloid- β (1-42) (A β 42) fragment in comparison to amyloid- β (1-40) (A β 40). The enzymatic variations in PSEN1 and PSEN2 are genetically sufficient to cause AD (Gandy and DeKosky, 2013). This, so-called, amyloidogenic pathway can also be increased due to mutations in the APP protein, affecting its proteolytic cleavage in favor of amyloidogenic A β 42 – compared to the less aggregation-prone A β 40 peptide isoform. In genetic cases, APP mutations lead to an increase of APP cleavage by proteases, which mostly generate A β 42 peptide fragments from APP (O'Brien and Wong, 2011). Additionally, duplication of the APP gene, either of the gene locus itself, or the chromosome as in trisomy 21, leads to an increased production of A β 42 peptides and ultimately to the development of an AD phenotype (McNaughton et al., 2012).

Mutations in APP and members of the APP cleaving complexes account for approximately 60 to 70 percent of early onset AD, but for less than 1 percent of all AD cases, and therefore only explain a small proportion of overall AD clinical cases. Additional rare genetic variants were recently identified in two genes, namely TREM2 and SORL1 (Guerreiro et al., 2013; N. et al., 2015), which are involved in autophagy and lysosomal protein degradation (Buggia-prévot and Thinakaran, 2014; Ulland et al., 2017) – cellular mechanisms essential for the processing of misfolded and aggregated peptides and proteins in almost all cell types, including neurons (Klionsky, 2007). This emphasizes the role of misfolding proteins and their clearance mechanisms in AD pathogenesis. Overproduction of aggregation-prone proteins or peptides such as A β 42 and insufficient

clearance mechanisms such as deficiencies in autophagy or lysosomal activity, ultimately harm affected neuronal cells and might therefore be accountable for AD (Nikoletopoulou et al., 2015; Orr and Oddo, 2013).

In line with this hypothesis, a recent genetic case-control study that analyzed whole-exome sequencing data to find AD-related variants in sporadic cases, including late-onset AD, was able to identify four genes – PSD2, TCIRG1, RIN3 and RUFY1 – in which mainly rare missense variants are strongly associated with late onset and early onset AD (Kunkle et al., 2017). Interestingly, all four genes are likely involved in endolysosomal transport (Bohdanowicz and Grinstein, 2013; Cataldo et al., 1997; Kajihio et al., 2003; Sun-Wada et al., 2009), This further supports the amyloid-hypothesis and highlights the importance of cellular A β aggregate clearance mechanisms in AD pathogenesis.

Besides these rather rare genetic risk factors, variants in the apolipoprotein E (ApoE) have been established as – by far - the most important susceptibility gene for late-onset AD (LOAD) (Bettens et al., 2013). The human APOE gene is located on chromosome 19 and is encoding three different isoforms: ApoE ϵ 2 (ApoE2), ApoE ϵ 3 (ApoE3) and ApoE ϵ 4 (ApoE4). Differences between the isoforms are limited to two amino acid changes, but have a rather strong effect on the protein's structure and function, and a dramatic impact on the risk to develop AD (Zhong and Weisgraber, 2009). Genetic variants in the APOE gene mainly result in the expression of a certain predominant isoform. The ApoE4 isoform hereby represents the main genetic risk factor: one copy of the genetic variant leading to ApoE ϵ 4 expression results in a five year earlier disease onset, whereas two copies of the risk allele shift onset up to 10 years earlier (Noguchi et al., 1993; Pastor et al., 2003). Harboring the most common isoform ApoE3 results in an average risk to develop AD, whereas being genetically equipped with an ApoE2 isoform acts in a protective way. Interestingly, the increased risk of ApoE4 carriers to develop AD is directly associated with an increased deposition of misfolded A β (ApoE4 > ApoE3 > ApoE2). This has been clearly shown in AD animal models as well as in human studies (Bales et al., 2009; Castellano et al., 2011; Koffie et al., 2012; Youmans et al., 2012). Furthermore, it has been found that ApoE is strongly involved in A β clearance and in maintaining A β in a soluble rather than in an insoluble, aggregated state (Bu et al., 2012; Tai et al., 2013). ApoE in fact, directly interacts with A β and the subsequent binding of ApoE to membrane proteins, such as the low-density lipoprotein receptor (LDLR), the low-density receptor-related protein 1 (LRP1) and sortilin, initiates A β endocytosis and mediates cellular A β

uptake (Bu et al., 2012; Carlo et al., 2013). Most notably, when the interaction between A β and ApoE is blocked, intraneuronal accumulation of A β is reduced (Kuszczyk et al., 2013).

Thus, the genetic landscape of AD-associated mutations and risk variants results in, on the one hand, an increased production of the aggregation-prone A β 42 peptide isoforms from its precursor protein and, on the other hand, affects cellular uptake and clearance mechanisms of misfolded proteins on multiple levels. Ultimately, this might lead to an excessive disturbance of cellular protein homeostasis, where intracellular protein aggregates sequester essential factors of cellular functions (Yang and Hu, 2016). Furthermore, constant recycling of misfolded, aggregated proteins and peptides is of high importance, in order to maintain a sufficient, cellular energy metabolism. Thus, malfunctions in endosomal-lysosomal uptake and autophagic flux, might finally result in metabolic dysregulation, cellular nutritional deficiencies and neuronal cell death (Kaur and Debnath, 2015; Singh and Cuervo, 2011).

2.4 Intracellular A β 42 deposition and cellular degradation

As introduced above, even though the pathological hallmark of AD was initially described as extracellular A β plaque formation, A β peptides do not only accumulate extracellularly, but also form insoluble intracellular aggregates in neuronal cells (LaFerla et al., 2007; Ripoli et al., 2014; Takahashi et al., 2017). In transgenic mouse models of AD, the formation of intracellular A β aggregates is generally observed prior to the appearance of extracellular amyloid plaques, indicating that intracellular aggregate formation is an early event in pathogenesis potentially preceding extracellular A β plaque deposition (Takahashi et al., 2013). Additionally, the intracellular accumulation of A β peptides could also be found prior to extracellular plaque formation in AD patients with Down Syndrome (Gyure et al., 2001).

Within the cytoplasm of neurons in AD patients, individual endosomes in fact show dramatically enlarged volumes when compared to their sizes in unaffected individuals indicating intracellular A β 42 aggregate deposition in the endolysosomal compartment (Cataldo et al., 2004). APP itself can be internalized into early-endosomes and is discussed to be processed within the endocytotic pathway, which thereby represents a location of intracellular A β 42 generation (Cabrejo et al., 2006; Martin et al., 1995; Rovelet-Lecrux et al., 2006). Additionally, within lysosomes, which are the common endpoint of

the endocytotic and endolysosomal pathway, degradation of misfolded, accumulated proteins such as A β 42 is mediated. In fact, some of the earliest pathologic changes in AD are characterized by accumulation of A β peptides within this endolysosomal system, suggesting a malfunction of this essential pathway (Peric and Annaert, 2015). Even in blood exosomes from yet cognitively normal individuals, which later developed AD, increased levels of autolysosomal proteins are detectable, indicating a very early intracellular A β accumulation and lysosomal dysfunction in AD pathogenesis (Goetzl et al., 2015).

Additionally, recent studies have shown that neurons and glia can internalize extracellular A β aggregate species through receptor-mediated endocytosis to remove these structures from the extracellular space (Yeh et al., 2016). However, A β aggregates entering mammalian cells were shown to be able to convert soluble intracellular A β polypeptides into an aggregated state through a prion-like seeding mechanism (Fritschi et al., 2014; Sowade and Jahn, 2017). Thus, neuronal and glial uptake of A β peptides or A β aggregates and their subsequent degradation in the endolysosomal system are very likely important processes in controlling A β levels, and malfunctions in this processing pathways might therefore sustain the pathological cascade in AD. In fact, spreading of A β peptides via cell-to-cell transfer was shown to be dependent on insufficient cellular clearance and thereby potentially drives disease progression (Domert et al., 2014). Thus, reduction of the A β 42 load within the central nervous system and in particular, enhanced degradation of intracellular A β 42 aggregates could be a promising approach to slow neurodegeneration and progression in AD.

2.5 Molecular therapeutic strategies in Alzheimer's disease

As deposition of A β peptides is a major pathological hallmark of AD and insufficient clearance mechanisms might account for disease, numerous efforts to pharmacologically lower the A β load in brains have been undertaken (Cummings et al., 2014; Doody et al., 2014; Salloway et al., 2014). One of the first strategies followed was to find inhibitors of proteases mainly responsible for cleavage of the APP protein in favor of the amyloidogenic A β 42 peptide. As amyloidogenic peptides are generated by cleavage of the APP fragment by the γ -secretase complex (Zhang et al., 2011), one logical approach was to find inhibitors of this protease and thereby decrease cleavage and ultimately reduce the production of aggregation-prone A β 42 peptides (Wolfe, 2012). Different γ -secretase inhibitors were identified and strongly pushed towards clinical evaluation, as

preclinical studies clearly showed a reduction in brain A β 42 deposition and a reduction of cognitive decline in rodent AD models (Stanton et al., 2010). Furthermore, high concentrations of γ -secretase inhibitors in phase II trials were able to effectively block A β 42 production in humans, giving hope for this therapeutic approach (Wolfe, 2012). However, the unforeseen side effect of γ -secretase inhibitors, inhibition of notch signaling – a highly conserved pathway involved in neurogenesis (Artavanis-Tsakonas et al., 1999) severely limited dosage in coming phase III trials due to safety concerns (Coric et al., 2012; Doody et al., 2013). Currently, γ -secretase inhibitors are therefore under optimization in order to increase specificity and to reduce inhibition of notch signaling (Strömberg et al., 2015).

As initial cleavage of APP by β -site amyloid precursor protein cleaving enzyme 1 (BACE1) is a prerequisite for subsequent generation of amyloidogenic A β peptides from the APP fragment C99 by γ -secretase (Zhang et al., 2011), additionally, BACE1 inhibitors were developed as A β 42 lowering and potential AD disease-modifying drugs. However, BACE1 inhibitors, which went into clinical trials, were not able to improve clinical outcomes for AD patients. A leading theory for failure, besides insufficient potency or poor pharmacokinetics, is that therapeutics aiming at lowering A β 42 production would need to unfold their effects very early in the course of disease to be able to delay neurodegeneration (Mullard, 2017). Therefore, BACE1 inhibitors are now being evaluated in patient cohorts with prodromal AD (Cummings et al., 2017).

Another therapeutic approach is the development of A β -specific antibodies to reduce A β pathology in AD patient brains and thereby slow cognitive decline. Currently, there are still ongoing clinical trials evaluating A β -specific antibodies (Cummings et al., 2017). However, so far all A β -targeting antibodies, even though able to reduce cerebral amyloid plaque load, have failed to exhibit significant positive effects on neurodegeneration and clinical outcome (Mullard, 2017). At first, most A β targeting antibodies were raised against the aggregation-prone A β 42 peptide species (Prins and Scheltens, 2013). It is not clear however, whether these antibodies would still recognize the APP protein and might therefore not be able to trigger sufficient immune response and induce adequate phagocytosis of misfolded, accumulated A β 42 aggregate species. Regarding this, specific antibodies were raised against neo-epitopes on the surface of aggregated A β species (Prins and Scheltens, 2013; van Dyck, 2017). One of the most promising candidates currently represents Aducanumab, in fact an A β aggregate-specific antibody,

which was isolated from a memory B-cell of a healthy-aged, elderly individual (Sevigny et al., 2016). As A β aggregate formation and deposition is not restricted to AD patients, but also affects healthy-aged individuals, there might be protective antibodies within the central nervous system's (CNS) antibody repertoire of elderly individuals (Geylis et al., 2005). Potentially, A β aggregate or A β seed-targeting antibodies are able to slow disease progression by preventing cell-to-cell transfer and spreading of misfolded A β throughout the CNS.

An additional strategy lies in the identification of direct A β aggregation modulating small molecules. It was previously shown that A β -binding molecules are capable of interfering with A β aggregation, thereby slowing down the formation of compact, β -sheet-rich structures or furthermore, redirecting the aggregation cascade towards a different substructure, which exhibits less toxic effects to neuronal cells (Bieschke et al., 2011; Nie et al., 2011). In fact, numerous small molecules, are currently under clinical evaluation (Parsons and Rammes, 2017). Besides small molecules, which show beneficial neuroprotective, anti-inflammatory, metabolic effects or counteract neurotransmitter imbalance in AD, direct, anti-amyloid compounds represent 13% of the current AD drug pipeline (Cummings et al., 2017). One major aim of this approach is to inhibit the formation of toxic, oligomeric A β peptide species, which – in the role of so-called “amyloid- β derived diffusible ligands” (ADDLs) (Liu et al., n.d.) (Wen et al., 2018) – specifically bind to postsynaptic receptors and thereby act as neurotoxins (Shi et al., 2016).

As stated above, the endolysosomal system and autophagic flux are the major pathways identified to be responsible for A β clearance. Therefore, enhancing autophagic clearance represents an additional potential strategy to increase A β aggregate degradation. In fact, increasing degradation by autophagy-stimulating compounds does result in increased A β clearance (Kovács et al., 2017; Tian et al., 2011). Most recently, it was shown that boosting endogenous clearance mechanisms by increasing expression of sequestosome 1 – also known as ubiquitin-binding protein p62, an autophagosome cargo protein, which marks other proteins for selective autophagy – does efficiently lower A β load and rescues cognitive deficits in an AD mouse model (Caccamo et al., 2017). Ultimately, small molecules directly targeting accumulating A β aggregates in cells, could potentially combine both effects: leading to the formation of less proteotoxic amyloid species and enhancing degradation through a compound-mediated conformational change. Thus, identifying small molecules, which reduce intracellular A β aggregate load might be an

effective therapeutic approach to treat AD.

2.6 Aim of the work

In order to identify small molecules, which increase cellular A β clearance, the first aim of this work was to model the phenomenon of intracellularly accumulating A β 42 aggregates, which are taken up from the extracellular space and accumulate within multivesicular bodies of the endolysosomal pathway. The cell model system should be intensively characterized for its A β 42 aggregate uptake mechanism, the localization and biochemical properties of accumulating A β 42 aggregates to evaluate its potential and suitability as a disease model for AD pathology.

In a next step, the model system clearly exhibiting major characteristics of *in vivo* pathology should be scaled up to a high-throughput capable, cell-based screening assay for the identification of small molecules reducing the abundance of endocytotically-derived intracellular A β 42 aggregates. In a proof-of-principle approach it was the aim to show that this assay is able to identify compounds, which lead to a significant reduction of intracellularly accumulating A β 42 aggregates.

Then, the cellular A β 42 aggregate reductive effect of the most potent hit compound should be validated using independent biochemical readouts and its concentration-dependent effect should be evaluated in titration experiments. Further, the aim was to assess, whether the compound-mediated cellular A β 42 reduction was able to ameliorate A β 42's seeding activity and whether compound treatment does in fact counteract A β 42-induced toxicity in neuronal cells.

Next, it was the aim to elucidate the mechanism of how the compound-mediated reduction of the cellular A β 42 aggregate load is mediated and whether the direct modulation of A β 42 aggregate formation and the compounds' remodeling propensity accounts for increased cellular A β 42 clearance.

Finally, it should be resolved, whether structural remodeling of A β 42 aggregates through EGCG is responsible for the increased A β 42 degradation through lysosomal enzymes – providing a potential mechanistic explanation for the strong, cellular A β 42 aggregate degradation promoting effect of direct amyloid-targeting polyphenols.

3 Material and Methods

3.1 A β 42 peptide stock solutions

Synthetic A β 42 peptides produced via solid-state peptide synthesis were dissolved in (1,1,1,3,3,3)-Hexafluoroisopropanol (HFIP) overnight, sonicated for 30 min, aliquoted and lyophilized with a vacuum concentrator. Monomeric A β solutions (200 μ M) were prepared from HFIP treated peptides by dissolution of the lyophilized peptide in 10 mM NaOH, water bath sonication for 5 min and subsequent dilution in low salt buffer (LSB) to desired assay concentrations. Lyophilization and handling of A β 42 solutions was performed in Protein Lobind tubes to minimize binding of peptides to plastic surfaces.

3.2 Preparation and fluorescent labeling of A β 42 aggregates

A β 42 aggregates were prepared from 20 μ M peptide stock solutions by incubation in LSB at 37°C for 18 h under constant agitation (300 rpm). For fluorescent labeling of A β 42 aggregates, 20 μ M A β 42 peptide stock solutions diluted in LSB were mixed with 5% A β 42 peptides which have been N-terminally labeled with the fluorophore 5-Carboxytetramethylrhodamine (TAMRA) in solid-state peptide synthesis. Then, mixed A β 42 peptide solutions were likewise aggregated at 37°C for 18 h under constant agitation (300 rpm). For cellular uptake experiments, aggregation products were additionally tip sonicated at lowest intensity for 1 min.

3.3 Atomic Force Microscopy (AFM)

Sheet mica was glued to conventional microscope slides and 20 μ l sample solution was adsorbed for 15 min onto the freshly cleaved mica, washed with filtered, deionized water (5 \times 40 μ l) and dried overnight. As controls, only aggregation buffer was added to the mica slide. Sample images were recorded with a digital multimode NanoWizard II atomic force microscope using a cantilever with a resonance frequency f_0 of 75 kHz (Bruker AFM Probes) in intermittent contact mode.

3.4 Fluorescence polarization-based A β 42 aggregation assay

N-terminally 5-Carboxyfluorescein (FAM) -labeled A β 42 peptide was dissolved in 1 mM NaOH to 50 μ M and stored as a stock solution at -20°C (A β 42-FAM tracer). In A β 42 aggregate reactions 0.05 μ M A β 42-FAM tracer was combined with 10 μ M unlabeled A β 42 peptides in low salt buffer. For seeded aggregation reactions 80 nM (monomer equivalent)

performed A β 42 aggregates were added as seeds. The aggregation mixtures were replenished with LSB to a total volume of 40 μ l/well. Fluorescence polarization was measured every 15 min at 37 °C in a fluorescence plate reader with a polarization module (M1000/M1000 PRO, Tecan) at an excitation wavelength of 470 \pm 5 nm and an emission wavelength of 528 \pm 20 nm in 384 well plates with 5 s shaking before each read. Values are means of four technical replicates. Polarization values are calculated as dimensionless millipolarization units (mP) with the plate reader software i-control (Tecan).

3.5 Neuroblastoma cell culture and treatment with A β 42(-TAMRA) aggregates

Neuroblastoma SH-EP cells (RRID: CVCL_0524) were cultured in Dulbecco's modified eagle medium (DMEM) containing 10% FCS, 25 mM D-Glucose, 100 units/ml penicillin and streptomycin, respectively. Incubation was carried out at 37°C with 5% (v/v) CO₂. For A β 42 aggregate internalization, cells were treated with 0.6 or 1 μ M unlabelled or A β 42-TAMRA aggregates which were directly infused into the cell culture medium.

3.6 Preparation of cell lysates for biochemical analysis

Cell lysates for biochemical analysis were prepared as follows: 2.2 x 10⁶ SH-EP cells were seeded into T25 cell culture flasks. After adhesion overnight, cells were treated with A β 42-TAMRA aggregates, directly infused into the cell culture medium, as described above for indicated timeframes. Then, cells were washed with PBS, trypsinized and collected in fresh medium. For compound validation experiments, cells were incubated with aggregates for 6 h, washed and trypsinized, before being seeded into 6-well cell culture plates on EGCG or dimethyl sulfoxide (DMSO) dilutions. After compound incubation for 20 h, cells were collected in fresh medium, transferred to Protein Lobind tubes and centrifuged for 3 min at 150 g in a microcentrifuge. After an additional washing step in PBS, cell pellets were lysed with 150 μ l cell lysis buffer and incubated for 30 min at 4°C. Protein concentrations of resulted cell lysates were determined using a bicinchoninic acid protein assay kit and were subsequently stored at -80°C before being analyzed.

3.7 Polyacrylamide gel electrophoresis and Western blotting

For analysis of samples using polyacrylamide gel electrophoresis (PAGE), 20 μ g protein from cell lysate was added to LDS sample buffer before being boiled for 5 min at 95°C in Protein Lobind tubes in a microcentrifuge tube incubator. Then, samples were loaded

onto SDS-PAGE gels along with pre-stained protein standard. After electrophoresis for 35 mins at 200 V with 2-(*N*-morpholino)ethanesulfonic acid (MES) running buffer, separated protein from cell lysates was wet blotted onto a nitrocellulose membrane in transfer buffer. Membranes were blocked with 3% milk powder in PBS-T for 1 h at room temperature (RT). Then, membranes were incubated with primary antibodies in blocking solution overnight at 4°C, followed by washing in PBS-T and subsequent incubation with horseradish peroxidase (HRP)-conjugated secondary antibodies for an additional hour at RT. Before being visualized, membranes were washed twice with PBS-T and once in PBS. For detection, HRP substrate was added and chemiluminescence was measured in a LAS-3000 Imaging System. Quantification analysis were performed using ImageJ software and intensities were normalized to loading control.

3.8 Native and denaturing filter retardation assays

For analysis of insoluble A β 42 aggregates in denaturing filter retardation assays (detection of SDS-stable aggregates), samples were prepared by adding them to an equal volume of 4% sodium dodecyl sulfate (SDS) and 100 mM dithiothreitol (DTT) followed by boiling samples at 98°C for 5 min. For analysis of A β 42 aggregates under non-denaturing conditions in a native filter retardation assay (detection of Nonidet P-40 (NP40) stable aggregates), samples were mixed with an equal volume of 1% NP40 solution. Then, detergent (SDS or NP40) treated samples were filtered through a cellulose acetate membrane with 0.2 μ m pore diameter size in a custom-made filter apparatus. Membranes were blocked in blocking solution for 1 h at RT. A β 42 aggregates retained on the filter membrane were then detected using the 6E10 antibody (1:2000) and an anti-mouse HRP-conjugated secondary antibody. In case of TAMRA-labeled A β 42 aggregates, additional detection of the fluorescent signal intensities on the filter membrane by exciting with a green light source (520 nm) and detecting with a long-pass emission filter (>575 nm) in a LAS-3000 Imaging System (Fujifilm) was performed. Signal intensities were quantified from technical triplicates after background subtraction using Aida Image Analyzer Software.

3.9 Automated fluorescence microscopy and quantification of aggregates in cells

Cells were treated with A β 42-TAMRA aggregates as described above for indicated times. To ensure removal of non-incorporated and surface-bound aggregates, A β 42 containing

medium was aspirated, cells were washed with PBS, trypsinized and collected in fresh medium. Then, cells were seeded into 96-well cell culture plates at an initial density of 4.5×10^4 cells per cm^2 . After adhesion for at least 3 h, cells were fixed in 2% paraformaldehyde (PFA) for 20 mins at RT, followed by nuclei staining with Hoechst (1:2500). Cells were then washed twice with phosphate-buffered saline (PBS) before fluorescent microscopy was performed in a high-content screening system (HCS) using an objective with 20-fold magnification. After image acquisition, automated data analysis was performed using HCS Software. For quantification, individual cells were detected from Hoechst fluorescent signals (excitation (Ex)/emission (Em) 353/483 nm) and total TAMRA fluorescent areas per cell (Ex/Em 555/580 nm) were measured and calculated from technical triplicates. To assess the suitability of the cell-based A β 42 degradation assay for high-throughput screening, we determined its z-factor (Zhang et al., 1999). DMSO treated samples served as negative and EGCG treated samples as positive control. The z-factor was then determined from formula (1).

$$z \text{ factor} = 1 - \frac{3(\sigma_p + \sigma_n)}{|\mu_p - \mu_n|} = 1 - \frac{3(3.6 + 6.5)}{|44.2 - 100|} = 0.47 \quad (1)$$

3.10 Immunofluorescence microscopy and staining of cells with dyes

SH-EP cells were washed with PBS and fixed with 2% PFA for 20 min at RT. Then, Hoechst staining (1:2500) followed by permeabilization with 0.1% Triton X-100 in PBS and blocking with 1% bovine serum albumin (BSA) in PBS-T was performed. For immunofluorescence staining, cells were incubated with primary antibodies overnight at 4°C or for 2 hr at 37°C, washed with PBS-T and subsequently stained with secondary antibodies for 1 h at RT and washed with PBS before being visualized. Lipid rafts were stained with 10 mg/ml of the monosialotetrahexosylganglioside (GM1)-binding, fluorescein isothiocyanate (FITC) conjugated cholera toxin subunit B (FITC-CTB) and incubated for 1 h at RT. Staining of β -sheet-rich intracellular aggregates was performed with 10 $\mu\text{g/ml}$ of the amyloid-binding compound Thioflavin S (ThS) for 10 min at RT.

3.11 Confocal microscopy

For confocal microscopy, 9.0×10^4 SH-EP cells per well were seeded on fibronectin-coated (1:100) cover slips in 24-well cell culture plates. After fixation and fluorescent staining was performed (see above), cover slips were transferred to conventional microscope slides using fluorescence mounting medium before image acquisition with a

Leica SP5 confocal microscope was performed (Advanced Light Microscopy Facility, MDC). Cells were identified from Hoechst fluorescent signals (Ex/Em 353/483 nm), TAMRA, FITC and ThS fluorescent images were acquired at excitation wavelengths of Ex/Em 555/580, 490/525 and 384/429 nm, respectively. Co-localization analysis of TAMRA and FITC fluorescent puncta was performed using Fiji Software.

3.12 Screening of a polyphenol compound library

A compound library containing 20 polyphenol molecules was utilized for the focused screen. Compounds were purchased from Sigma-Aldrich. All compounds were at analytical grade (> 95% purity or higher) and dissolved in DMSO at 20 mM and stored at -20 °C. To test their cellular A β 42 degradation promoting effect, cells previously treated with A β 42-TAMRA for 6 h as described above were washed with PBS, trypsinized and collected accordingly. Then, A β 42-TAMRA aggregate harboring cells were seeded onto 10 μ M compound dilutions or DMSO only as control and incubated for additional 20 h. Automated fluorescent microscopy and data analysis to determine cellular A β 42 aggregate loads was performed as described above.

3.13 Thioflavin T A β 42 aggregate binding and seeding assay

For quantification of β -sheet rich aggregates in cells, lysates were prepared as described above and 30 μ g cell lysate of each sample was transferred to a 384-well plate and incubated with 6 μ M ThT for 10 min at RT before fluorescence intensities were measured (Ex/Em 420/485 nm) in a fluorescence microplate reader (M1000).

For A β 42 aggregation kinetics *in vitro*, 20 μ M A β 42 peptide solutions were prepared as described above and mixed with equimolar amounts of ThT in a 384-well plate. For compound studies, additional equimolar amounts of EGCG, derivatives or DMSO as control were added to *in vitro* A β 42 aggregation reactions (total volume 40 μ l). Then, fluorescence intensities (Ex/Em 420/485 nm) were measured every 20 mins in a fluorescence microplate reader (M1000).

To evaluate seeding-activity of intracellular A β 42 aggregates, cells were first mechanically lysed in a tissue homogenizer. Protein concentrations were then determined using the BCA assay and 1 μ g of cell lysate was added to *in vitro* A β 42 aggregation reactions monitored from ThT fluorescence intensities over time as described above. For quantification of seeding-activity, aggregation kinetics were non-

linearly fitted and time-points at which the half maximal ThT signal intensity was reached (t_{50}) were calculated using GraphPad PRISM Software. Then, the t_{50} value of treated samples was subtracted from control samples' t_{50} values resulting in a value for seeding-activity (Δt_{50} (h)), which resembles the acceleration or deceleration of spontaneous A β 42 aggregation.

3.14 Preparation of neuronal primary cultures from rat hippocampi

Animal tissue preparation and neuronal cell isolation was performed by Dr. Aline Schulz (AG Meier, Max Delbrück Center for Molecular Medicine). All animals were sacrificed according to the permit given by the Office for Health Protection and Technical Safety of the regional government of Berlin (LaGeSo, T0122/07, to Prof. Jochen Maier) and in compliance with regulations laid down in the European Community Council Directive. Cell culture plates were coated with 0.005% poly-DL ornithine hydrobromide in H₂O at 37°C overnight and further incubated with DMEM containing 10% FCS for several hours. The pregnant rats were sacrificed by cervical dislocation, embryos were dissected and moved into ice-cold standard salt solution (SSS). The brains of each embryo were isolated and collected in ice-cold SSS. Then, meninges of brains were removed, and hippocampi were isolated. Hippocampal tissue was cut into small pieces and treated with trypsin solution for 5 mins at 37°C. Trypsinization was stopped with DNase-Ovomucoid solution. To singularize cells, tissue was grinded, cells were counted and plated at an initial density of 6.8×10^4 cells per cm² in coated 96-well cell culture plates. Hippocampal neuron cultures were sustained in 2% B27- and 1% FCS-supplemented neurobasal medium containing 25 μ M β -mercaptoethanol, 0.25 mM L-glutamine and 0.05% Penicillin/Streptomycin (Brewer et al., 1989). To eliminate glia cells from the culture, cells were treated with 5 μ M cytarabine (AraC) on day *in vitro* two.

3.15 Mitochondrial metabolic rate assay (MTT)

For analysis of SH-EP cell mitochondrial metabolic rate, neuroblastoma cells were cultured as described and seeded at an initial density of 2.0×10^4 cells per well into 96-well cell culture plates. In case of mitochondrial metabolic analysis in neurons, primary rat hippocampal neurons were prepared as described above. Neuroblastoma cells or primary neurons were treated with 1 μ M preformed A β 42 aggregates or aggregation buffer as control. Then, cells were treated with indicated EGCG concentrations and further incubated for 24 h. To evaluate cell viability, cells were treated with MTT (3-(4,5-

dimethylthiazol-2-yl)-2,5-diphenyltetrazolium bromide) reagent and incubated for additional 4 h at 37°C. Then, stop solution was applied, incubated for 1 h and absorbance at 570 nm was measured in a fluorescence microplate reader (M200).

3.16 Mouse embryonal fibroblast (MEF) cell culture

Wild-type (autophagy related 5 protein (ATG5) +/+) and ATG5 knockout (ATG5 -/-) MEFs were cultured in DMEM containing 10% FCS, 25 mM D-Glucose, 100 units/ml penicillin and streptomycin, respectively. Incubation was carried out at 37°C with 5% (v/v) CO₂. For A β 42-TAMRA aggregate internalization, 0.6 μ M of aggregate solution was directly infused into the cell culture medium. After A β 42 aggregate uptake, cells were trypsinized, washed and transferred to 96-well cell culture plates onto compound dilutions as described above. Immunofluorescence staining was performed as described above. Aggregate loads were quantified using automated fluorescence microscopy.

3.17 Cathepsin B enzyme activity assay

SH-EP cells were cultivated and treated with A β 42-TAMRA aggregates as described above. Then, cells were washed, trypsinized, collected in fresh medium and 90×10^4 cells were seeded onto EGCG or DMSO as control in 6-well cell culture plates. After incubation for 18 h, medium was aspirated, cells were washed in PBS, mechanically detached from the surface and collected in Protein Lobind tubes. After centrifugation for 3 min at 150 g, supernatant was removed and 100 μ l M2 lysis buffer was added to cell pellets. After lysis for 30 mins at 4°C, protein concentrations were determined using a BCA assay kit and all samples were adjusted to total protein concentration of 1 μ g/ μ l in M2 lysis buffer. Then, 25 μ g lysate was added to 50 μ M of the cathepsin B (CatB) substrate Z-Arg-Arg-7-amido-4-methylcoumarin hydrochloride (Z-RR-AMC) diluted in cell free system buffer and incubated for 1 h at 37°C. AMC fluorescence intensities were measured using a fluorescence microplate reader (M200).

3.18 EGCG derivative library

EGCG derivatives commercially available were purchased from Sigma-Aldrich. (+)-EGC, EGC-3,5-DHB, EGC-3,4-DHB, EGC-3-FB, EGC-4-FB, EGC-4-HB, EGC-Biotin, Rhodamine B Linker and EGC-Rhodamine B were custom synthesized, identity checked by nuclear magnetic resonance (NMR) spectroscopy and kindly provided by collaborators at the Heinrich-Heine University Düsseldorf (Angelika Motzny, Prof. Dr. Constantin

Czekelius). All compounds were at analytical grade (> 95% purity or higher) and dissolved in DMSO to 20 mM or 60 mM and stored at -20°C or -80°C. To test their cellular A β 42 degradation promoting effect, A β 42 *in cell* degradation assay was performed as described above. *In vitro* aggregation inhibiting effects were assessed in ThT aggregation kinetics (see above for experimental details).

3.19 Co-localization studies of EGCG and intracellular A β 42 aggregates

SH-EP cells were treated with 0.6 or 1 μ M preformed A β 42-TAMRA or A β 42-HiLyte aggregates for 6 h as described above. After trypsinization and washing to remove extracellular and surface-bound aggregates, 9.0×10^4 cells per well were seeded onto fibronectin (1:100) and poly-L-lysine (1:100) coated cover slips in 24-well cell culture plates. Then, cells were treated with 30 μ M of biotin- or rhodamine B-labeled EGCG derivatives (EGCG #25, #44) and DMSO or rhodamine B with the linker only (EGCG-control #37) as control. After 3 h of incubation, SH-EP cells were fixed in 2% PFA and prepared for confocal microscopy as described above. In case of the biotin-labeled EGCG derivative, cells were fixed, blocked in 1% BSA, permeabilized with 1% Triton-X and additionally stained with Streptavidin-Cy5.

3.20 EGCG-mediated remodeling of A β 42 aggregates

20 μ M A β 42 peptides were preaggregated as described above (in LSB, 37°C, 300 rpm, 18 h). For remodeling, two approaches were chosen: EGCG-aggregation samples were aggregated in presence of three-fold molar excess of EGCG (20 μ M A β 42: 60 μ M EGCG), in EGCG-disaggregation samples preformed A β 42 aggregates (18 h) were incubated for an additional 24 h in the presence of a three-fold excess of EGCG. Then, EGCG-aggregation and -disaggregation samples were analyzed for changes in morphology and size distribution of aggregates by AFM and transmission electron microscopy.

3.21 Transmission electron microscopy (TEM)

Samples were diluted to 2 μ M (monomeric concentration) in LSB. Then, 5 μ l of sample solution was adsorbed to carbon-coated copper grids for 1 min. Residual buffer was removed with filter paper and the grid was negatively stained with 5% uranyl acetate. Images were acquired in a Philips CM-100 transmission electron microscope.

3.22 Density gradient centrifugation

Native and EGCG-remodeled A β 42 aggregates were subjected to iodixanol gradient centrifugation. The assay principle was published by Brener O. et al. naming the method quantitative determination of interference with A β aggregate size distribution (QIAD) (Brener et al., 2015). The published protocol was slightly adapted to analyze the EGCG-mediated remodeling effect. Therefore, a discontinuous gradient of iodixanol was prepared in an 11 x 34 mm polyallomer ultracentrifuge tube, from bottom to surface: 130 μ l of 50%, 130 μ l of 40%, 130 μ l of 30%, 390 μ l of 20%, 130 μ l of 10% and 50 μ l of 5% (w/v) iodixanol. Then the gradient was overlaid by 50 μ l of the analyzed A β 42 aggregate sample solution. Ultracentrifugation was performed at 4°C with a TLA-55 rotor at 55.000 rpm for 3 h. After centrifugation, 14 fractions of 70 μ l were harvested by upward displacement and pellet (~30 μ l) was collected as 15th fraction. All fractions were denatured with 2% SDS and 50 mM DTT and boiled at 95°C for 5 mins. Then fractions were analyzed for A β content in dot blot assays using the 6E10 antibody.

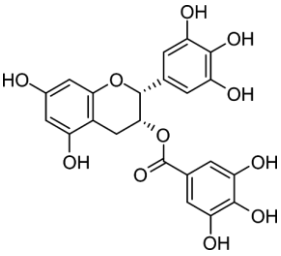
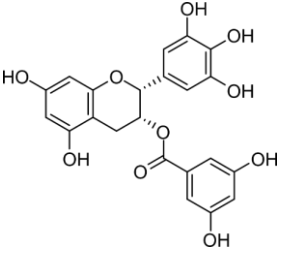
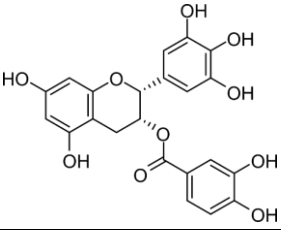
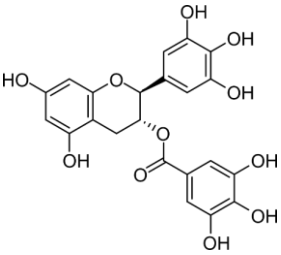
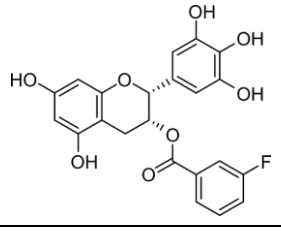
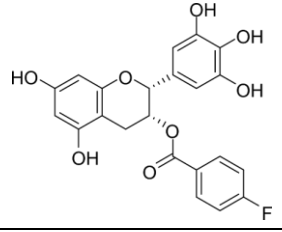
3.23 *In vitro* Cathepsin B activity and cleavage of A β 42 aggregates

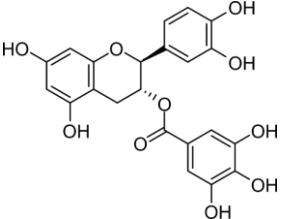
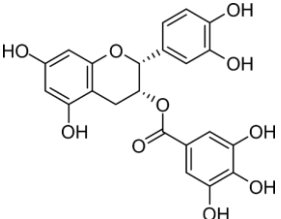
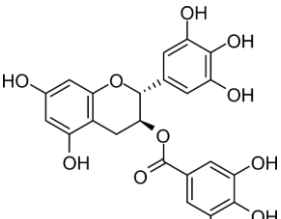
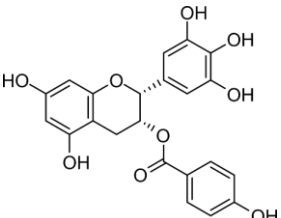
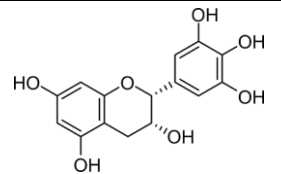
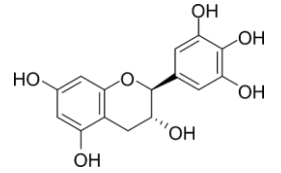
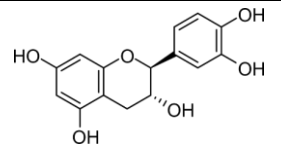
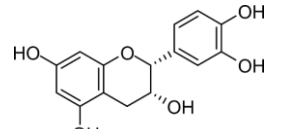
For *in vitro* CatB activity and cleavage studies of native and remodeled A β 42 aggregates, CatB purified from human liver was purchased (Enzo Life Sciences), aliquoted at stock concentration of 437 μ g/ml and stored at -80°C. For analysis of direct compound effects on enzyme activity *in vitro*, CatB was prediluted to 100 μ g/ml in H₂O containing 0.1% Brij-35 and 4 mM L-Cysteine for enzyme preactivation, which was carried out for 5 min at RT. Next, fluorescent cathepsin substrate Z-R-R-AMC was diluted in cathepsin *in vitro* assay buffer to 10 μ M. Preactivated enzyme was added to substrate solution at a final concentration of 1 μ g/ml. Then, 10 μ M EGCG, CatB inhibitor CA074 or DMSO as control were added to enzyme-substrate mixtures. Samples were transferred to a 384-well plate and AMC fluorescence intensity was measured in triplicates over time in a fluorescence microplate reader (M1000, Em/Ex: 348/440 nm). For *in vitro* CatB cleavage of A β 42 aggregates, morphology and size distribution of EGCG-induced, remodeled A β 42 aggregates were analyzed using AFM, TEM and gradient centrifugation. Native and remodeled aggregate species were then digested with CatB and analyzed for cleavage efficiency. Therefore, 5 μ g/ml preactivated CatB or enzyme buffer as control was added to 10 μ M A β 42 aggregate solutions and incubated for 4 h at 37°C. Digestion reactions were stopped with 1x protease inhibitor (PI) cocktail and phenylmethylsulfonyl fluoride

(PMSF). Samples were analyzed in dot blot and filter retardation assays using 6E10 and SySy28703 A β -detecting antibodies.

3.24 Material and equipment

Table 1. EGCG derivatives

Compound	Structure
(-)-Epigallocatechin gallate Abbr.: EGCG	
(-)-Epigallocatechin 3,5-dihydroxybenzoate Abbr.: EGC-3,5-DHB , #25	
(-)-Epigallocatechin dihydroxybenzoate Abbr.: EGC-3,4-DHB , #19	
(-)-Gallocatechin gallate Abbr.: (-)- GCG	
(-)-Epigallocatechin 3-fluorobenzoate Abbr.: EGC-3-FB , #20	
(-)-Epigallocatechin 4-fluorobenzoate Abbr.: EGC-4-FB , #13	

<p>(-)-Catechin gallate</p> <p>Abbr.: CG</p>	
<p>(-)-Epicatechin gallate</p> <p>Abbr.: ECG</p>	
<p>(+)-Gallocatechin gallate</p> <p>Abbr.: (+)-GCG, #8</p>	
<p>(-)-Epigallocatechin 4-hydroxybenzoate</p> <p>Abbr.: EGC-4-HB, #24</p>	
<p>(-)-Epigallocatechin</p> <p>Abbr.: EGC</p>	
<p>(-)-Gallocatechin</p> <p>Abbr.: GC</p>	
<p>(-)-Catechin</p> <p>Abbr.: C</p>	
<p>(-)-Epicatechin</p> <p>Abbr.: EC</p>	

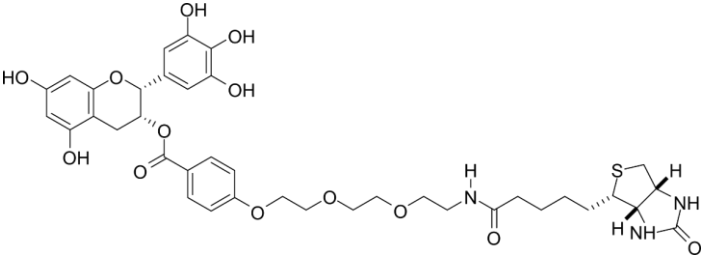
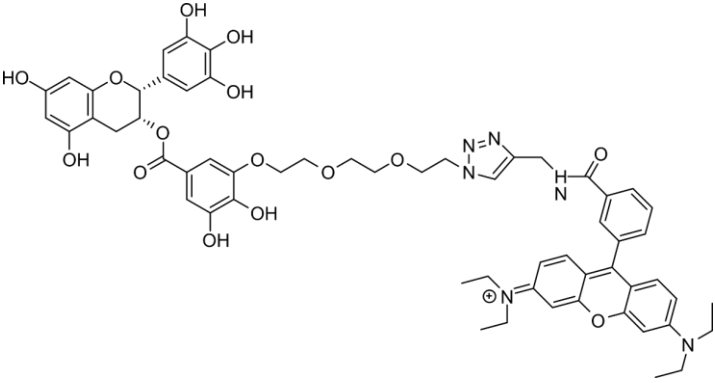
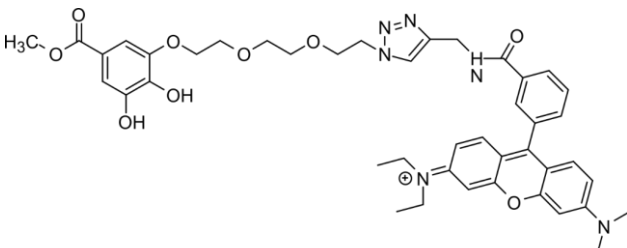
<p>(-)-Epigallocatechin 4-biotinbenzoate</p> <p>Abbr.: EGC-Biotin, #26</p>	
<p>(-)-Epigallocatechin 3-rhodaminB-4,5-dihydroxybenzoate</p> <p>Abbr.: EGCDHB-RhodaminB, #35</p>	
<p>Rhodamin B linker control</p> <p>Abbr.: EGCG-control #44</p>	

Table 2. List of recombinant proteins and peptides

Peptide / protein ▲	Application	Origin / synthesis method	Provider	Ref.#
5-TAMRA-Amyloid β -Protein (1-42) (A β 42-TAMRA)	Preformed aggregate labeling	Solid-state peptide synthesis	Bachem	H-7448
FAM-Amyloid β -Protein (1-42) (A β 42-FAM)	Fluorescence polarization assay	Solid-state peptide synthesis	AnaSpec	AS-23525-05
Amyloid β -Protein (1-42) (A β 42)	Preformed aggregate production, aggregation assay	Solid-state peptide synthesis	Bachem	H-1368
Cathepsin B	In vitro A β 42 cleavage assay	Purified from human liver	Enzo Life Sciences	BML-SE198-0025

HiLyte 488 Fluor -Amyloid β -Protein (1-42) (A β 42-HiLyte)	Prefomed aggregate labeling	Solid-state peptide synthesis	AnaSpec	AS-60479-01
--	-----------------------------	-------------------------------	---------	-------------

Table 3. List of antibodies

Antibody ▲	Specificity	Host & type	Working concentration	Manufacturer / Provider
Anti-Amyloid β (SySy218703)	Amyloid- β (AAs 37-42)	Rabbit, polyclonal	1:1000	Synaptic Systems (SySy)
anti-Amyloid- β (4G8)	Amyloid- β (AAs 17-24)	Mouse, monoclonal	1:1000	BioLegend
anti-Amyloid- β (6E10)	Amyloid- β (AAs 1-16)	Mouse, monoclonal	1:1000	BioLegend
anti-Cathepsin B (ab58802)	Cathepsin-B	Mouse, monoclonal	1:1000	abcam
anti-EEA1	Early endosome antigen 1	Rabbit, polyclonal	1:100	Cell Signaling Technology
anti-Lamp2 (51-2200)	Lysosomal associated membrane protein 2	Mouse, monoclonal	1:1000	Invitrogen
anti-Mouse IgG	Mouse IgG (H + L) (HRP conjugated)	Goat, polyclonal	1:2000	Sigma-Aldrich
anti-Mouse IgG	Mouse IgG (H + L) (Alex488 conjugated)	Goat, polyclonal	1:1000	ThermoFisher Scientific
anti-Tubulin	α -Tubulin	Mouse, monoclonal	1:2000	Sigma-Aldrich

Table 4. List of dyes, fluorophores and substrates

Dye / fluorophore	Abbreviation	Ex / Em (nm) ▲	Provider
Z-Arg-Arg 7-amido-4-methylcoumarin	Z-R-R-AMC	348 / 440	Sigma-Aldrich
Hoechst 33342	Hoechst	353 / 483	Life Technologies
Thioflavin S	ThS	384 / 429	Sigma Aldrich
Thioflavin T	ThT	440 / 485	Sigma-Aldrich
FITC-Cholera toxin B	FITC-CTB	490 / 525	Sigma-Aldrich
5-Carboxyfluorescein	FAM	494 / 521	AnaSpec
Alexa Fluor™ 488	Alex488	498 / 520	ThermoFisher
HiLyte Fluor™ 488	HiLyte	501 / 527	AnaSpec
Lysotracker™ Green	Lysotracker	504 / 511	Sigma-Aldrich
Carboxy tetramethyl-rhodamine	TAMRA	555 / 580	Bachem
3-(4,5-dimethylthiazol-2-yl)-2,5-diphenyltetrazolium bromide	MTT	absorption at 562	ThermoFisher

Table 5. Laboratory kits, chemicals and stock solutions

Description ▲	Substance / Product	Manufacturer / Provider
Antibiotic-Antimycotic (AB-AM)	Penicillin, Streptomycin, Amphotericin B	Gibco
B27	B-27™ Supplement	Gibco
BCA assay kit	Pierce™ BCA Protein Assay Kit	ThermoFisher Scientific
Benzonase®	Endonuclease from <i>Serratia marcescens</i>	Merck Millipore
Brij-35	Brij™-35, 30% solution	Sigma-Aldrich
Cytochalasin D	Cytochalasin D, C8273	Sigma-Aldrich
D-Glucose	Glucose solution	Gibco
DMEM	various	Gibco
EIPA	5-(N-ethyl-N-isopropyl) amiloride, A3085	Sigma-Aldrich
FCS	Fetal calf (bovine) serum	Gibco
Fibronectin	Fibronectin from bovine plasma	Gibco
HFIP	1,1,1,3,3,3-Hexafluoro-2-propanol	Sigma-Aldrich
HRP substrate	Pierce ECL Western Blotting Substrate	Thermo Fisher Scientific
Iodixanol	OptiPrep™ Density Gradient Medium	Sigma-Aldrich
L-Cysteine	(R)-2-Amino-3-mercaptopropionic acid	Sigma-Aldrich
LDS sample buffer	NuPAGE LDS sample buffer (4x)	Invitrogen
Milk powder	Low-fat powdered milk	Carl Roth
Mounting medium	Dako S3032	Agilent / Dako
Penicillin and Streptomycin	Penicillin-Streptomycin	Gibco
PMSF	Phenylmethylsulfonyl fluoride	Roche
Protease inhibitor cocktail	cOmplete™, EDTA-free	Roche
Protein ladder	SeeBlue Plus2	Thermo Fisher Scientific
SDS	Sodium dodecyl sulfate	Sigma-Aldrich
Triton™ X-100	polyethylene glycol <i>tert</i> -octylphenyl ether	Sigma-Aldrich
Tween® 20	polyethylene glycol sorbitan monolaurate	Sigma-Aldrich

Table 6. List of buffer solutions

Buffer solution (abbr.)	Ingredient	Final concentration	Purpose ▲
Low salt buffer (LSB) pH = 7.4	KH ₂ PO ₄ K ₂ HPO ₄ NaCl	2.0 mM 8.0 mM 10.0 mM	Aggregation buffer
Cell free system buffer pH = 7.4 (Zhou et al., 2013)	HEPES-NaOH KH ₂ PO ₄ NaCl MgCl ₂ EGTA Pyruvate D-Sucrose D-Mannitol AEBFS PMSF DTT	10.0 mM 2.5 mM 2.0 mM 2.0 mM 0.5 mM 5.0 mM 68.0 mM 220.0 mM 1.0 mM 0.1 mM 1.0 mM	CatB activity in cells
Cathepsin in vitro assay buffer pH = 6.0	KH ₂ PO ₄ Na ₂ HPO ₄ EDTA	105.6 mM 14.4 mM 1.2 mM	CatB <i>in vitro</i> assay
Cell lysis buffer pH = 8.1	Tris EDTA MgCl ₂ NaCl PMSF NP40 PI cocktail Benzonase	50.0 mM 1.0 mM 5.0 mM 100.0 mM 1.0 mM 1.0 % 1.0 x 1.0 x	Cell lysis for analysis of intracellular Aβ ₄₂ aggregates
M2 lysis buffer pH = 7.4 (Cold Spring Harbor Protocols, 2007)	Tris NaCl NaF Na ₃ PO ₄ Na ₃ VO ₄ β-glycerol PO ₄ EDTA AEBSF	50.0 mM 150.0 mM 50.0 mM 5.0 mM 0.1 mM 40.0 mM 1.0 mM 1.0 mM	Cell lysis for Cathepsin activity assay

	PMSF	0.1 mM	
Phosphate buffered saline (PBS) pH = 7.4	KH ₂ PO ₄	1.8 mM	Multiple
	Na ₂ HPO ₄	10.0 mM	
	KCl	2.7 mM	
	NaCl	137.0 mM	
PBS + Tween (PBS-T); pH = 7.4	+ Tween	0.05 %	
MES SDS running buffer pH = 7.3	MES	50.0 mM	PAGE
	Tris	50.0 mM	
	EDTA	1.0 mM	
	SDS	0.1 %	
Standard salt solution (SSS) pH = 7.4	NaCl	135.0 mM	Primary neuron preparation
	KCl	5.0 mM	
	CaCl ₂ x 2*H ₂ O	1.25 mM	
	MgCl ₂ x 6*H ₂ O	0.5 mM	
	MgSO ₄ x 7*H ₂ O	0.5 mM	
	NaHCO ₃	1.0 mM	
	HEPES	10.0 mM	
	D-Glucose	25.0 mM	
	AB-AM	1 x	
Trypsin solution pH = 8.0	PBS	1 x	Primary neuron preparation
	D-Glucose	20.0 mM	
	HEPES	15.0 mM	
	EDTA	1.0 mM	
	Trypsin	0.25 %	
	AB-AM	1 x	
DNase-Ovomucoid solution pH = 7.4	Hank's MEM	1 x	Primary neuron preparation
	MgCl ₂ x 6*H ₂ O	0.44 mM	
	HEPES	25.0 mM	
	D-Glucose	20.0 mM	
	MgSO ₄ x 7*H ₂ O	50.0 mM	
	Ovomucoid	30 mg/ml	
	DNase	1380 U/ml	
Transfer buffer (TB-wet) pH = 8.3	Tris	25.0 mM	Western Blot (wet)
	Glycine	192.0 mM	
	Methanol	10.0 %	

Table 7. Plate types and specifications

Application ▲	Plate format	Provider	Description	Ref.#
A β 42 aggregation in vitro (ThT), ThT cell lysate measurements	384-well	BD Falcon	Black, clear bottom	353962
BCA Assay	96-well	Nunc	Clear, polystyrene	P7366
Cell-based screening assay	96-well	BD Falcon	Black, clear bottom, tissue culture	353219
Cover slip sample preparation for confocal microscopy	24-well	Greiner	CELLSTAR® clear	662160

Table 8. List of laboratory instruments and equipment

Instrument ▲	Model	Provider
AFM	NanoWizard® II	JPK Instruments
AFM Mica	Agar mica	NanoWorld AG
Cellulose acetate membrane	OE66	Schleicher and Schuell
Centrifuge	Allegra X-12	Beckman Coulter
CO2 incubator	CB 160	Binder
Confocal microscope	TCS SP5	Leica
Electrophoresis system	XCell SureLock™	ThermoFisher Scientific
Filter assay unit	Hybrid manifold	Life Technologies
Fluorescence microplate reader	M200	Tecan
Fluorescence microplate reader	M1000	Tecan
High-content array scanner	Cellomics™ ArrayScan VTI HCS	ThermoFisher Scientific
Imaging System	LAS-3000	Fujifilm
Light microscope	Axio Imager	Zeiss
Microcentrifuge tube incubator	Thermomixer	Eppendorf AG
Nitrocellulose membrane	BA85 0.45 μ m	Protran / Whatman
Protein low-binding tubes	Protein Lobind	Eppendorf
SDS-PAGE Gels	NuPAGE Bis-Tris (1 mm, 4-12%)	Invitrogen

Semi-dry blotting unit	Trans-Blot® SD Semi-Dry Transfer Cell	BioRad
TEM	CM-100	Philips
TEM copper grid	„Glimmer“ V3, G250-2	PLANO GmbH
Tip sonicator	Ultrasonicator 450	Branson
Tissue homogenizer	Precellys 24	Bertin Instruments, USA
Ultracentrifuge	TL 100	Beckman Coulter
Ultracentrifuge tubes	Polyallomer tubes, #357448	Beckmann Coulter
Vacuum concentrator	SpeedVac Plus SC110A	Savant
Water bath sonicator	SONOREX Digitec	Bandelin
Wet blotting unit	Mini Trans-Blot® Cell	BioRad

Table 9. List of Software used

Software ▲	Application	Provider	Version
AIDA Image Analyzer	Dot blot and filter retardation assay analysis	Elysia-raytest GmbH	3.21
GraphPad PRISM	Figures and statistical analysis	GraphPad Software Inc.	7
i-control	Fluorescence/Absorption-based assays	TECAN	2.0
ImageJ (Fiji – “Fiji is just ImageJ”)	Image Analysis	National Institute of Health	1.51n

4 Results

4.1 Fluorescent labeling and characterization of preformed A β 42 aggregates

To establish a cell-based screening assay which is high-throughput capable and not dependent on antibody staining for the detection of intracellular A β 42 aggregate load, fluorescently labeled A β 42 aggregates were prepared from *in vitro* aggregation reactions. Therefore, synthesized A β 42 peptides were used, which were N-terminally labeled with the fluorophore 5-Carboxytetramethylrhodamine (TAMRA). TAMRA-labeled A β 42 peptides were incorporated into A β 42 aggregates by mixing 5% of fluorescently-labeled

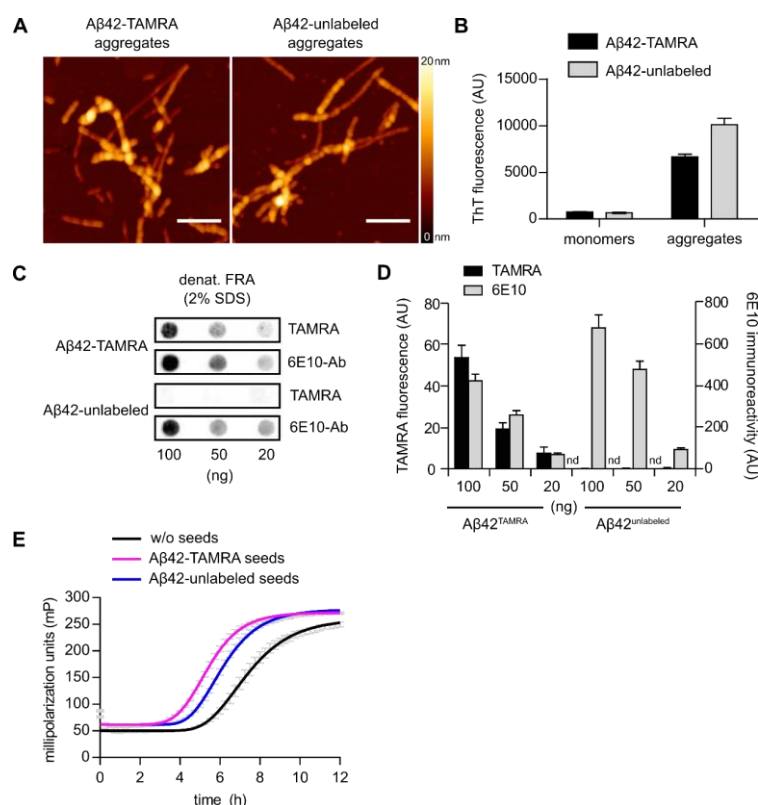


Figure 2. Characterization of preformed A β 42 aggregates. **(A)** Atomic force microscopy of TAMRA- and unlabeled A β 42 aggregates showing similar aggregate morphology and fibril heights. 10 μ M A β 42 peptides were incubated for 18 h at 37°C. Scale bars: 300 nm. **(B)** Characteristic fluorescence spectrum shift of ThT upon A β 42 aggregate binding indicates high β -sheet content. A β 42 monomers show no ThT binding capacity. A β 42:ThT ratio, 1:1; 10 μ M. **(C)** Biochemical analysis of preformed A β 42 aggregates. SDS-stability was assessed in denaturing filter retardation assays. Signals were detected from TAMRA or 6E10 antibody signals. **(D)** Quantification of SDS-stable A β 42 aggregates in C. **(E)** Seeding activity of labeled and unlabeled A β 42 aggregates. A β 42-TAMRA aggregates are seeding competent in A β 42 fluorescence polarization assay. Bars represent means with error bars indicating standard deviation. *In vitro* analysis was performed in technical triplicates. _____

with 95% unlabeled peptides and incubation of mixed A β 42 peptide solutions for 18 h under constant agitation in low salt buffer (LSB). As smaller particles with an increased overall surface are potentially more efficiently internalized, resulting aggregation products were additionally sonicated after incubation. TAMRA-labeled A β 42 aggregate species were analyzed in atomic force microscopy and it was investigated whether fluorescent labeling results in changes on aggregate morphology. Fluorescently labeled aggregates were similar in morphology and fibril heights compared to unlabeled A β 42 aggregates when analyzed by AFM (**Figure 2**, A). Resulting aggregate species were further characterized by analyzing their ThT binding properties. Binding of ThT to β -sheet-rich amyloid structures typically results in a characteristic shift of its fluorescence spectrum (Biancalana and Koide, 2010) and is widely used to stain for A β 42 pathology in AD model systems and patient brain material (Luna-Muñoz et al., 2008). As expected, when monomeric A β 42 peptides were stained, ThT did not shift its spectrum, but for aggregated A β 42 species a typical fluorescence shift could be detected. This was observed for unlabeled as well as fluorescently labeled A β 42 aggregates (**Figure 2**, B). The slightly reduced fluorescent signal of ThT bound to TAMRA-labeled A β 42 aggregates is potentially due to partial absorption of ThT fluorescence by the TAMRA fluorophores. The A β 42 aggregate species found in patient tissue are typically detergent-resistant and are in parts not solubilized by SDS treatment (Masters and Selkoe, 2012). Therefore, the preformed A β 42 aggregates were analyzed in filter retardation assays under denaturing conditions (2% SDS). *In vitro* prepared A β 42 aggregates contained SDS-resistant aggregate species, which could be detected with the A β 42-antibody 6E10 (**Figure 2**, C). Additionally, high-ordered structures retained on the filter membrane showed strong TAMRA-fluorescence, indicating that A β 42-TAMRA peptides are successfully incorporated into SDS-stable A β 42 aggregates (**Figure 2**, D). Taken together, the structural and biochemical characterization of preformed, TAMRA-labeled A β 42 aggregates shows that *in vitro* prepared A β 42 aggregates exhibit major characteristic properties of aggregate species found in AD patient tissue.

4.2 A β 42 aggregates are rapidly internalized by SH-EP cells and are directed towards the endolysosomal pathway

In order to establish a cell-based aggregation degradation assay for compound testing, it was next examined, whether SH-EP neuroblastoma cells take up preformed A β 42 aggregates after adding them to the culture medium. Therefore, unlabeled and TAMRA-labeled aggregates were used, which were produced and characterized as stated above (**Figure 2**). To test whether monomeric or aggregated A β 42 species are preferentially internalized by SH-EP cells, A β 42 aggregates, soluble A β 42 peptides or aggregation buffer alone as a control were added to the cell culture medium. After 6 h, cells were

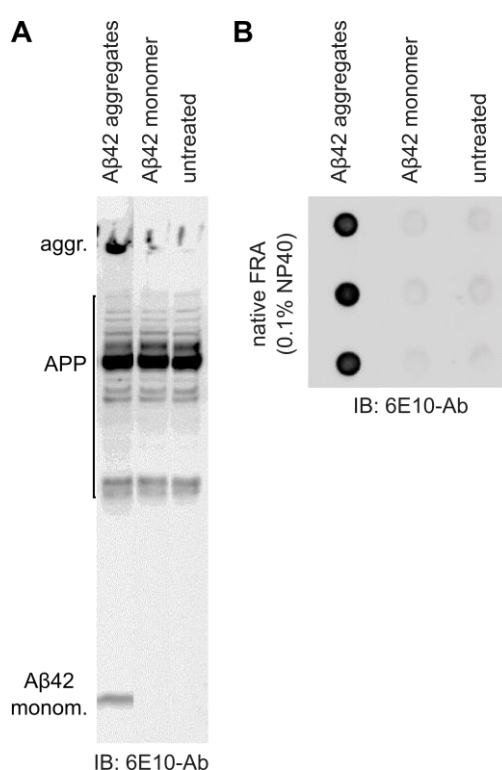


Figure 3. Biochemical analysis of SH-EP cell lysates after treatment with A β 42 aggregates. **(A)** Western blot from SH-EP cell lysates treated with A β 42 aggregates, A β 42 monomer or aggregation buffer only. 6E10 antibody detects SDS-stable aggregates in gel pockets as well as an A β 42 monomer band. APP, its different isoforms, dimers, trimers, oligomers and APP fragments are detectable. **(B)** Native filter retardation assay from SH-EP cell lysates treated with A β 42 aggregates, monomer or buffer as control. Only lysates from SH-EP cells treated with preformed A β 42 aggregates show strong aggregate accumulation. No spontaneous formation of A β aggregates from endogenous APP detectable. *Shown are the results from one representative experiment, analysis was performed in technical triplicates.* ____

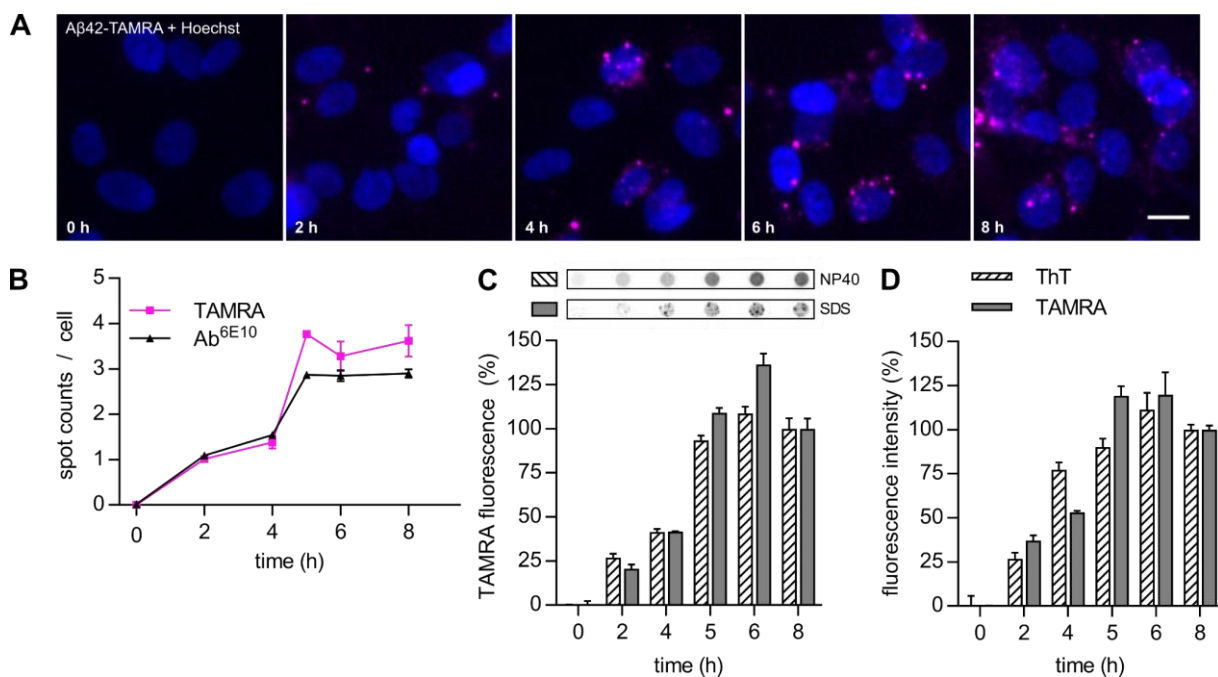


Figure 4. A β 42 aggregate internalization and cellular aggregate formation. **(A)** Fluorescence microscopy images show increasing formation of TAMRA-positive puncta over time. *Scale bar: 20 μ m.* **(B)** Quantification of cellular, TAMRA-positive puncta over time. For validation, cells were co-stained with A β -antibody 6E10. **(C)** Denaturing (SDS) and native (NP40) filter retardation assay analysis of SH-EP lysates after A β 42-TAMRA aggregate internalization for indicated timeframes. A β 42 aggregates were detected from TAMRA fluorescent signals, data was normalized to intensities at 8 h. **(D)** Thioflavin T binding assay from cell lysates with A β 42 aggregate. With increasing cellular aggregate load, TAMRA and Thioflavin T fluorescence intensities increase over time indicating build-up of β -sheet-rich cellular inclusions. *Depicted are means from three individual experiments with error bars representing standard deviation.* _____

lysed, and cell lysates were subsequently analyzed by SDS-PAGE and Western blotting. Successful A β 42 aggregate uptake was evaluated by staining Western blots with the 6E10 antibody. As the 6E10 antibody, besides reacting to A β 42 peptides, additionally detects endogenous APP, this could serve as a loading control. Only when neuroblastoma cells were treated with preformed A β 42 aggregates, SDS-stable aggregate species were detectable in the gel pockets (**Figure 3, A**). An additional band was detectable at the size of monomeric A β 42 peptide, which presumably resembles the product from non-detergent resistant A β 42 aggregates or soluble, monomeric A β 42 peptides. (**Figure 3, A**). In contrast, when equimolar amounts of monomeric A β 42 peptides were added to the cell culture medium, neither aggregates nor A β 42 monomers

could be detected in the cell lysate. The absence of A β 42 monomer in the cell lysate from treated SH-EP cells is probably due to immediate, efficient degradation of monomeric A β 42 peptides by SH-EP cells or inefficient uptake of the monomeric peptide (Jin et al., 2016). Native filter retardation assays further confirmed that only aggregate treated cells contain A β 42 aggregates and that there is no aggregate formation over time upon monomer treatment in these cells. There was also no spontaneous build-up of intracellular A β 42 aggregates observed in control cells due to endogenous APP cleavage or the release of A β peptides (**Figure 3, B**).

To evaluate the time-dependency of the uptake process, SH-EP cells were treated with 0.6 μ M of A β 42-TAMRA aggregates; cells were fixed after different incubation intervals, and cellular aggregate loads were analyzed performing fluorescence microscopy (**Figure 4, A**). To validate whether TAMRA fluorescent puncta in fact consist of A β 42 aggregates, fluorescent puncta per cell were quantified from TAMRA, as well as from 6E10 antibody signals after immunofluorescence staining. It was found that, in treated cultures, fluorescently labeled and antibody positive puncta are first detectable after 2 h. The abundance of these structures increases over time and reaches saturation after 8 h of incubation, indicating that A β 42-TAMRA aggregates are rapidly internalized in a time-dependent manner (**Figure 4, B**).

The observation of fluorescent puncta suggests that intracellular, insoluble A β 42 inclusions are formed in SH-EP cells. To confirm that the increase of fluorescent puncta detected over time resembles the build-up of intracellular A β 42 aggregates, cell lysates from different time points were analyzed using filter retardation assays. In line with the microscopic analysis, increasing A β 42 aggregate loads could be detected with filter retardation assays under native as well as under denaturing conditions, indicating the build-up of detergent-soluble and -insoluble cellular A β 42 aggregates (**Figure 4, C**). As A β 42 aggregates found in patient material consist of compact β -sheet structures (Masters and Selkoe, 2012), it was further analyzed, whether the resulting protein aggregate species in SH-EP cells are β -sheet rich by incubating cell lysates with the β -sheet binding dye ThT. With increasing intracellular A β 42 aggregate accumulation, ThT fluorescence intensity of cell lysates increased accordingly indicating the build-up of compact, β -sheet-rich, intracellular A β 42 aggregates. To verify that the high ThT signals in A β 42 aggregate

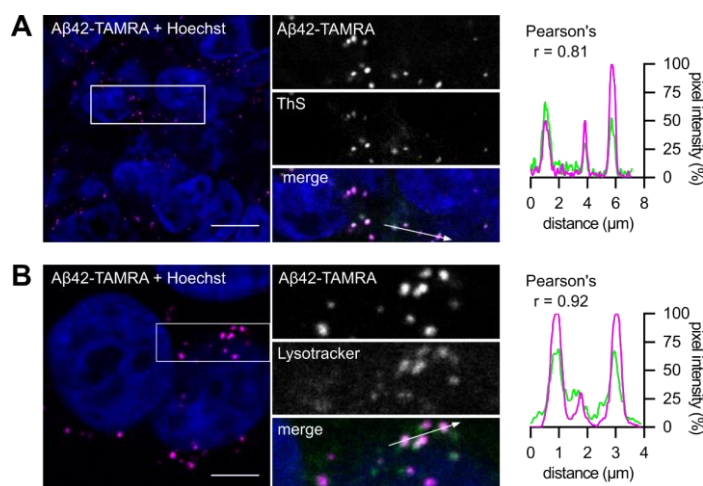


Figure 5. Intracellular A β 42 aggregates accumulate in acidic organelles. **(A)** Staining of intracellular A β 42 aggregates shows highly ThS positive puncta. Co-localization analysis of ThS and TAMRA signals confirm that TAMRA-labeled A β 42 aggregates contain β -sheet-rich amyloid peptide structures. *Scale bar: 10 μ m.* **(B)** Internalized A β 42 aggregates accumulate in acidic organelles. Aggregates strongly co-localize with the Lysotracker dye. *Scale bar: 5 μ m. Showing one representative image and co-localization analysis from multiple observations. Images were kindly provided by Simona Kostova*

containing lysates are due to ThT binding to intracellular A β 42 aggregates, it was further analyzed whether Thioflavin directly co-localizes with intracellular A β 42 aggregates in SH-EP cells. For cell culture and tissue stainings of amyloids, ThS instead of ThT is typically used (Sun et al., 2002). Therefore, cells with intracellular A β 42 were fixed, stained with ThS and analyzed for co-localization by confocal microscopy. In fact, intracellular A β 42 aggregates in the neuroblastoma cells were highly ThS-positive and strongly co-localized with A β 42-TAMRA aggregates (**Figure 5, A**). Finally, it was analyzed to which cellular compartment intracellular A β 42 aggregates localize in SH-EP cells. In pathological studies it has been observed, that protein aggregates – including A β 42 aggregates – taken up from the extracellular space mainly localize to acidic organelles (Hu et al., 2009). Thus, SH-EP cells were stained with the acidic organelle accumulating dye Lysotracker. Strong co-localization of Lysotracker fluorescence intensity with intracellular A β 42-TAMRA aggregates was observed by confocal microscopy, suggesting distinct localization of A β 42 aggregates to acidic organelles in this model system (**Figure 5, B**).

Taken together, treating neuroblastoma cells with *in vitro* preformed A β 42 aggregates

leads to the formation of SDS-stable, ThT-positive intracellular aggregates, which accumulate in acidic organelles. These characteristics resemble well the biochemical properties and spatial distribution of intracellular A β 42 aggregates found in AD patients (Masters and Selkoe, 2012). Hence, modelling the pathology of intracellular A β 42 aggregates in SH-EP cells is a suitable approach to develop a screening assay for the identification of small molecules promoting A β 42 aggregate degradation.

4.3 A β 42 aggregates are internalized through actin-dependent, lipid raft-mediated macropinocytosis

As compounds potentially identified by this screening assay should especially target intracellular A β 42 aggregates shuttling between neuronal cells, it was investigated, whether the cell model internalizes A β 42 aggregates through *in vivo* described A β 42 internalization pathways. Different mechanisms of A β aggregate uptake have been described and are discussed. Among these receptor-mediated endocytosis at lipid rafts plays a particular important role for neuronal aggregate uptake and cell-to-cell transfer (Lai and McLaurin, 2011). To assess whether lipid raft mediated uptake is involved in this neuroblastoma model system, SH-EP cells were treated with A β 42-TAMRA aggregates, fixed after 2 h of incubation and then stained with the ganglioside GM1 binding protein cholera toxin B (CTB), which marks lipid rafts on the cell surface (Blank et al., 2007). TAMRA fluorescent puncta partly co-localized with FITC-CTB, indicating binding of A β 42 aggregates to lipid rafts on the cell surface (**Figure 6, A**). Partial co-localization of A β 42 aggregates with CTB most likely resembles transient binding to lipid rafts throughout the uptake process. The receptor mediated, active endocytosis at lipid rafts is a β -actin dependent process (Head et al., 2014). To gain further evidence that this process is responsible for A β 42 aggregate uptake in this model system, I tested whether treatment with a β -actin polymerization inhibitor prevents A β 42 aggregate uptake. Therefore, neuroblastoma cells were treated with increasing concentrations of the actin-polymerization inhibitor cytochalasin D prior to A β 42 aggregate treatment and the remaining uptake was evaluated. In a concentration-dependent manner, inhibition of β -actin polymerization lead to a strong decrease in cellular A β 42 aggregate loads (**Figure 6, B**). To further pin down the A β 42 aggregate uptake mechanism, it was tested which

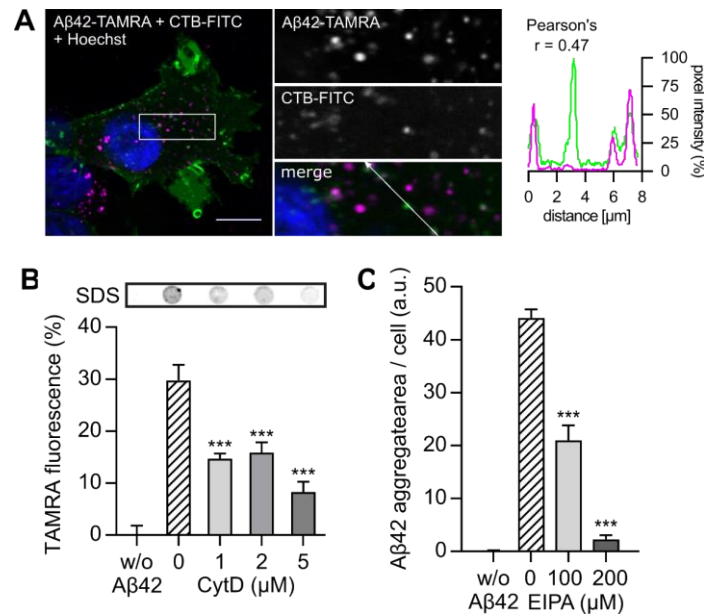


Figure 6. Aβ42 aggregate internalization via lipid-raft mediated macropinocytosis. **(A)** Confocal microscopy shows Aβ42 aggregates partly co-localizing with lipid rafts on the cell surface. SH-EP cells were treated with Aβ42-TAMRA aggregates and fixed after 2 h. Lipid rafts are stained with the ganglioside GM1 binding subunit B of cholera toxin conjugated to FITC. TAMRA and FITC fluorescence intensities were quantified along white arrow in the merged image. Fluorescent signals clearly overlap at several locations indicating Aβ42 aggregates transiently bind to lipid rafts on the cell surface. *Representative image shown with co-localization analysis using the Pearson's correlation coefficient.* **(B)** Filter retardation assays of denatured (2% SDS) lysates from SH-EP cells treated with Aβ42 aggregates and increasing concentrations of cytochalasin D (CytD) show effective uptake inhibition. TAMRA fluorescence intensities from Aβ42-TAMRA aggregates retained on the filter membrane were quantified. **(C)** Amount of intracellular Aβ42-TAMRA aggregates after pretreatment of SH-EP cells with macropinocytosis inhibitor EIPA. Internalized Aβ42 aggregate loads were quantified from total TAMRA intensities. *Depicted are the means from technical triplicates of one representative experiment. Error bars representing standard deviation. One-way ANOVA with Dunnett's post-test, *** p < 0.001.* ____

particular form of endocytosis is involved in SH-EP cells. Macropinocytosis, a form of clathrin-independent endocytosis, which mediates non-selective uptake of solute molecules and large gulps, is highly active in macrophages and dendritic cells (Bloomfield and Kay, 2016). As it has been described to be particularly involved in Aβ42 uptake

(Mandrekar et al., 2009) it was investigated whether SH-EP cells take up preformed A β 42 aggregates via this distinct pathway. Prior to A β 42-TAMRA aggregate addition to the cell culture media, SH-EP cells were treated with 5-(N-ethyl-N-isopropyl) amiloride (EIPA). This agent effectively inhibits macropinocytosis in the micromolar range (Koivusalo et al., 2010). Consequently, when increasing concentrations of EIPA were applied, an almost complete uptake inhibition of A β 42 aggregates could be observed (**Figure 6, C**).

This suggests that SH-EP cells internalize A β 42 aggregates via β -actin dependent, lipid-raft-mediated macropinocytosis – an aggregate uptake pathway, especially described to be involved in microglia-mediated clearance of A β 42, which is likely involved in propagation and cell-to-cell spreading of A β 42 aggregates (Zeineddine and Yerbury, 2015). Therefore, this neuroblastoma cell model system involves an A β 42 aggregate uptake mechanism which is highly relevant in A β 42 processing *in vivo* and thus presents a suitable cell model system to assess the effects of small molecules in promoting the degradation of A β 42 aggregate species particularly involved in this pathophysiological process.

4.4 A cell-based screening assay facilitates the identification of small molecules promoting the clearance of intracellular A β aggregates

Next, this model system was used to identify chemical compounds that influence the levels of intracellular A β aggregates. Therefore, a cell-based semi-automated screening assay was established for compound testing in microtiter plates. The principle of the assay is schematically shown in **Figure 7 A**. First, SH-EP cells are treated with preformed A β 42-TAMRA aggregates to promote the formation of intracellular aggregates. Next, the cells are washed and trypsinized to remove non-internalized A β 42 aggregates from the cell culture. The intracellular A β 42 aggregate harboring cells are then seeded into microtiter plates onto 10 μ M compound dilutions and are further incubated for 20 h. After fixation and cell nuclei staining, remaining A β 42 aggregate loads per cell are quantified using a microscopic high content fluorescence imaging system.

As a proof-of-principle study, a focused library of 20 polyphenol compounds was tested (**Figure 7, B**), since several compounds of this chemical subgroup have been shown to exhibit effects on amyloid- β aggregation *in vitro* and *in vivo* (Bieschke, 2013; Stefani and Rigacci, 2013). Among these 20 compounds, 5 significantly promoted the degradation of A β 42 aggregates, whereas 15 compounds exhibited no effects on the abundance of

intracellular A β 42 aggregates. Notably, the green tea flavonoid epigallocatechin gallate (EGCG) (**Figure 7, C**), which was previously shown to directly target preformed β -sheet-rich A β 42 aggregates and to promote their dissociation *in vitro* (Bieschke et al., 2010; Ehrnhoefer et al., 2008), exhibited the most potent effect. It reduced the intracellular A β 42 aggregate load by 56% at a concentration of 10 μ M (**Figure 7, B, C**). Two further

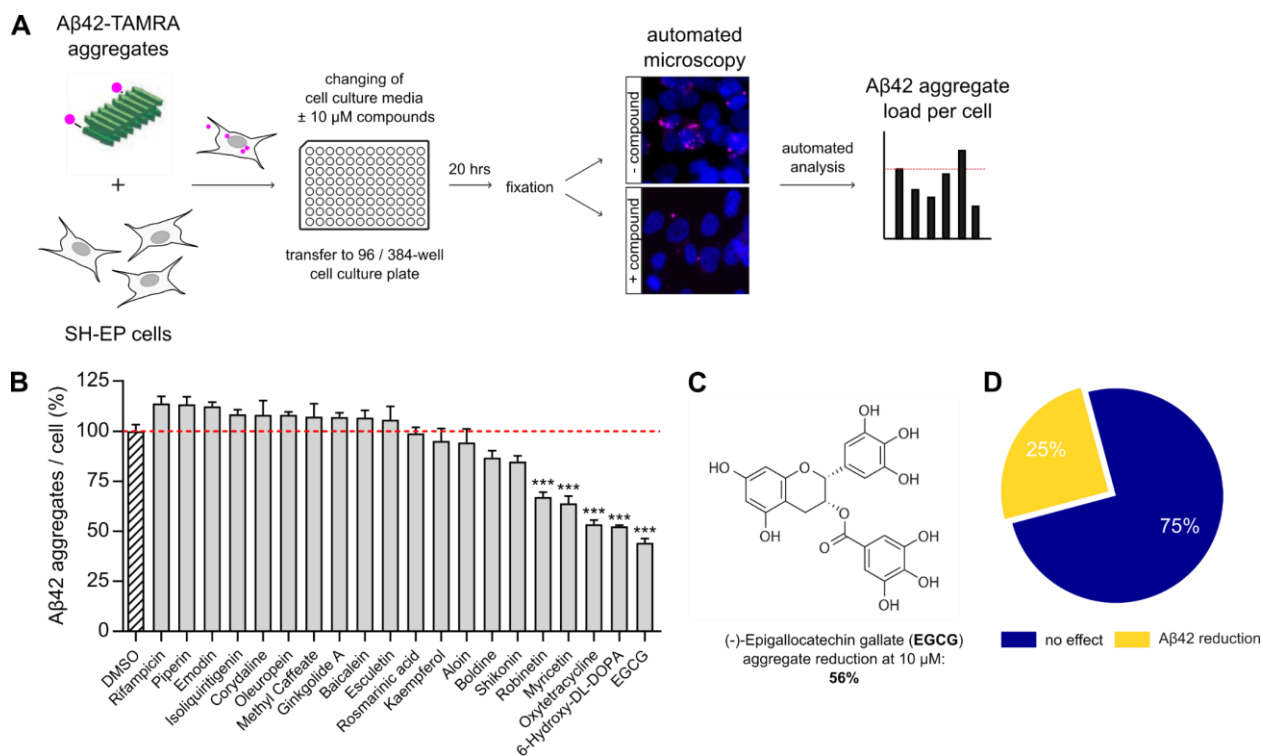


Figure 7. Cell-based screening assays identifies polyphenols increasing A β 42 aggregate degradation. **(A)** Schematic representation of the screening assay. SH-EP cells are treated with 0.6 μ M A β 42-TAMRA aggregates and incubated for 6 h. Cells are washed, trypsinized and transferred to cell-culture plates containing 10 μ M compound dilutions. After incubation for additional 20 h, cells are fixed, and A β 42 aggregate loads per cell are quantified in a high-content fluorescent imaging system. **(B)** Results from the focused library screen. A β 42 aggregate loads are quantified from total fluorescent intensities per cell and normalized to solvent control (DMSO). **(C)** Molecular structure of the most potent polyphenol – Epigallocatechin gallate (EGCG) – reducing cellular A β 42 aggregates in SH-EP cells by $56 \pm 3.6\%$ at a concentration of 10 μ M. **(D)** Summary of the effects of the aggregation-modulating compounds on intracellular A β 42 aggregate levels. 25% of the tested compounds showed a significant A β 42 aggregate reduction. *Depicted are the means of three individual experiments with error bars representing standard deviation. One-way ANOVA with Dunnett's post-test, *** $p < 0.001$.*

flavonoids were among the hit compounds: Robinetin and Myricetin (**Figure 7, B**) – two naturally occurring polyphenols which previously showed neuroprotective effects in cellular model systems of neurodegeneration (Regitz et al., 2014). Moreover, Myricetin showed potent inhibition of A β fibril formation *in vitro* (Hirohata et al., 2007) and was effective in reducing A β pathology aggregates in an AD transgenic mouse model (Hamaguchi et al., 2009). Oxytetracycline, an FDA-approved antibiotic and derivative of tetracycline, likewise strongly reduced the levels of intracellular A β 42 aggregates (**Figure 7, B**). Notably, this compound has also been shown to inhibit A β aggregate formation *in vitro* (Inbar et al., 2008) and was further described to inhibit the interaction of A β oligomers with ephrin type-B receptor 2 – a receptor tyrosine kinase important for learning and memory functions (Suzuki et al., 2016). Additionally, 6-Hydroxy-DL-DOPA, a derivative of the Parkinson drug Levodopa (Poskanzer, 1969) showed the second strongest effect reducing the abundance of intracellular A β 42 aggregates by 48%. Interestingly, dopamine itself was previously identified in a screen for A β binders and aggregation inhibitors *in vitro* (Inbar et al., 2008). Thus, the identified compounds that lead to a reduction of intracellular A β 42 aggregates *in cells* are either themselves or structurally related to *in vitro* aggregation inhibitors.

Next, the effects of EGCG on the abundance of intracellular A β 42 aggregates was assessed in independent titration experiments with increasing compound concentrations. The A β 42 decreasing effect was strongly concentration-dependent and a half maximal inhibitory compound concentration (IC₅₀) of 6.3 μ M was determined (**Figure 8, A**). To validate the reduction of cellular A β 42 aggregate loads using a different readout, additional immunofluorescence stainings with the 6E10 antibody were performed. Similar to the reduction of TAMRA fluorescent signals from A β 42 aggregates, a concentration-dependent effect on the abundance of intracellular A β 42 aggregates could be observed. However, the effects obtained with the antibody readout were slightly lower compared to the TAMRA fluorescent signals, resulting in a 6E10 IC₅₀ of 14.5 μ M compared to 6.3 μ M for TAMRA aggregate-based detection (**Figure 8, B**).

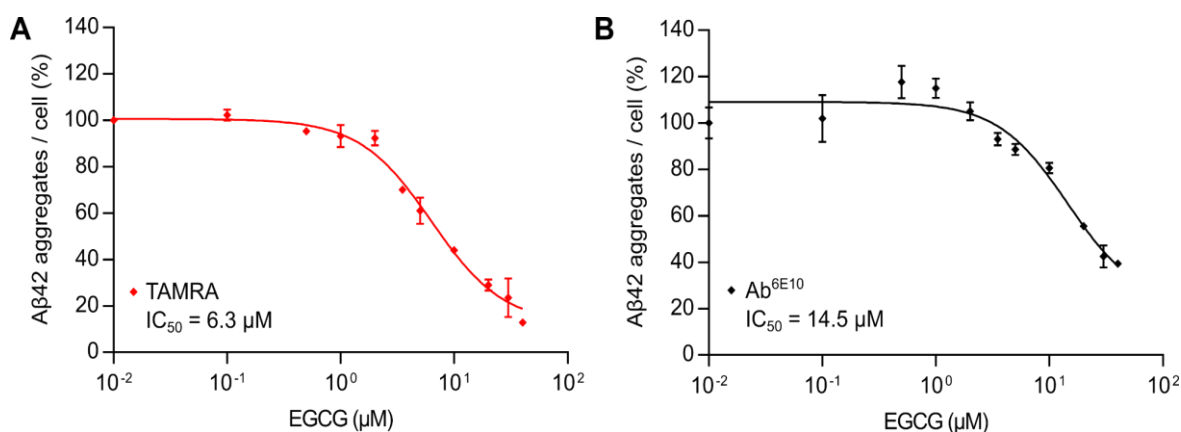


Figure 8. Titration experiment with increasing concentrations of EGCG. **(A)** Cellular Aβ42 aggregate loads were determined from total TAMRA fluorescence intensities. Data points were non-linearly fitted and an IC₅₀ value was determined at a concentration of 6.3 μM. **(B)** Validation titration experiment; Compound effects were followed by immunofluorescent staining of aggregates with the Aβ-specific antibody 6E10. EGCG-mediated promotion of cellular Aβ42 degradation is lower when quantified from antibody signals resulting in an IC₅₀ value of 14.5 μM. *Depicted data points represent means from three individual experiments with error bars representing standard deviation.* _____

This discrepancy may result from a quenching effect of EGCG on the TAMRA fluorophore. To evaluate this in detail, non-peptide coupled TAMRA fluorophores were incubated with increasing concentrations of EGCG. Here, no EGCG-mediated reduction of TAMRA fluorescence was observed (**Figure 9, A**, TAMRA fluorophore). However, there could still be an effect of EGCG on the TAMRA-fluorophore when it is incorporated into Aβ42-TAMRA aggregates as EGCG has been shown to directly bind Aβ42 aggregates *in vitro* (Ehrnhoefer et al., 2008) and thereby might accumulate in close proximity to the fluorophores. In fact, when increasing concentrations of EGCG were added to Aβ42-TAMRA peptides or preformed aggregates *in vitro*, a strong reduction of TAMRA fluorescence intensity of the aggregates could be observed (**Figure 9, A**). This could indeed resemble EGCG-mediated quenching of TAMRA fluorescence upon Aβ42 aggregate binding or – as EGCG has been shown to remodel Aβ42 aggregates into off-pathway oligomers (Lopez del Amo et al., 2012) – indicates EGCG-mediated remodeling

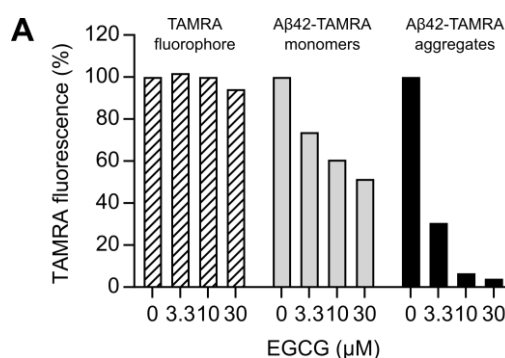


Figure 9. Analysis of the effect of EGCG on TAMRA fluorescence. **(A)** Increasing EGCG concentrations were added to non-peptide coupled TAMRA fluorophores, Aβ42-TAMRA peptide monomers and labeled Aβ42-TAMRA aggregates *in vitro*. No reduction of TAMRA fluorescent intensity on the dye itself could be detected, whereas EGCG strongly reduced TAMRA fluorescent intensities when labeled to Aβ42 peptides or incorporated into Aβ42 aggregates. ____

of Aβ42-TAMRA aggregates leading to a change in their fluorescence.

As EGCG apparently reduces TAMRA fluorescence of labeled Aβ42 aggregates itself, additional validation experiments were performed to evaluate the Aβ42 aggregate degradation promoting effect in the neuroblastoma cell model system. In these experiments, the abundance of intracellular Aβ42 aggregates after EGCG treatment were additionally analyzed by filter retardation assays. When lysates from EGCG treated SH-EP cells were filtered through a membrane to quantify cellular aggregates, they likewise showed a strong reduction in cellular Aβ42 aggregate loads. This could be observed from Aβ-specific antibody signals (4G8) retained on filter membranes as well as when measuring the fluorescent intensities of retained TAMRA-labeled aggregate species. **(Figure 10, A, w/ Aβ42)**. As control, increasing EGCG concentrations were added to SH-EP cells, which did not contain intracellular Aβ42 aggregates. Here, the detected background signals from cell lysates was not changed – neither from TAMRA nor from antibody signals **(Figure 10. w/o Aβ42)**. Taken together, these experiments showed that the established assay is suitable for the screening of small molecules, which can promote the degradation of preformed intracellular Aβ42 aggregates. With the assay, five compounds that significantly decrease the abundance of intracellular Aβ42 aggregates

were identified, of which EGCG showed the strongest effect. Furthermore, IC_{50} values for the most potent hit compound EGCG (TAMRA: $6.3 \mu\text{M}$; 6E10-antibody: $14.5 \mu\text{M}$) were

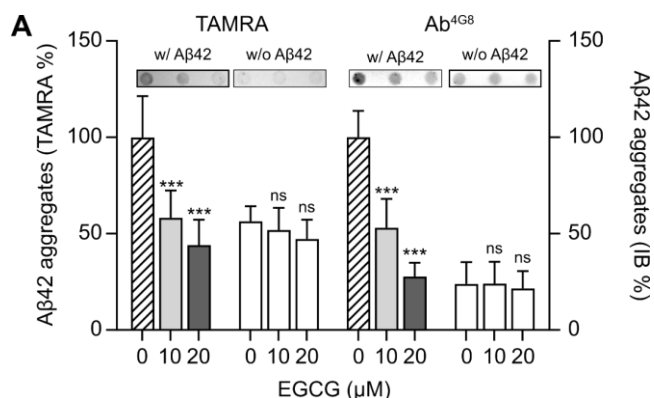


Figure 10. Validation of EGCG-mediated A β 42 aggregate degradation. **(A)** Filter retardation assays of native protein extracts (NP40) from SH-EP cells confirm A β 42 aggregate degradation promoting effect of EGCG. In the left panel, total TAMRA fluorescent intensities are quantified – on the right, cellular A β 42 aggregates retained on filters are detected with the A β -specific antibody 4G8. *Depicted bars represent means from three individual experiments with error bars showing standard deviation. One-way ANOVA with Dunnett's post-test, *** $p < 0.001$. ____*

determined and the EGCG-mediated effects could be validated using independent biochemical readouts. This validation is of critical importance as a direct effect of the compound molecule on the assay readout – as TAMRA fluorescence intensity here – must be excluded.

4.5 EGCG-mediated degradation mitigates A β 42 seeding activity and rescues A β 42-induced toxicity

As intracellular A β 42 aggregates might be highly relevant in disease progression and – when spreading from cell-to-cell – were shown to seed A β aggregation of soluble A β peptides in pathologically unaffected neuronal cells (Sowade and Jahn, 2017; Ziegler-Waldkirch et al., 2018), it was evaluated whether an EGCG-mediated decrease of intracellular A β 42 aggregates influences their seeding activity. Therefore, SH-EP cells with intracellular A β 42 aggregates were treated with or without $30 \mu\text{M}$ EGCG and cell extracts were analyzed for their A β seeding activity. To exclude that residual EGCG in cell extracts and not its degradation promoting effect influences seeding activity, additionally non-A β 42 aggregate containing cells were treated with or without EGCG as

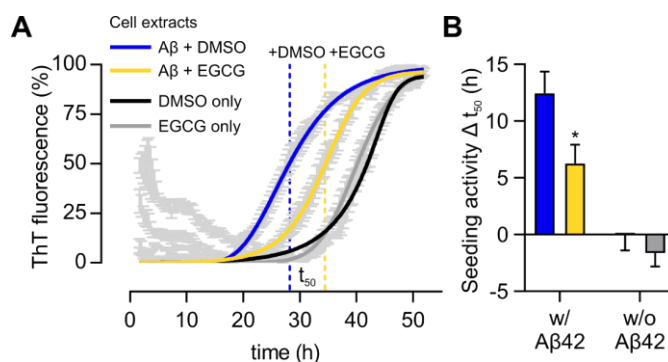


Figure 11. Seeding activity of cell extracts from SH-EP cells with intracellular A β 42 aggregates. **(A)** Addition of cell extracts from SH-EP cells treated with or without 30 μ M EGCG for 20 h. Intracellular A β 42 aggregates accelerate spontaneous A β 42 aggregation, whereas treatment with EGCG significantly reduced this seeding effect. Residual EGCG from cell extracts (EGCG only) shows no effect on spontaneous A β 42 aggregation. **(B)** Quantification of seeding activity from the Δt_{50} values. Intracellular A β 42 aggregate containing SH-EP cell extracts accelerated spontaneous A β 42 aggregation by \sim 12 h. EGCG treatment reduced this acceleration by \sim 6 h (\sim 50%). Bars show mean of one representative experiment performed in technical triplicates. Error bars representing standard deviation. Student's *t*-test, * $p < 0.05$. ____

a control. After 20 h of compound or solvent control incubation, cells were lysed and the cell extracts' seeding activity was investigated. Therefore, cell extracts were added to *in vitro* A β 42 aggregation reactions, which were then monitored over time by quantification of ThT fluorescence intensities. For quantification of seeding activity, A β 42 aggregation kinetics were non-linearly fitted and time points were calculated, where the half-maximal ThT intensity was reached (t_{50}). Seeding activity of cell extracts was quantified from the shift of the t_{50} time point (Δt_{50}) in relation to unseeded aggregation reactions. Expectedly, the addition of cell extracts harboring intracellular A β 42 aggregates exhibited a significant seeding effect on spontaneous A β 42 aggregation *in vitro* by shortening the lag phase and accelerating the aggregation process (+DMSO, **Figure 11, A**). When extracts from SH-EP cells treated with 30 μ M EGCG (+ EGCG, **Figure 11, A**) were analyzed with *in vitro* seeding assays, they showed a significantly reduced seeding activity compared to DMSO treated samples. In the control experiments, no effect of residual EGCG in cell extracts on spontaneous A β 42 aggregation could be observed (**Figure 11, B**).

Whether the reduction of intracellular A β 42 aggregates or an additional compound-induced aggregate modification accounts for the observed reduction in seeding activity

remains unclear. However, these results clearly demonstrate that treatment of cells containing intracellular A β 42 aggregates with A β 42 degradation promoting compounds such as EGCG, is able to mitigate the cell extracts' seeding-activity and might therefore be a promising approach to impede seeding and spreading of A β aggregates.

Next, it was investigated whether the EGCG-mediated reduction of intracellular A β 42 aggregates does rescue A β 42-induced toxicity. As intracellular, proteotoxic A β aggregates have been described to compromise physiological cellular functions and to decrease mitochondrial metabolism (Liu and Schubert, 2002), the MTT (3-(4,5-dimethylthiazol-2-yl)-2,5-diphenyltetrazolium bromide) assay was utilized to examine whether EGCG treatment influences mitochondrial metabolic activity of SH-EP cells after treatment with A β 42 aggregates. Addition of 1 μ M preformed A β 42 aggregates to the cell culture medium of SH-EP cells did lead to a decline in their mitochondrial metabolic activity. However, when cells were treated with increasing concentrations of EGCG, the proteotoxic effect of A β 42 aggregates could be significantly rescued in a concentration-dependent manner (**Figure 12, A**). As hippocampal neurons are one of the most affected

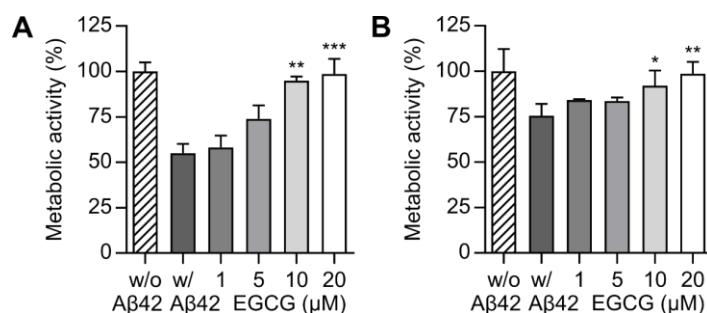


Figure 12. EGCG treatment rescues A β 42-induced toxicity. **(A)** A β 42 aggregate treatment affects mitochondrial metabolic activity of SH-EP cells, which can be rescued by treating cells with increasing concentrations of EGCG. 1 μ M of A β 42 aggregates added to cell culture medium strongly reduce mitochondrial metabolic activity indicated by a decreased MTT reduction capacity of the SH-EP cell pool. Treatment with the polyphenol EGCG counteracts A β 42 induced toxicity in a concentration-dependent manner; addition of 10 and 20 μ M compound significantly improves mitochondrial metabolic activity **(B)** Mitochondrial metabolic activity of rat hippocampal neurons is accordingly impaired when neurons are treated with 1 μ M of A β 42 aggregates. Addition of 10 and 20 μ M EGCG likewise significantly restores metabolic impairment. *Bars show mean of three individual experiments with error bars representing standard deviation. One-way ANOVA, * $p < 0.05$, ** $p < 0.002$, *** $p < 0.001$.* _____

cell populations in patients suffering from AD (West et al., 1994), it was further tested whether similar effects of EGCG treatment could be observed with primary neuronal cultures prepared from rat hippocampi. Adding *in vitro* preformed A β 42 aggregates to the cell culture medium resulted in an impairment of neuronal mitochondrial activity (w/ A β 42, **Figure 12**, B). Notably, when hippocampal neurons were treated with EGCG, A β 42-induced toxicity could also be reproducibly rescued in a concentration dependent manner (**Figure 12**, B).

The results from the seeding and toxicity experiments show that EGCG treatment not only decreases the abundance of intracellular A β 42 aggregates, but is additionally able to reduce their cellular seeding-activity and furthermore can rescue A β 42-mediated toxicity by restoring A β 42-induced mitochondrial impairment.

4.6 Intracellular A β 42 aggregates accumulate in lysosomes and the EGCG-mediated effect is dependent on lysosomal enzyme activity

As EGCG-mediated reduction of intracellular A β 42 aggregates seems to be an effective approach to reduce their cellular seeding activity and toxicity, it was next investigated how this effect is mechanistically exhibited. Therefore, the exact localization of intracellular A β 42 aggregates in SH-EP cells was first analyzed in detail. *In vivo*, A β 42 aggregates are mainly detected in multivesicular bodies, which include early endosomes, late-endosomes and lysosomes (Takahashi et al., 2002). To assess the subcellular localization of internalized A β 42 aggregates in SH-EP cells, markers of different cellular compartments of the endosomal-lysosomal trafficking pathway and the cellular A β processing process (Fukuda, 1991) were fluorescently stained and co-localization with TAMRA-labeled A β 42 aggregates was analyzed in confocal microscopy. As it was of main interest to elucidate where the intracellular A β 42 aggregates accumulate, when the cells are treated with compounds, their localization was investigated 6 h after aggregate addition. In fact, it was found that in neuroblastoma cells at this time point, actively internalized A β 42 aggregates partially co-localized with the early endosome marker EEA1 (**Figure 13**, A), but mainly co-localized with the late endosome and lysosome-associated membrane protein 2 (LAMP2) (**Figure 13**, B). Lysosomes have been widely described to be the major compartment for degradation of misfolded proteins and protein aggregates composed of α -synuclein, huntingtin, tau and A β (R.A. Nixon, 2013). This suggests that the EGCG-mediated A β 42 aggregate degradation promoting effect is exhibited when the

aggregates have already accumulated in the lysosome.

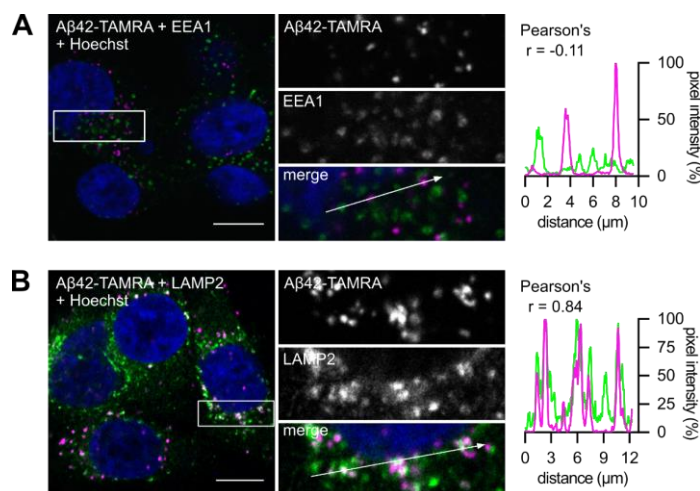


Figure 13. Co-localization of internalized Aβ42-TAMRA aggregates with lysosomal markers. **(A)** Co-localization analysis with the early-endosome marker EEA1 shows no or only very partial co-localization 6 h after Aβ42 aggregate treatment. **(B)** Clear co-localization with the lysosome-associated membrane protein 2 (LAMP2) after 6 h of Aβ42 aggregate uptake. Scale bars: 20 μm. Showing representative image sections from confocal microscopy of multiple co-localization events. Correlation coefficient Pearson's *r* depicted. Images were kindly provided by Simona Kostova. ____

As autophagy – a major cellular pathway for degradation of misfolded proteins and protein aggregates – forms autophagosomes, which subsequently fuse with lysosomes (Menzies et al., 2015) and even EGCG itself has been reported to stimulate autophagy (Lee et al., 2015; Zhou et al., 2014), it was investigated whether the EGCG-mediated effect is dependent on autophagic activity. Therefore, a mouse embryonal fibroblast (MEF) cell line lacking the ATG5 protein – a key regulator of autophagy (Kishi-Itakura et al., 2014) – was used to test, whether the EGCG-mediated effect relies on active autophagy. Interestingly, the EGCG-mediated promotion of Aβ42 aggregate degradation was reduced in autophagy deficient MEFs in comparison to wildtype cells. EGCG was significantly less efficient in promoting intracellular Aβ42 aggregate degradation in ATG5 knockout cells (**Figure 14, A**).

As intracellular Aβ42 aggregates taken up by neuroblastoma cells mainly accumulated in lysosomes – the common endpoint of endocytosis and autophagy (Ganley et al., 2011), it was further evaluated whether lysosomal enzyme activity is required for the observed EGCG-mediated effect on Aβ42 aggregates. Therefore, SH-EP cells were treated with

inhibitors of lysosomal enzyme activity and increasing concentrations of EGCG and then intracellular A β 42 aggregate loads were evaluated. Bafilomycin A1 – a potent inhibitor of the ATP-dependent proton pump V-ATPase within the lysosomal membrane – prohibits acidification of the lysosome and thereby reduces lysosomal enzyme activity (Mauvezin

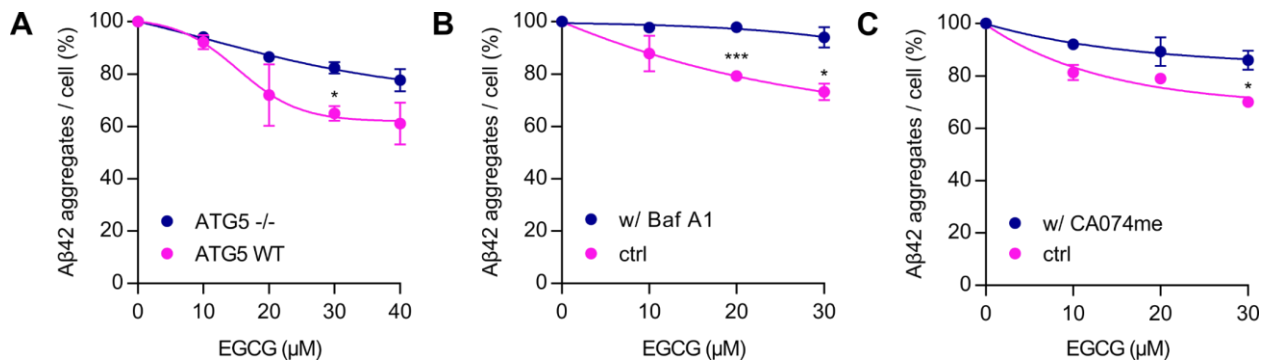


Figure 14. EGCG-mediated promotion of cellular A β 42 degradation is dependent on autophagy and lysosomal enzyme activity. **(A)** ATG5 knockout MEFs show less EGCG-mediated reduction of cellular A β 42 aggregate levels when compared to the effect in wildtype MEFs. **(B)** Inhibition of lysosomal acidification and autophagosome-lysosome fusion with Bafilomycin A1 does almost completely abrogate EGCG-mediated A β 42 aggregate degradation in SH-EP cells. **(C)** Solely inhibiting the lysosomal enzyme cathepsin B using a specific inhibitor (CA074me) does reduce the EGCG-mediated effect in the SH-EP cell model. *A β 42 aggregates were quantified from total intensity of 6E10-antibody signals per cell. Data points show mean of two or three individual experiments with error bars representing standard deviation. Student's t-test was used for statistical analysis comparing wildtype or untreated with knockout or inhibitor treated cells, * $p < 0.05$, *** $p < 0.001$.* ____

and Neufeld, 2015). When SH-EP cells harboring intracellular A β 42 aggregates were additionally treated with Bafilomycin A1, EGCG was no longer able to promote cellular aggregate degradation (**Figure 14, B**). It was further tested, whether lysosomal enzymes previously described to be able to degrade amyloid aggregates, were involved in this process. Within the lysosome, mainly a family of cysteine proteases – cathepsins – have been shown to be able to degrade aggregated A β 42 peptides (Nixon et al., 2001). Especially the family member cathepsin B (CatB) came to attention as it is tightly regulated by cystatin C, of which a polymorphism is linked to an increased risk for AD (Sun et al., 2008). Furthermore, cathepsin B was described to degrade cellular A β 42 aggregates (Mueller-Steiner et al., 2006). Consequently, it was tested whether treating

SH-EP cells with a selective cathepsin B inhibitor influences the EGCG-mediated degradation effect. In fact, only inhibiting this single cathepsin family member was sufficient to reduce the EGCG-mediated effect (**Figure 14, C**).

Taken together, these results clearly show that the EGCG-mediated increase of cellular A β 42 aggregate degradation is dependent on ATG5-related autophagy and is in particular dependent on lysosomal degradation as it can be completely blocked by inhibiting lysosomal enzyme activity.

4.7 EGCG treatment increases maturation of Cathepsin B and boosts lysosomal enzyme activity

As it has been previously reported that EGCG is able to increase acidification of lysosomes (Zhong et al., 2015), this effect might be responsible for an increased A β 42 aggregate degradation in neuroblastoma SH-EP cells. On the one hand, the optimal enzyme activity of CatB is at pH ~6 (Almeida et al., 2000), whereas on the other hand, activation of CatB via enzymatic cleavage of its pro-enzyme is increased at low pH (Pungerčar et al., 2009). To first investigate whether EGCG has an influence on CatB expression and maturation, SH-EP cells were treated with increasing concentrations of EGCG and Bafilomycin A1 as a negative control and cell lysates were analyzed by

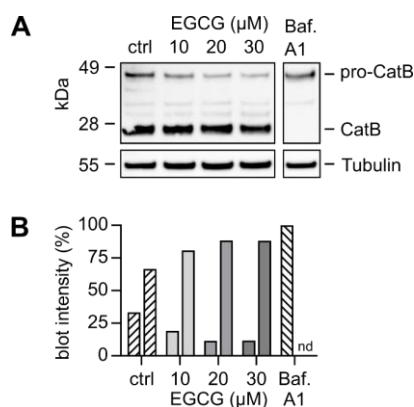


Figure 15. EGCG treatment increases CatB maturation. **(A)** CatB-specific antibody detects pro-CatB (46 kDa) and the heavy chain of the mature CatB isoform (25 kDa) in SH-EP cells harboring intracellular A β 42 aggregates. Increasing EGCG concentrations positively affect CatB maturation, whereas Bafilomycin A1 completely inhibits maturation of the pro-enzyme. **(B)** Quantification of A. EGCG treatment leads to a decrease of pro-CatB and increases maturation of CatB, whereas no mature CatB could be detected when lysosomal acidification was inhibited with Bafilomycin A1. *Bars show signal intensities of pro-CatB and CatB normalized to loading control.* ____

Western blotting for CatB expression. For detection of the enzyme, a CatB specific antibody was used, which is able to recognize the pro-enzyme as well as the matured, active isoform (**Figure 15, A**). Whereas treatment with Bafilomycin A1 did completely prevent the maturation of CatB, reduced levels of the pro-enzyme and increased CatB maturation could be observed in EGCG-treated SH-EP cells. Total CatB levels stayed relatively stable (**Figure 15, B**). Next, it was investigated, whether the increase in CatB maturation does in fact lead to an increased cellular enzymatic activity. For this, a fluorescence-quenched CatB substrate (Z-R-R-AMC) was used, which – when cleaved by CatB between its arginine residues – becomes released and unquenched. With this assay, a potential EGCG-induced increase of enzymatic CatB activity can be quantified from the increasing AMC fluorescence intensity over time. SH-EP cells were treated with increasing concentrations of EGCG, Bafilomycin A1 and the CatB inhibitor CA074me and were subsequently lysed and analyzed for CatB enzyme activity. The fluorescent CatB substrate was finally added to SH-EP cell lysates and CatB enzyme activity was quantified. EGCG treatment of neuroblastoma cells did result in an increased enzymatic activity of CatB in the cell lysate. In contrast, in the control samples, where lysosomal activity was inhibited and where EGCG-mediated promotion of A β 42 degradation is

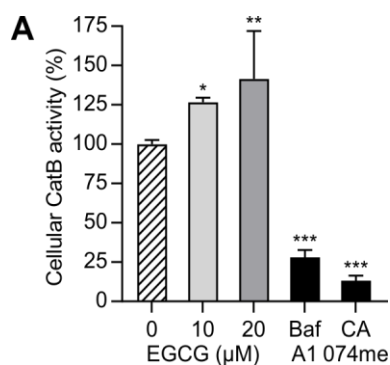


Figure 16. EGCG treatment increases CatB enzyme activity in SH-EP cells. **(A)** Cleavage of the CatB-specific fluorescent substrate by SH-EP cell lysates. Treatment of living cells with 10 or 20 μM EGCG significantly increase their lysates' CatB enzyme activity. As control, SH-EP cells were treated with Bafilomycin A1 or the CatB inhibitor CA074me which resulted in a strong reduction of substrate turnover. *Bars show means from two individual experiments, error bars represent standard deviation, * $p < 0.05$, ** $p < 0.002$, *** $p < 0.001$.* _____

strongly reduced, the CatB activity was almost completely abolished (**Figure 16**, A).

4.8 *In-cell* potency of EGCG and structural related derivatives strongly correlates with modulation of A β 42 aggregation *in vitro*

It has been previously shown that EGCG and related structural derivatives of the catechin family inhibit misfolding and aggregation of amyloid- β , α -synuclein, transthyretin and other aggregation-prone, disease-associated proteins *in vitro* (Bieschke et al., 2010; Ferreira et al., 2011). Furthermore, it was shown that EGCG remodels mature A β 42 fibrils into SDS-resistant, off-pathway oligomers. Therefore, apart from increasing lysosomal enzyme activity in SH-EP cells, a direct effect of EGCG on intracellular A β 42 aggregates might promote their degradation in cells. To test this hypothesis, first EGCG and structural related derivatives were analyzed for their effects on preformed A β 42 aggregate degradation in the established cellular compound screening assay. Then, it was further assessed, whether derivatives promoting cellular degradation are also modulators of A β 42 aggregation *in vitro*.

After treatment of cells with EGCG derivatives (10 μ M) for 20 h, total aggregate loads per cell were quantified and compared to untreated controls (**Figure 17**, A). I found that unmodified EGCG represented the most potent compound reducing the intracellular A β 42 aggregate levels by >50% as observed in the previous experiments (**Figure 8**, A). Interestingly, removal of hydroxyl groups from the gallate ring led to a strong reduction of *in-cell* potency. For dihydroxybenzoate derivatives where only one hydroxyl group was removed from the gallate group, still a robust aggregate decreasing effect could be measured – nearly as potent as EGCG. Derivatives with only a single hydroxyl group on the gallate moiety though, were not sufficient to exhibit an effect in the cell model system. As hydroxyl groups on EGCG undergo fast oxidation by forming ketones (Palhano et al., 2013), additional fluorbenzoate derivatives were synthesized. Presumably these compounds are protected from oxidation, but should show similar binding properties as hydroxyl groups. Interestingly, a single fluorbenzoate EGC derivative (EGC-3-FB) was still – yet less potently – promoting the degradation of cellular A β 42 aggregates. Comparing the potency of the 3,4,5-trihydroxyphenyl chromane with 3,4-dihydroxyphenyl chromane derivatives additionally shows the importance of the third hydroxyl group in the

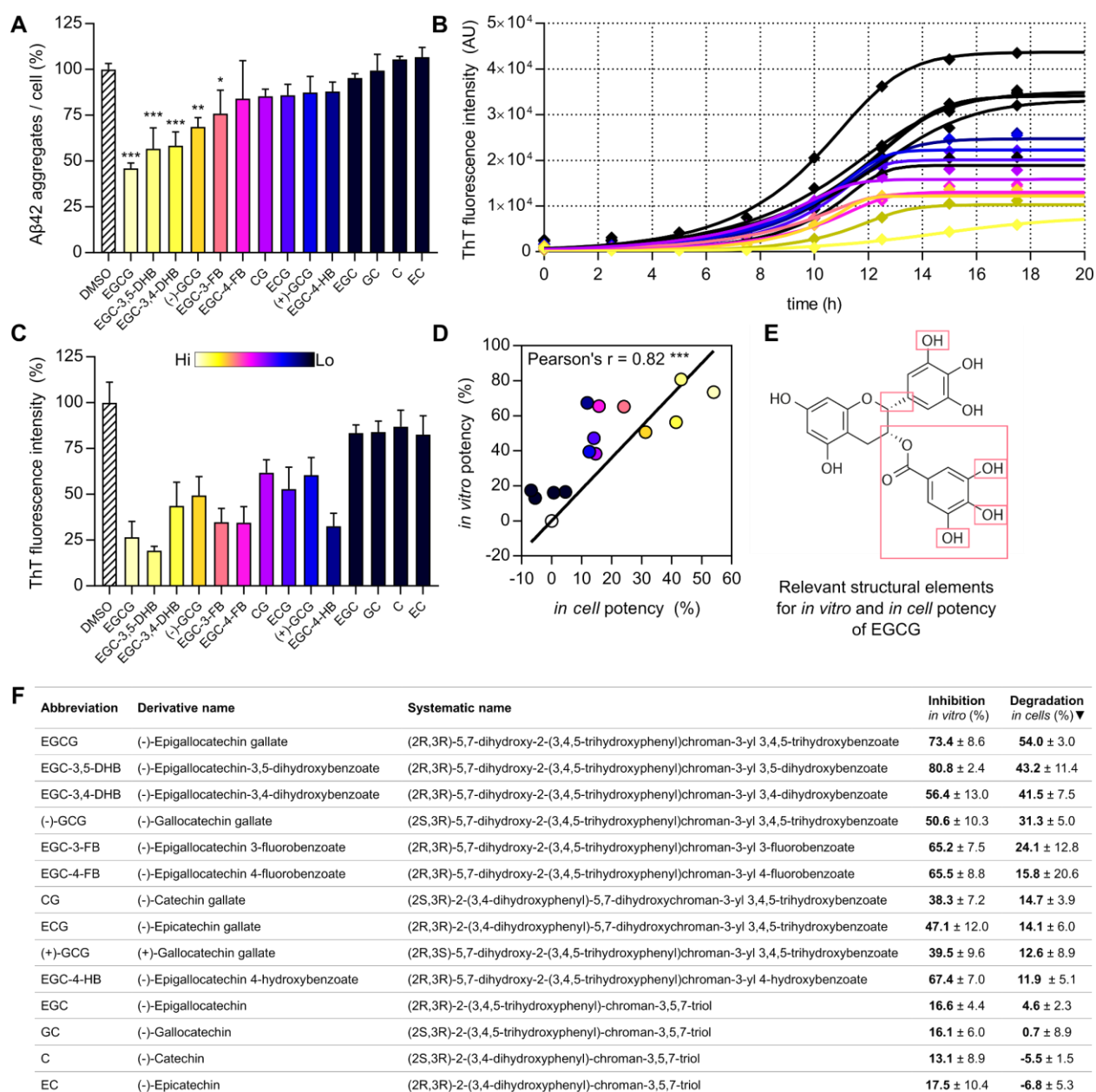


Figure 17. EGCG derivatives' *in cell* potency correlates with *in vitro* A β 42 aggregation inhibition. **(A)** Cellular A β 42 aggregate levels 20 h after treatment with 10 μ M EGCG or structural derivatives. EGCG and four derivatives significantly promote degradation of intracellular A β 42 aggregates. **(B)** Spontaneous aggregation of 10 μ M A β 42 peptides in the presence of equimolar amounts of EGCG or derivative monitored by ThT fluorescence. **(C)** Quantification of B shows inhibition of spontaneous A β 42 aggregation or competitive binding to A β 42 aggregates of EGCG and derivatives with ThT. **(D)** Pearson correlation of derivatives' *in vitro* and *in cell* potency. **(E)** Structure of EGCG. Framed moieties are relevant for potency. **(F)** Overview of derivatives and their effects. Bars show mean of two or three individual experiments, error bars indicate standard deviation. Values in percent were normalized to solvent treated control samples. Statistical analysis: One-way ANOVA and Pearson's Correlation Coefficient, * $p < 0.05$, ** $p < 0.002$, *** $p < 0.001$.

phenyl group for *in cell* potency and is in line with the stronger effects observed for gallo catechol derivatives over catechins on *in vitro* aggregation effects observed for gallo catechol derivatives over catechins on *in vitro* aggregation (Bieschke et al., 2010).

Interestingly, the stereochemical orientation is additionally important for compound activity. When comparing the activities of EGCG, (-)-GCG and of (+)-GCG, the epi-orientation clearly shows to exhibit a stronger degradation promoting effect *in cells* (**Figure 17, A, C, E**).

To investigate whether the observed compound effects *in cells* correlate with their *in vitro* effects on A β 42 aggregation, the compounds were additionally investigated in a Thioflavin T (ThT) binding assay. Soluble A β 42 peptides were incubated in the presence or absence of equimolar concentrations of EGCG or EGCG derivatives, and the spontaneous formation of A β 42 aggregates was followed by quantification of ThT fluorescence intensity (**Figure 17, B**). For quantification of the A β 42 aggregation modulating effect, the maximally reached ThT signal intensity compared to untreated control aggregation reactions was quantified. It was found that structural modification of EGCG shows a clear effect on its inhibition of A β 42 aggregation *in vitro* (**Figure 17, C**). Interestingly, derivatives which showed an A β 42 aggregation inhibiting effect, lead to a reduction of A β 42 aggregates *in cells*. However, it is important to mention that observing a compound effect on ThT fluorescence intensity in A β 42 aggregation studies *in vitro* can originate from different events: from an actual reduction in the formation of β -sheet rich A β 42 aggregates or, from competitive binding of the compound and ThT to β -sheet rich structures. Furthermore, a compound-mediated reduction of ThT intensity in A β aggregation studies does indicate a direct interaction of the compound molecule with A β 42 aggregates *in vitro*. Interestingly, EGCG derivatives, which were potent promoters of A β 42 aggregate degradation in cells, did also exhibited a strong modulation of A β 42 aggregation *in vitro*. However, the fluorobenzoate derivatives EGC-3-FB and EGC-4-FB, which presumably do not undergo spontaneous oxidation and therefore are more stable molecules, showed stronger effects *in vitro* than in cells. This discrepancy might result from a decreased ability to overcome the cellular membrane and spontaneous hydroxyl group oxidation on EGCG into ketones might be beneficial for its biological activity, while not being detrimental for its potency. To further analyze whether the observed compound effects on intracellular A β 42 aggregates and the effects observed *in vitro* on A β 42 aggregation are correlated, a statistical analysis of the obtained datasets was performed. Interestingly,

I found that the effects of EGCG and its closely related derivatives on A β 42 aggregation *in vitro* are strongly correlated with the ability of the compounds to promote aggregate degradation *in cells*. The direct effect on A β 42 aggregation of EGCG and related derivatives strongly correlates with their ability to promote aggregate degradation *in cells* (**Figure 17, D**). This suggests that besides the EGCG-mediated stimulation of lysosomal enzyme activity in cells, its ability to directly modulate the formation of A β 42 aggregates may be responsible for promoting cellular A β 42 aggregate degradation.

4.9 EGCG directly targets intracellular A β 42 aggregates

In order to evaluate, whether EGCG is capable of directly targeting intracellular A β 42 aggregates, our collaborators first synthesized a biotin-coupled EGCG derivative for aggregate-compound co-localization studies in mammalian cells. Linkage was performed at the 3-hydroxyl group of the gallate moiety, fusing it to a single hydroxybenzoate EGCG derivative (**Figure 18, A**). Treatment of intracellular A β 42 aggregate harboring SH-EP cells with this EGCG-Biotin derivative and subsequent staining with a Streptavidin-Cy5 fluorescent dye, did not result in any specific accumulation of fluorescence at A β 42-TAMRA labeled aggregates (**Figure 18, B**). However, the compound EGC-4-HB, which lacks two hydroxyl groups on the gallate moiety was also not able to promote the degradation of intracellular A β 42 aggregates (**Figure 17, A**). Thus, the absence of any co-localization with the EGCG-Biotin derivative, might have simply resulted from the fact, that the basic molecular structure used for this experiment was not optimal to interact with A β 42 aggregates. Therefore, using click-chemistry (Kolb et al., 2001) an additional fluorescently labeled EGCG derivative was synthesized (EGCG-Rhodamine B), in which the rhodamine B fluorophore was coupled at the gallate group that still harbors two additional hydroxyl groups (**Figure 17, C**). To control for unspecific binding of the linker or dye itself, additionally a compound consisting of the rhodamine B dye, the ethylene glycol linker and the gallate group was generated (**Figure 17, E**). As TAMRA and Rhodamine B highly overlap in their fluorescent spectrum and are therefore unsuitable for co-localization studies, HiLyte™ Fluor 488 labeled A β 42 (A β 42-HiLyte) aggregates were prepared and added to mammalian cells. Strikingly, when SH-EP cells treated with the EGCG-Rhodamine B derivative were subsequently analyzed by confocal microscopy, a clear co-localization of the compound and intracellular A β 42-HiLyte aggregates could be detected (**Figure 17, D**). Most notably, when correlating HiLyte and Rhodamine B fluorescent intensities in representative image sections, a strong correlation was

detectable by calculating Pearson's Correlation Coefficients (**Figure 18**, D, i., ii.). In contrast, the treatment of cells with the control compound (Linker-Rhodamine B) (**Figure 18**, E), did not result in any Rhodamine B accumulation at A β 42 aggregates and only showed a very poor correlation of signal intensities (**Figure 18**, F). This indicates that the observed binding of EGCG to intracellular A β 42 aggregates is highly specific. Thus, the ability of EGCG to directly target and dissociate intracellular aggregates might be responsible for the observed, strong aggregate degradation promoting effect *in cells*.

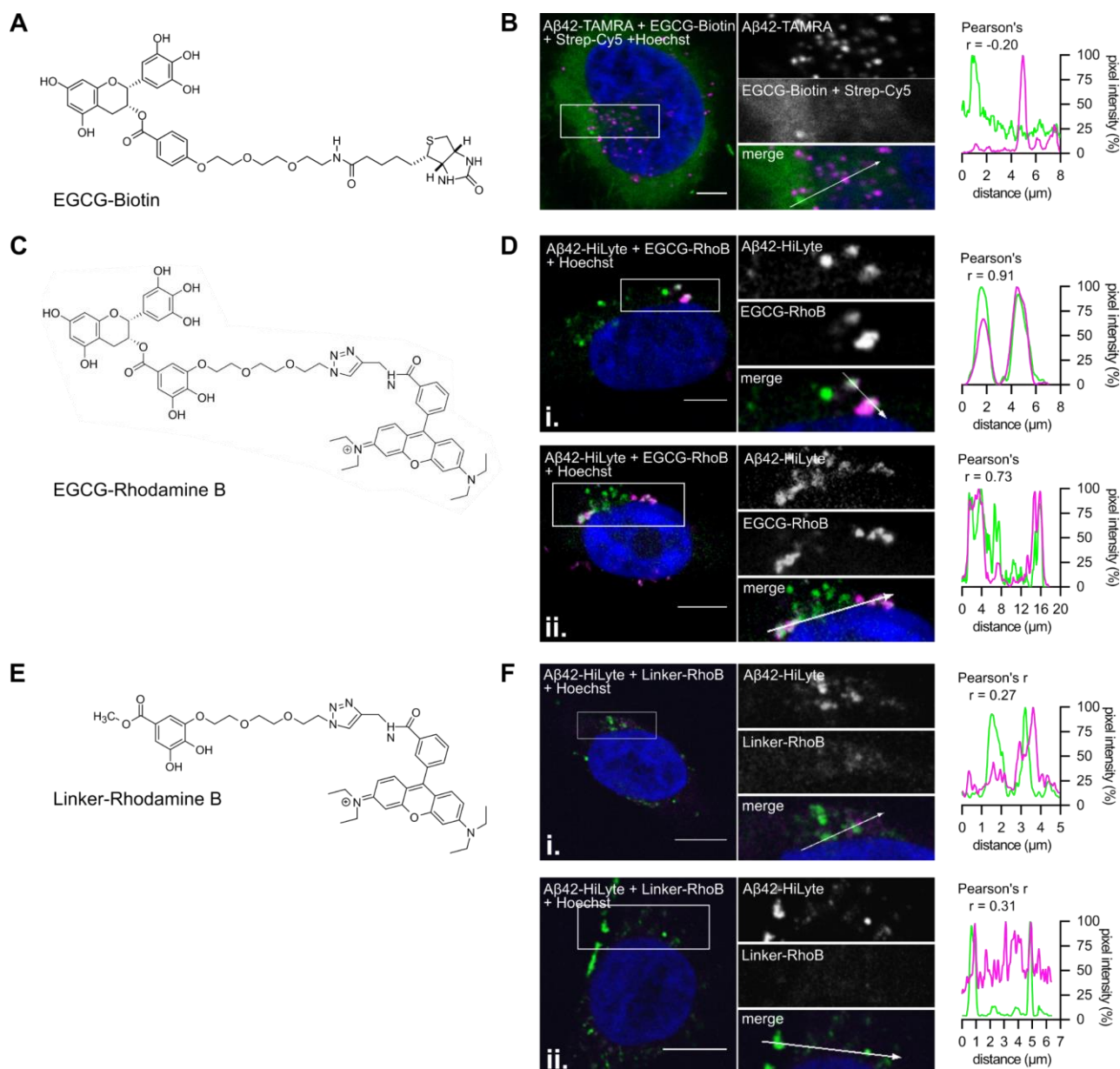


Figure 18. EGCG derivatives for cellular co-localization studies in SH-EP cells. **(A)** Biotin-labeled EGCG derivative lacking two hydroxyl groups at the former gallate ring. **(B)** EGCG-Biotin counterstained with Streptavidin-Cy5 shows strong background signal in confocal microscopy. Sporadic Cy5 fluorescence clustering does not co-localize with intracellular Aβ42-TAMRA aggregates (Pearson's $r = -0.20$). **(C)** Rhodamine B coupled EGCG derivative with ethylene glycol linker synthesized using click chemistry. **(D)** Representative image sections show clear co-localization of Aβ42-HiLyte aggregates with enrichment of rhodamine fluorescence from EGCG-Rhodamine B derivative (Pearson's $r = 0.91$ (i.) and 0.73 (ii.)). **(E)** Rhodamine B control derivative with gallate group, ethylene glycol linker and fluorescent dye. **(F)** No detectable enrichment of Rhodamine B control derivative (Pearson's $r = 0.27$ and 0.31). *Representative images and image sections from two individual experiments shown. Scale bars: 5 μm .* _____

4.10 EGCG-mediated remodeling of A β 42 aggregates facilitates cleavage through the lysosomal enzyme Cathepsin B

Considering that EGCG directly targets intracellular A β 42 aggregates (**Figure 18**) and is known to induce the formation of off-pathway A β 42 aggregates (Ehrnhoefer et al., 2008), it was obvious to ask whether these A β 42 aggregate species undergo more efficient lysosomal cleavage and degradation. To test this, structural remodeling of A β 42 peptides and aggregates into off-pathway aggregate species was induced by adding EGCG to A β 42 aggregates and the CatB cleavage efficiency of the generated A β 42 substructures was analyzed. To first outline that EGCG directly increases CatB activity *in vitro* by enhancing its enzymatic activity in a cell-free environment, the effect of EGCG on the turnover of the chromogenic, CatB specific substrate z-Arg-Arg-amino-4-methylcoumarin (Z-R-R-AMC) was analyzed. As a positive control, the CatB inhibitor CA074 was added – the unestered equivalent of CA074me, which was used in the cell-based assay – to inhibit CatB enzyme activity. CatB substrate turnover was then followed by monitoring AMC fluorescence intensity by cleavage between the arginine residues of Z-R-R-AMC (**Figure 19, A**). For quantification, the turnover rates per minute in the early exponential phase were calculated for each reaction. Whereas expectedly, the CatB inhibitor CA074 significantly reduced CatB enzymatic activity, no direct effect of EGCG on AMC turnover

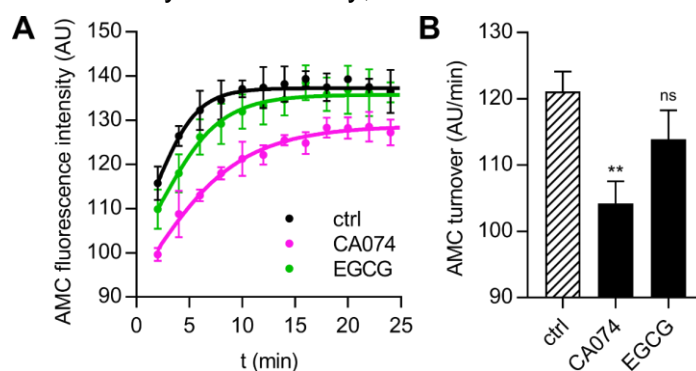


Figure 19. Enzymatic cathepsin B activity *in vitro* is not modulated by EGCG at assay concentrations. **(A)** CatB substrate turnover in presence of EGCG, CatB inhibitor CA074 and solvent control measured by increasing AMC fluorescence over time. **(B)** Quantification of substrate turnover per minute in exponential phase. CatB inhibitor significantly reduces substrate turnover, whereas EGCG shows no effect on CatB enzyme activity. *Data points and bars depict mean from experiment performed in technical triplicates with error bars representing standard deviations. Statistical analysis: One-way ANOVA, ** $p < 0.002$.* ____

could be observed (**Figure 19**, B). Excluding a direct effect of EGCG on CatB activity, it was next investigated, whether EGCG-induced A β 42 aggregates influence the cleavage by CatB. Therefore, A β 42 peptides were first preaggregated for 18 h as previously described (**3.2**). Then, EGCG or DMSO was added to preformed A β 42 aggregates and samples were incubated for an additional 24 h. To assess whether EGCG was able to induce the aggregate remodeling, the morphologies of preformed untreated and treated A β 42 aggregates were analyzed by AFM and EM. Here, in line with previous studies, it could be observed that fibrillar A β 42 aggregates are partly disrupted and that the formation of oligomeric structures is induced (**Figure 20**, A, B). The formation of EGCG-

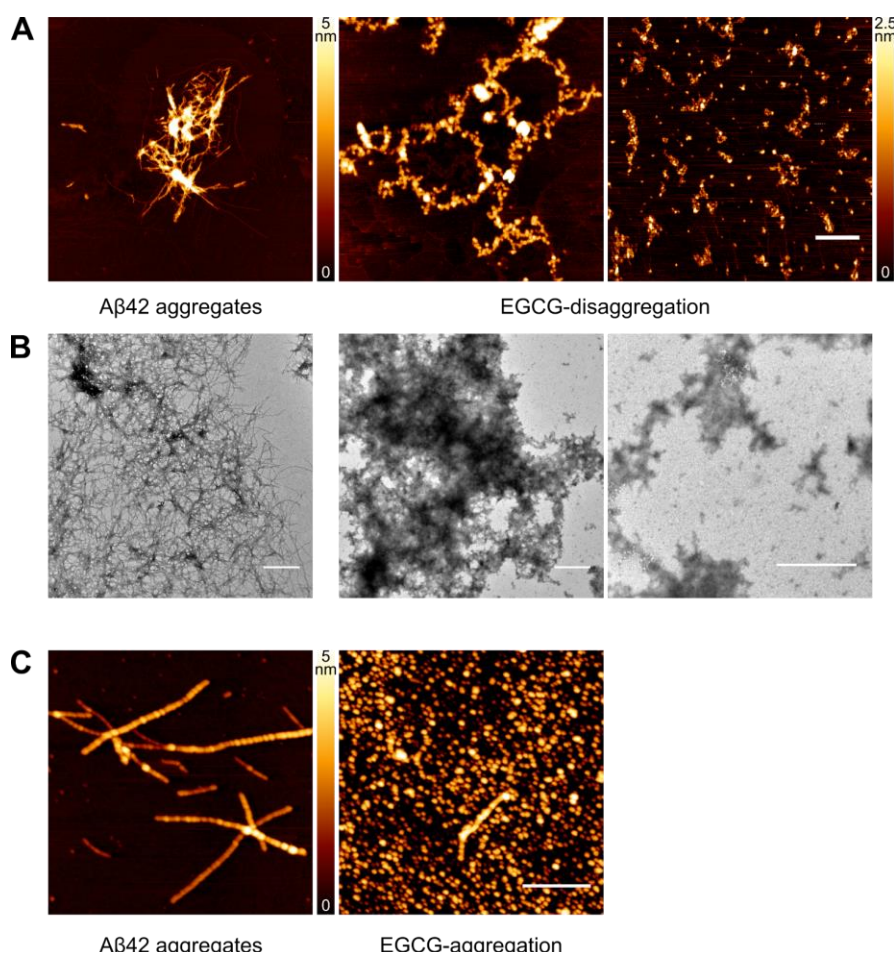


Figure 20. EGCG-induced A β 42 aggregate remodeling. **(A)** Incubation of 10 μ M high molecular weight, fibrillar A β 42 aggregates with excess amounts of EGCG for 24 h results in fibril disruption and formation of amorphous substructures. Samples analyzed by AFM. **(B)** Similar morphological changes are observed when samples are analyzed by TEM. **(C)** Aggregation of 10 μ M soluble A β 42 peptides in presence of equimolar concentrations of EGCG hinders fibril formation and results in the formation of stable amorphous A β 42 oligomers. Samples analyzed by AFM. *Scale bars: 500 nm. Representative image sections from three independent remodeling experiments.* ____

induced A β 42 aggregate species was even more pronounced, when A β 42 peptide aggregation reactions were performed in the presence of EGCG, resulting in an almost complete off-pathway oligomer population (**Figure 20, C**).

To quantify the EGCG-mediated remodeling of preformed A β 42 aggregates, the reaction products were additionally analyzed by density gradient centrifugation. Therefore, the recently published QIAD method was slightly modified. With this method, compound effects on the formation of aggregate species and their size distribution can be precisely monitored (Brener et al., 2015). In the density gradient, the preformed A β 42 aggregates

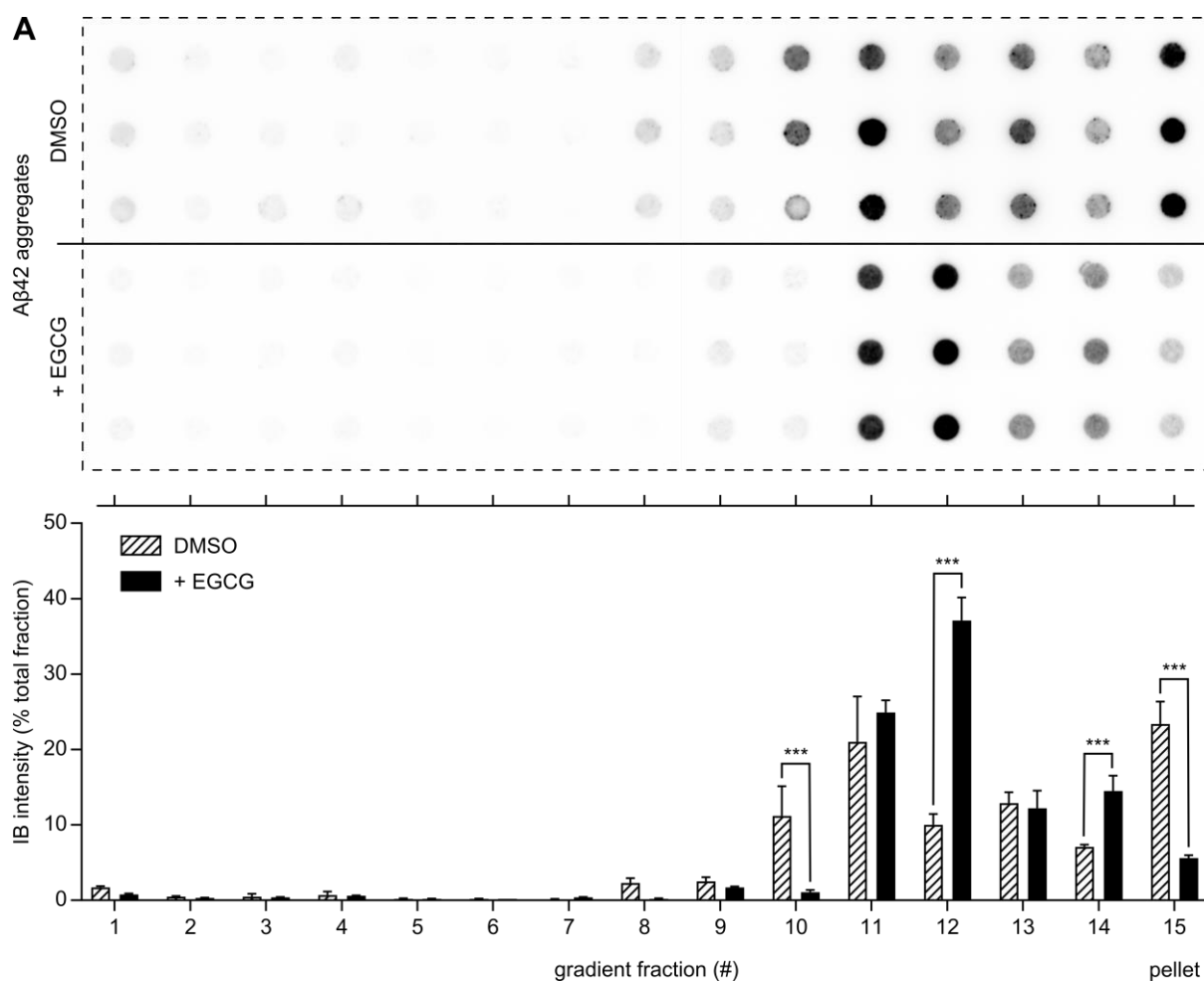


Figure 21. Quantification of EGCG-mediated structural A β 42 aggregate remodeling using gradient centrifugation. **(A)** Preformed A β 42 aggregate solutions (**DMSO**) consist of various protein aggregate sizes resembled by a wide distribution over gradient fractions. Enrichment of high molecular weight A β 42 aggregates in the pellet fraction is detected. Addition of EGCG (**+ EGCG**) redirects A β 42 aggregates into a defined subspecies, which strongly accumulates in fraction #12. *Data bars show mean from technical triplicates of one representative experiment. Error bars represent standard deviation. Statistical analysis: One-way ANOVA, *** $p < 0.001$.* ____

were distributed relatively equally over fractions 10 to 14 and also enriched in the pellet fraction (15) (DMSO, **Figure 21**, A), indicating the presence of mainly large A β 42 aggregate species and some smaller structures. When EGCG-remodeling was conducted, the aggregate distribution changed indicating the formation of smaller aggregate species. Interestingly, a strong enrichment of A β 42 species within fraction #12 could be observed (+EGCG, **Figure 21**, A), which most likely represents the previously characterized, EGCG-induced oligomeric species (Bieschke et al., 2011).

To next assess whether EGCG-mediated remodeling of preformed A β 42 aggregates influences their cleavage through the lysosomal protease CatB, A β 42 aggregate species were produced and digested with the lysosomal enzyme. To evaluate whether EGCG-mediated remodeling does indeed facilitate enzyme cleavage, reaction products were analyzed in dot blot assays for A β content. Additionally, the specific degradation of SDS-stable A β 42 aggregate species by CatB was evaluated by filter retardation assays. It

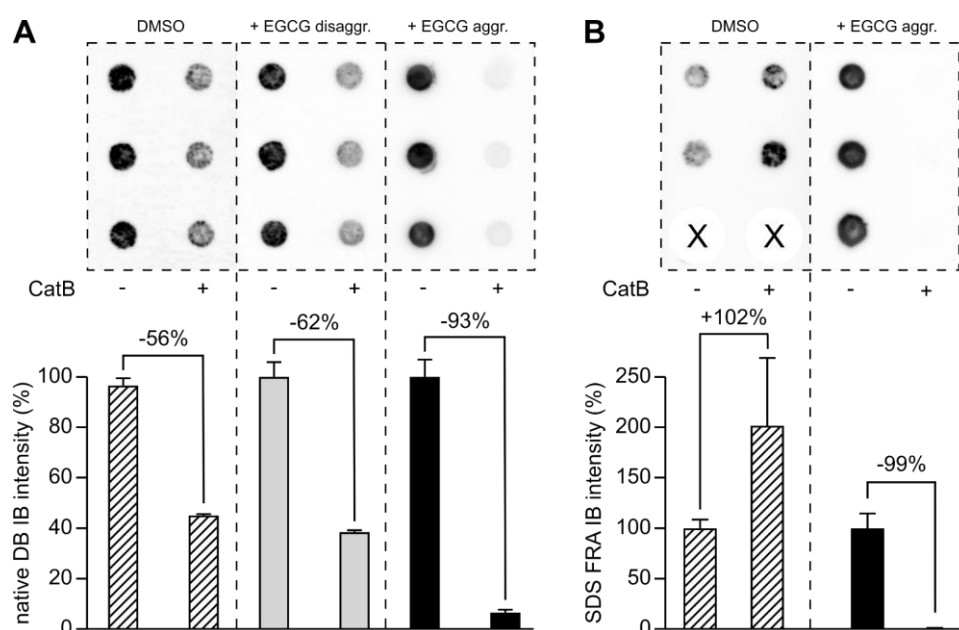


Figure 22. EGCG-mediated A β 42 aggregate remodeling facilitates lysosomal enzyme cleavage. **(A)** *In vitro* CatB digestion of fibrillar and EGCG-induced A β 42 aggregate species. 10 μ M preformed A β 42 aggregates were digested with 5 μ g/ml CatB for 4 h and analyzed by dot blot assays. EGCG-induced A β 42 subspecies are most efficiently degraded. **(B)** Specific analysis of SDS-stable A β 42 aggregates in filter retardation assays. CatB cleavage of solvent treated, SDS-stable A β 42 aggregates results in A β signal increase of SDS-FRA. EGCG-induced, SDS-stable A β 42 aggregate subspecies are not detectable in SDS-FRAs after CatB digestion. *Data bars depict means from one representative experiment with error bars indicating standard deviation.* _____

could be seen that, fibrillar A β 42 aggregates (as shown in Figure 21) are partially degraded by cathepsin B *in vitro*, reducing the abundance of A β 42 aggregate species by 56% (DMSO, **Figure 22**, A). However, when mature fibrillar aggregates are incubated with EGCG for 24 h to induce their remodeling prior to enzymatic digestion, cathepsin B cleavage is increased, leading to a reduction of 62% (+EGCG disaggr., **Figure 22**, A). This effect is even more pronounced, when A β 42 aggregates were preformed in the presence of EGCG. Under this condition, almost the whole aggregate population consists of the previously described, SDS-stable, off-pathway oligomeric aggregate species (**Figure 20**, C), which are indeed highly detergent stable, but surprisingly were efficiently degraded by the lysosomal enzyme cathepsin B (+EGCG aggr., **Figure 22**, A). Strikingly, when only analyzing the degradation of SDS-stable A β 42 aggregate species, a complete enzymatic digestion of the EGCG-induced aggregate species could be observed, whereas cathepsin B was not able to degrade SDS-stable, fibrillar A β 42 aggregates (**Figure 22**, B). This strongly indicates that the direct effect of EGCG on fibrillar A β 42 aggregates leads to the formation of structures, which are much more easily degraded by lysosomal enzymes – a key pathway in cellular A β 42 proteolysis and the potential mechanism for the EGCG-induced increase in intracellular A β 42 aggregate degradation.

5 Discussion

Previous approaches pursued to reduce cellular A β 42 aggregate loads mainly focused on enzymatic inhibition of APP cleaving enzymes or antibody-mediated immunological clearance of A β 42 plaques. Targeting intracellular A β 42 aggregates with small molecules potentially represents a promising approach to slow AD progression by increasing insufficient cellular clearance. Additionally, compound-mediated modification and reduction of intracellular A β 42 aggregates might reduce their cell-to-cell transfer and pathological spreading of misfolded A β 42 species in AD (Bieschke, 2013; Eisele et al., 2015). A β 42 lowering drugs developed to date, mainly targeted the production of aggregation-prone A β 42 peptides or the reduction of extracellular A β plaques (Cummings et al., 2017). Additionally, previous small molecule screening assays mainly tried to identify *in vitro* A β 42 aggregation inhibitors (Wang et al., 2014) or – in a cellular context – stimulators of cellular protein degradation pathways such as proteasome and autophagy activators (Eisele et al., 2015; Hwang et al., 2017). In this study, using a cell-based high-throughput compound screening assay it was aimed to identify small molecules, which significantly reduce the abundance of intracellular A β 42 aggregates. Further, the mechanism behind the cellular A β 42 aggregate reductive effect of the most potent hit compound – EGCG – was investigated.

5.1 A cell-based, high-throughput compound screening assay recapitulating intracellular A β 42 aggregate pathology

A cell-based compound screening assay, which is able to identify small molecules lowering intracellular A β 42 aggregate load needs to clearly recapitulate features of *in vivo* aggregate pathology. Preformed A β 42 aggregate species have been shown to convert soluble A β peptides into an aggregated state in a prion-like seeding process and continuous cell-to-cell spreading of A β 42 species might drive AD progression. Thus, a suitable cellular model of intracellular A β 42 formation for compound screening should make use of similar uptake mechanisms as observed *in vivo*. A major pathway for internalization of large gulps – including misfolded, aggregated proteins – from the extracellular space (Wang et al., 2017) is macropinocytosis. This pathway was described to be a mechanism through which uptake and subsequent degradation of protein aggregates within the endolysosomal system takes place (Mandrekar et al., 2009). Furthermore, when uptake through macropinocytosis is followed by insufficient clearance, this showed to induce seed-induced aggregate formation (Bloomfield and Kay, 2016;

Zeineddine and Yerbury, 2015). After internalization, intracellular A β 42 aggregates *in vivo* mainly accumulate in enlarged multivesicular bodies – a specialized subset of endosomes, which are able to fuse with lysosomes for subsequent degradation (R. A. Nixon, 2013).

In the work of this thesis, first a suitable cellular model system for uptake and accumulation of intracellular A β 42 aggregates was established. Modelling intracellular A β 42 aggregate pathology and their deposition in neuroblastoma SH-EP cells using preformed, fluorescently labeled A β 42 aggregates showed to involve actin-dependent, lipid-raft mediated macropinocytosis for aggregate uptake. Furthermore, the formation of SDS-stable, ThT-positive A β 42 intracellular aggregates accumulating in the endolysosomal system could be observed. Thus, this cell model clearly exhibits main characteristics of intracellular *in vivo* pathology (Biancalana and Koide, 2010; Krafft et al., 2003; Takahashi et al., 2017). Using fluorescently labeled A β 42 aggregates, the intracellular aggregate formation can additionally be easily monitored and quantified. This model could be effectively scaled up to a semi-automated, high-throughput capable, cell-based compound screening assay. Previously established assays for the identification of AD-modifying drugs mainly involved cell-free, *in vitro* aggregation inhibition assays (Wang et al., 2014). Compounds identified with these methods need extensive downstream investigations to analyze their *in-cell* potency. Therefore, cell-based compound screening assays are a powerful tool to directly identify biologically active small molecules (Michelini et al., 2010).

5.2 Direct A β 42 aggregate targeting compounds reduce cellular aggregate load, seeding activity and A β 42-induced toxicity

To elucidate the practicability of the assay, a focused proof-of-principle screen with a preselected polyphenolic compound library was performed. This chemical subgroup was found to effectively inhibit A β 42 aggregate formation in *cell-free* assays (Bieschke, 2013; Stefani and Rigacci, 2013) and was therefore investigated for its potency to reduce the abundance of cellular A β 42 aggregates. The cell-based compound screening assay efficiently identified 5 compounds within the tested polyphenol library, which significantly reduce cellular A β 42 aggregates. As it was found that the most potent compound – EGCG – did partially quench the fluorescence of TAMRA-labeled A β 42 aggregates, intensive validation experiments were performed. Antibody-based immunofluorescent and biochemical assays confirmed EGCG's strong A β 42 aggregate reductive effect on

intracellular A β 42 aggregate levels. High-throughput screening assays often make use of an increase or a decrease in bioluminescence or fluorescence to identify hit molecules (An, 2009; Fan and Wood, 2007). Subsequent validation experiments are of crucial importance as functional moieties of the compound molecule are able to interfere with assay readout signals. In the case of fluorescence, this can be caused by changes in pH, absorbance of the compound within the excitation or emission spectrum or by excited state reactions, energy transfer, complex-formation and collisional quenching (Simeonov and Davis, 2004). Interestingly, when the direct quenching effect of EGCG on the TAMRA fluorophore was evaluated in a cell-free environment, no quenching effect could be detected. However, EGCG quenched TAMRA fluorescence when coupled to A β 42. As EGCG is known to bind to A β 42 peptides and aggregates (Bieschke et al., 2010), this might be due to EGCG accumulation in close proximity to the fluorophore. Whereas, when the fluorophore and EGCG co-exist in solution, no direct interaction takes place and no quenching can be observed. Additionally, EGCG-induced remodeling of A β 42-TAMRA aggregates might affect fluorescence due to changes in the amino acid surrounding of the fluorophore. Thus, especially when the impact of small molecules on fluorescently labeled protein aggregates is investigated, intensive validation of compound-mediated effects in independent assays is essential.

Besides reducing intracellular A β 42 aggregate load, EGCG treatment of SH-EP cells with intracellular A β 42 aggregates additionally resulted in the reduction of the cell extracts' seeding activity. While it remains unclear whether this effect is in fact mediated through a structural remodeling of A β 42 aggregates into off-pathway structures or through the sole reduction of cellular A β 42 aggregates, it shows that direct aggregate targeting compounds provide an effective strategy to reduce seeding-activity in a cellular context. Additionally, EGCG treatment showed to reduce A β 42-induced mitochondrial toxicity in SH-EP cells as well as in primary neurons of rat hippocampi. Observing that a rescue of A β 42 aggregate-induced can be achieved with EGCG treatment indicates that it's cellular modulation of A β 42 aggregate levels is beneficial for cell viability.

5.3 A potential mechanism of the EGCG-induced reduction of intracellular A β 42 aggregates

Several cellular A β 42 aggregate lowering small molecules were previously identified (Wolfe, 2008). In fact, treatment with the most potent compound – EGCG – was previously shown to reduce cellular A β 42 aggregate load (Bieschke et al., 2010; Chang

et al., 2015; Li et al., 2006; Lin et al., 2009). However, although numerous potential cellular targets of EGCG were identified (Chang et al., 2015; Li et al., 2006; Lin et al., 2009), the main underlying mechanism responsible for its aggregate degrading effect in cells is still unknown. Therefore, this work further systematically investigated the underlying mechanism of EGCG-mediated reduction of the cellular A β 42 aggregate load.

Due to the fact that intracellular A β 42 aggregates in SH-EP cells mainly accumulated in lysosomes and cathepsins were previously described to be involved in A β aggregate clearance (Mueller-Steiner et al., 2006), I hypothesized that its aggregate degradation promoting effect is exhibited through lysosomal degradation. Systematic inhibition of autophagy, lysosomal acidification and the lysosomal enzyme CatB revealed that the EGCG-mediated reduction of the intracellular A β 42 aggregate load is dependent on lysosomal function and further on enzymatic activity of CatB. Total inhibition of CatB maturation completely abrogated the EGCG-mediated effect. As EGCG was previously described to enhance lysosomal acidification and might thereby enhance A β 42 aggregate cleavage (Zhou et al., 2014), it was tested whether EGCG treatment increases lysosomal enzyme activity in SH-EP cells. Interestingly, even in the absence of intracellular A β 42 aggregates, EGCG increased lysosomal enzyme activity. Additionally, an increased maturation of CatB through EGCG treatment could be detected. This increase might represent a potential mechanism for the increased degradation of intracellular A β 42 degradation after EGCG treatment. Interestingly, EGCG was recently described to increase lysosomal acidification and thereby counteract Epstein-Barr virus infection (Zhong et al., 2015). However, if enhancement of lysosomal enzyme activity through increased acidification is the main mechanism for EGCG's strong degradative effect, one would expect to see a reductive effect of EGCG when lysosomal acidification is inhibited with Bafilomycin A1. Complete lysosomal enzyme inhibition though did fully block the EGCG-mediated increase of A β 42 aggregate degradation and even high EGCG concentrations (30 μ M) were not able to initiate a reduction of cellular A β 42 aggregate levels. Therefore, besides EGCG-induced increase of lysosomal acidification, I hypothesized that an additional independent mechanism might be predominantly responsible for its A β 42 aggregate lowering effect.

The addition of EGCG to spontaneous A β 42 peptide aggregation reactions was shown to inhibit the formation of fibrillar A β 42 aggregates and leads to the formation of an off-pathway oligomeric species (Ehrnhoefer et al., 2008). Furthermore, binding of EGCG to

performed A β 42 aggregates induces the remodeling of fibrillar species (Bieschke et al., 2010). As the EGCG-mediated reduction of intracellular A β 42 aggregates was found here to be mediated through lysosomal degradation and as it was previously described that the remodeling of protein aggregates in lattice corneal dystrophy facilitates their proteolytic degradation (Stenvang et al., 2016), I hypothesized that the structural remodeling of A β 42 aggregates might increase degradation through lysosomal enzymes and thereby lead to an increased reduction of intracellular A β 42 load. Comparing the reduction of intracellular A β 42 aggregates of EGCG and structural derivatives revealed that compounds, which show *in vitro* A β 42 aggregation modulation, are potent in reducing cellular A β 42 load. This suggested that a direct *in cell* interaction of the compound molecules with A β 42 aggregates might be responsible for the observed effects. A prerequisite for this proposed mode of action is that EGCG is indeed able to bind to A β 42 aggregates *in cells*. Even though *in vitro* binding of fibrillar A β 42 aggregates has been shown (Bieschke et al., 2010), *in cell* binding evidence was lacking to date. In this work, labeling of EGCG with a rhodamine fluorophore did clearly show that EGCG directly binds intracellularly accumulating A β 42 aggregates. As EGCG is able to bind to A β 42 aggregates in cells, I hypothesized that the structural remodeling of A β 42 aggregates facilitates their cleavage through lysosomal proteases. This could represent the mechanistic explanation for the increased degradation of intracellular A β 42 aggregates upon compound treatment. EGCG-treatment of preformed A β 42 aggregates partially disrupted and disassembled fibrillar structures into smaller peptide species *in vitro*. Interestingly, the induced structures are more SDS-stable when compared to fibrillar A β 42 aggregates. However, the evaluation of A β 42 aggregate degradation with the lysosomal protease CatB of native and EGCG-remodeled A β 42 aggregates revealed that these structures— even though highly detergent stable – are more efficiently degraded by the lysosomal enzyme. Furthermore, when A β 42 aggregates were preformed in the presence of EGCG, which leads to the formation of a complete off-pathway oligomer

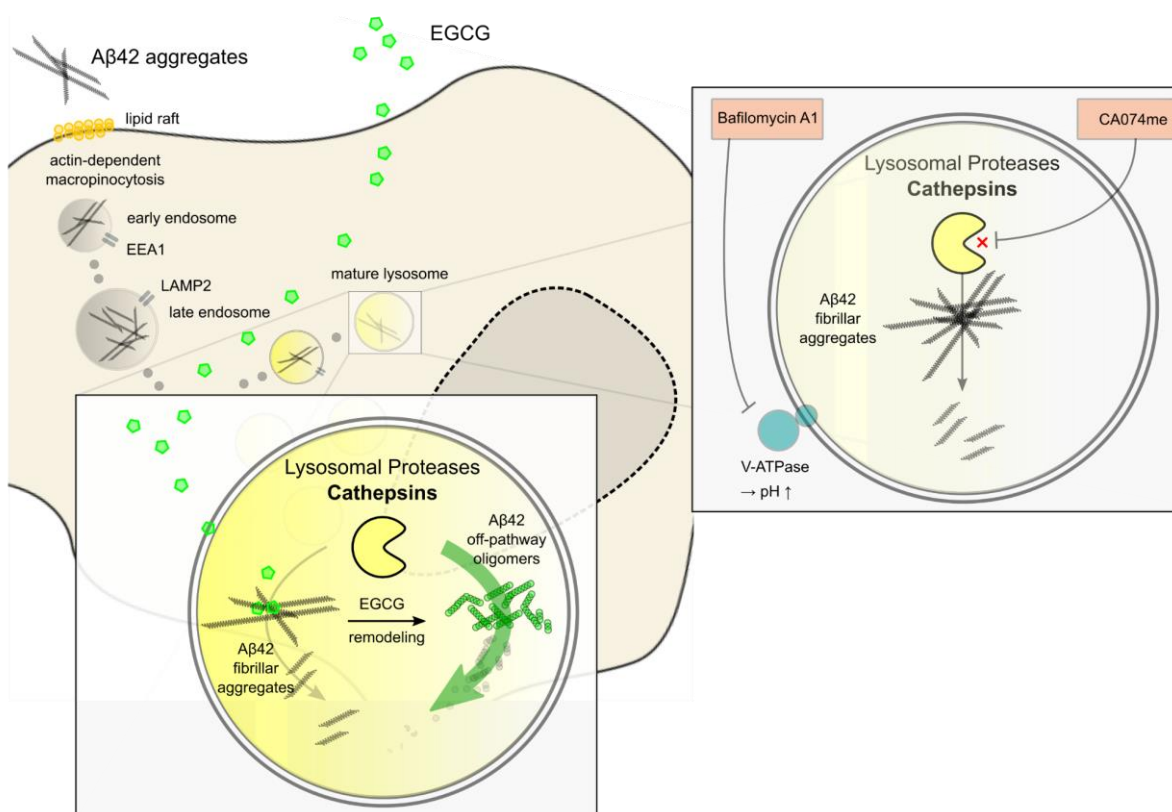


Figure 23. Model of EGCG-mediated reduction of cellular Aβ42 aggregates. Preformed Aβ42 aggregates are internalized via lipid-raft mediated macropinocytosis into early and late endosomes, which subsequently fuse with lysosomes for aggregate degradation. Fibrillar Aβ42 aggregates are inefficiently cleaved by lysosomal cathepsins and accumulate. Preventing lysosomal acidification and thereby CatB maturation or inhibition of CatB with a specific inhibitor blocks lysosomal degradation of Aβ42 aggregates. EGCG is able to enter cells and bind to intracellular Aβ42 aggregates potentially inducing their structural remodeling *in cells*. EGCG-induced off-pathway structures are efficiently degraded by the lysosomal enzyme CatB. ____

population, also a complete degradation of Aβ42 aggregates through CatB could be detected. In contrast, CatB was not able to degrade SDS-stable fibrillar Aβ42 aggregates.

Based on these results, we propose a mechanism for EGCG-induced reduction of cellular Aβ42 aggregate load. EGCG is able to cross the cellular membrane and bind to intracellularly accumulating amyloid aggregates. Binding to intracellular fibrillar Aβ42 aggregates induces structural remodeling into off-pathway structures. In contrast to fibrillar Aβ42 aggregates, these EGCG-induced oligomer species can be effectively degraded through lysosomal enzymes and thereby intracellular Aβ42 aggregate load is reduced.

Various approaches have been undertaken to lower A β 42 load in the brain of AD patients (Cummings et al., 2017). With this work, a novel approach and mechanism is presented. Identifying compounds, which selectively reduce intracellular A β 42 aggregates through enhancing endogenous clearance mechanisms by changing compact, fibrillar amyloid aggregates into amorphous subspecies might be an effective A β 42 lowering approach. Especially with the fact in mind that AD is a disease of the elderly and that with increasing age cellular protein clearance becomes inefficient (Tan et al., 2014), these small molecules might thereby counteract the deficient amyloid degradation. Additionally, as mutations in clearance mechanisms are causative for AD and insufficient clearance of protein aggregates is thought to be a driver in proteinopathies (Bloomfield and Kay, 2016; Zeineddine and Yerbury, 2015), this approach might be very specific in targeting common malfunctions in neurodegeneration responsible for progression in these diseases. It is to state that especially cathepsin-mediated lysosomal degradation is controversially discussed in AD pathogenesis. Cathepsin-mediated amyloid cleavage has been suspected to increase the production of aggregation-prone A β 42 species (Haque et al., 2008). Therefore, cathepsin inhibitors were proposed and evaluated as potential disease-modifying drugs. However, these did not exhibit strong beneficial effects in preclinical studies and more recent evidence, in line with this study, supports the idea that cathepsin are major essential enzymes for maintaining cellular protein homeostasis, are important for degradation of accumulating protein aggregates and mutations in cathepsins even cause neurodegeneration (R. A. Nixon, 2013; Perlenfein and Murphy, 2017; Sun et al., 2008) Thus, enhancing cathepsin-mediated, lysosomal clearance – e.g. through direct A β aggregate binding compounds represent a promising approach to increase insufficient clearance of lysosomal protein accumulation in AD and other neurodegenerative diseases.

6 References

- Almeida, P.C., Oliveira, V., Chagas, J.R., Meldal, M., Juliano, M.A., Juliano, L., 2000. Hydrolysis by cathepsin B of fluorescent peptides derived from human prorenin. *Hypertens. (Dallas, Tex. 1979)* 35, 1278–83. <https://doi.org/10.1161/01.HYP.35.6.1278>
- An, W.F., 2009. *Fluorescence-Based Assays*. Humana Press, Totowa, NJ, pp. 97–107. https://doi.org/10.1007/978-1-60327-545-3_7
- Artavanis-Tsakonas, S., Rand, M.D., Lake, R.J., 1999. Notch signaling: cell fate control and signal integration in development. *Science* 284, 770–6.
- Bales, K.R., Liu, F., Wu, S., Lin, S., Koger, D., DeLong, C., Hansen, J.C., Sullivan, P.M., Paul, S.M., 2009. Human APOE Isoform-Dependent Effects on Brain β -Amyloid Levels in PDAPP Transgenic Mice. *J. Neurosci.* 29, 6771–6779. <https://doi.org/10.1523/JNEUROSCI.0887-09.2009>
- Bettens, K., Sleegers, K., Van Broeckhoven, C., 2013. Genetic insights in Alzheimer's disease. *Lancet Neurol.* 12, 92–104. [https://doi.org/10.1016/S1474-4422\(12\)70259-4](https://doi.org/10.1016/S1474-4422(12)70259-4)
- Biancalana, M., Koide, S., 2010. Molecular mechanism of Thioflavin-T binding to amyloid fibrils. *BBA - Proteins Proteomics* 1804, 1405–1412. <https://doi.org/10.1016/j.bbapap.2010.04.001>
- Bieschke, J., 2013. Natural Compounds May Open New Routes to Treatment of Amyloid Diseases. *Neurotherapeutics* 10, 429–439. <https://doi.org/10.1007/s13311-013-0192-7>
- Bieschke, J., Herbst, M., Wiglenda, T., Friedrich, R.P., Boeddrich, A., Schiele, F., Kleckers, D., Miguel Lopez del Amo, J., Gr, rn A., Wang, Q., Schmidt, M.R., Lurz, R., Anwyl, R., Schnoegl, S., Frank, R.F., Reif, B., Walsh, D.M., Wanker, E.E., 2011. Small-molecule conversion of toxic oligomers to nontoxic β -sheet-rich amyloid fibrils. *Nat. Chem. Biol.* 8. <https://doi.org/10.1038/nChEMBio.719>
- Bieschke, J., Russ, J., Friedrich, R.P., Ehrnhoefer, D.E., Wobst, H., Neugebauer, K., Wanker, E.E., 2010. EGCG remodels mature alpha-synuclein and amyloid-beta

- fibrils and reduces cellular toxicity. *Proc. Natl. Acad. Sci. U. S. A.* 107, 7710–5.
<https://doi.org/10.1073/pnas.0910723107>
- Blank, N., Schiller, M., Krienke, S., Wabnitz, G., Ho, A.D., Lorenz, H.-M., 2007. Cholera toxin binds to lipid rafts but has a limited specificity for ganglioside GM1. *Immunol. Cell Biol.* 85, 378–382. <https://doi.org/10.1038/sj.icb.7100045>
- Bloomfield, G., Kay, R.R., 2016. Uses and abuses of macropinocytosis. *J. Cell Sci.* 129, 2697–705. <https://doi.org/10.1242/jcs.176149>
- Bohdanowicz, M., Grinstein, S., 2013. Role of Phospholipids in Endocytosis, Phagocytosis, and Macropinocytosis. *Physiol. Rev.* 93, 69–106.
<https://doi.org/10.1152/physrev.00002.2012>
- Brener, O., Dunkelmann, T., Gremer, L., van Groen, T., Mirecka, E.A., Kadish, I., Willuweit, A., Kutzsche, J., Jürgens, D., Rudolph, S., Tusche, M., Bongen, P., Pietruszka, J., Oesterhelt, F., Langen, K.-J., Demuth, H.-U., Janssen, A., Hoyer, W., Funke, S.A., Nagel-Steger, L., Willbold, D., 2015. QIAD assay for quantitating a compound's efficacy in elimination of toxic A β oligomers. *Sci. Rep.* 5, 13222.
<https://doi.org/10.1038/srep13222>
- Bu, G., Zhang, Y., Ladu, M.J., Xu, H., Li, J., Kanekiyo, T., Shinohara, M., 2012. Differential Regulation of Amyloid- β Endocytic Trafficking and Lysosomal Degradation by Apolipoprotein E Isoforms * □. *J. Biol. Chem* 287, 44593–44601.
<https://doi.org/10.1074/jbc.M112.420224>
- Buggia-prévot, V., Thinakaran, G., 2014. Sorting the Role of SORLA in Alzheimer ' s Disease. *Sci. Transl. Med.* 6, 9–11.
- Cabrejo, L., Guyant-Maréchal, L., Laquerrière, A., Vercelletto, M., De la Fournière, F., Thomas-Antérion, C., Verny, C., Letournel, F., Pasquier, F., Vital, A., Checler, F., Frebourg, T., Campion, D., Hannequin, D., 2006. Phenotype associated with APP duplication in five families. *Brain* 129, 2966–76.
<https://doi.org/10.1093/brain/awl237>
- Caccamo, A., Ferreira, E., Branca, C., Oddo, S., 2017. p62 improves AD-like pathology by increasing autophagy. *Mol. Psychiatry* 22, 865–873.

<https://doi.org/10.1038/mp.2016.139>

Carlo, A.-S., Gustafsen, C., Mastrobuoni, G., Nielsen, M.S., Burgert, T., Hartl, D., Rohe, M., Nykjaer, A., Herz, J., Heeren, J., Kempa, S., Petersen, C.M., Willnow, T.E., 2013. The pro-neurotrophin receptor sortilin is a major neuronal apolipoprotein E receptor for catabolism of amyloid- β peptide in the brain. *J. Neurosci.* 33, 358–70. <https://doi.org/10.1523/JNEUROSCI.2425-12.2013>

Castellano, J.M., Kim, J., Stewart, F.R., Jiang, H., DeMattos, R.B., Patterson, B.W., Fagan, A.M., Morris, J.C., Mawuenyega, K.G., Cruchaga, C., Goate, A.M., Bales, K.R., Paul, S.M., Bateman, R.J., Holtzman, D.M., 2011. Human apoE Isoforms Differentially Regulate Brain Amyloid- β Peptide Clearance. *Sci. Transl. Med.* 3, 89ra57-89ra57. <https://doi.org/10.1126/scitranslmed.3002156>

Cataldo, A.M., Barnett, J.L., Pieroni, C., Nixon, R.A., 1997. Increased neuronal endocytosis and protease delivery to early endosomes in sporadic Alzheimer's disease: neuropathologic evidence for a mechanism of increased β -amyloidogenesis. *J. Neurosci.* 17, 6142–51.

Cataldo, A.M., Petanceska, S., Terio, N.B., Peterhoff, C.M., Durham, R., Mercken, M., Mehta, P.D., Buxbaum, J., Haroutunian, V., Nixon, R.A., 2004. A β localization in abnormal endosomes: Association with earliest A β elevations in AD and Down syndrome. *Neurobiol. Aging* 25, 1263–1272. <https://doi.org/10.1016/j.neurobiolaging.2004.02.027>

Chang, X., Rong, C., Chen, Y., Yang, C., Hu, Q., Mo, Y., Zhang, C., Gu, X., Zhang, L., He, W., Cheng, S., Hou, X., Su, R., Liu, S., Dun, W., Wang, Q., Fang, S., 2015. (-)-Epigallocatechin-3-gallate attenuates cognitive deterioration in Alzheimer's disease model mice by upregulating neprilysin expression. *Exp. Cell Res.* 334, 136–145. <https://doi.org/10.1016/J.YEXCR.2015.04.004>

Cold Spring Harbor Protocols, 2007. M2 lysis buffer. *Cold Spring Harb. Protoc.* 2007, pdb.rec10773-rec10773. <https://doi.org/10.1101/pdb.rec10773>

Coric, V., van Dyck, C.H., Salloway, S., Andreasen, N., Brody, M., Richter, R.W., Soininen, H., Thein, S., Shiovitz, T., Pilcher, G., Colby, S., Rollin, L., Dockens, R., Pachai, C., Portelius, E., Andreasson, U., Blennow, K., Soares, H., Albright, C.,

- Feldman, H.H., Berman, R.M., 2012. Safety and Tolerability of the γ -Secretase Inhibitor Avagacestat in a Phase 2 Study of Mild to Moderate Alzheimer Disease. *Arch. Neurol.* 69, 1430. <https://doi.org/10.1001/archneurol.2012.2194>
- Cummings, J., Lee, G., Mortsdorf, T., Ritter, A., Zhong, K., 2017. Alzheimer's disease drug development pipeline: 2017. *Alzheimer's Dement. Transl. Res. Clin. Interv.* 3, 367–384. <https://doi.org/10.1016/J.TRCI.2017.05.002>
- Cummings, J.L., Morstorf, T., Zhong, K., 2014. Alzheimer's disease drug-development pipeline: few candidates, frequent failures. *Alzheimers. Res. Ther.* 6, 37. <https://doi.org/10.1186/alzrt269>
- Domert, J., Rao, S.B., Agholme, L., Brorsson, A.-C., Marcusson, J., Hallbeck, M., Nath, S., 2014. Spreading of amyloid- β peptides via neuritic cell-to-cell transfer is dependent on insufficient cellular clearance. *Neurobiol. Dis.* 65, 82–92. <https://doi.org/10.1016/j.nbd.2013.12.019>
- Doody, R.S., Raman, R., Farlow, M., Iwatsubo, T., Vellas, B., Joffe, S., Kieburtz, K., He, F., Sun, X., Thomas, R.G., Aisen, P.S., Siemers, E., Sethuraman, G., Mohs, R., Mohs, R., Semagacestat Study Group, 2013. A Phase 3 Trial of Semagacestat for Treatment of Alzheimer's Disease. *N. Engl. J. Med.* 369, 341–350. <https://doi.org/10.1056/NEJMoa1210951>
- Doody, R.S., Thomas, R.G., Farlow, M., Iwatsubo, T., Vellas, B., Joffe, S., Kieburtz, K., Raman, R., Sun, X., Aisen, P.S., Siemers, E., Liu-Seifert, H., Mohs, R., Alzheimer's Disease Cooperative Study Steering Committee, Solanezumab Study Group, 2014. Phase 3 trials of solanezumab for mild-to-moderate Alzheimer's disease. *N. Engl. J. Med.* 370, 311–21. <https://doi.org/10.1056/NEJMoa1312889>
- Ehrnhoefer, D.E., Bieschke, J., Boeddrich, A., Herbst, M., Masino, L., Lurz, R., Engemann, S., Pastore, A., Wanker, E.E., 2008. EGCG redirects amyloidogenic polypeptides into unstructured, off-pathway oligomers. *Nat. Struct. Mol. Biol.* 15. <https://doi.org/10.1038/nsmb.1437>
- Eisele, Y.S., Monteiro, C., Fearn, C., Encalada, S.E., Wiseman, R.L., Powers, E.T., Kelly, J.W., 2015. Targeting protein aggregation for the treatment of degenerative diseases. *Nat. Rev. Drug Discov.* 14, 759–780. <https://doi.org/10.1038/nrd4593>

- Fan, F., Wood, K. V., 2007. Bioluminescent Assays for High-Throughput Screening. *Assay Drug Dev. Technol.* 5, 127–136. <https://doi.org/10.1089/adt.2006.053>
- Ferreira, N., Saraiva, M.J., Almeida, M.R., 2011. Natural polyphenols inhibit different steps of the process of transthyretin (TTR) amyloid fibril formation. *FEBS Lett.* 585, 2424–2430. <https://doi.org/10.1016/j.febslet.2011.06.030>
- Fritschi, S.K., Langer, F., Kaeser, S.A., Maia, L.F., Portelius, E., Pinotsi, D., Kaminski, C.F., Winkler, D.T., Maetzler, W., Keyvani, K., Spitzer, P., Wiltfang, J., Kaminski Schierle, G.S., Zetterberg, H., Staufenbiel, M., Jucker, M., 2014. Highly potent soluble amyloid- β seeds in human Alzheimer brain but not cerebrospinal fluid. *Brain* 137, 2909–2915. <https://doi.org/10.1093/brain/awu255>
- Fukuda, M., 1991. Lysosomal membrane glycoproteins. Structure, biosynthesis, and intracellular trafficking. *J. Biol. Chem.* 266, 21327–30.
- Gandy, S., DeKosky, S.T., 2013. Toward the Treatment and Prevention of Alzheimer's Disease: Rational Strategies and Recent Progress. *Annu. Rev. Med.* 64, 367–383. <https://doi.org/10.1146/annurev-med-092611-084441>
- Ganley, I.G., Wong, P.-M., Jiang, X., 2011. Thapsigargin distinguishes membrane fusion in the late stages of endocytosis and autophagy. *Autophagy* 7, 1397–1399. <https://doi.org/10.4161/auto.7.11.17651>
- Geylis, V., Kourilov, V., Meiner, Z., Nennesmo, I., Bogdanovic, N., Steinitz, M., 2005. Human monoclonal antibodies against amyloid- β from healthy adults. *Neurobiol. Aging* 26, 597–606. <https://doi.org/10.1016/j.neurobiolaging.2004.06.008>
- Goetzl, E.J., Boxer, A., Schwartz, J.B., Abner, E.L., Petersen, R.C., Miller, B.L., Kapogiannis, D., 2015. Altered lysosomal proteins in neural-derived plasma exosomes in preclinical Alzheimer disease. *Neurology* 85, 40–47. <https://doi.org/10.1212/WNL.0000000000001702>
- Guerreiro, R., Wojtas, A., Bras, J., Carrasquillo, M., Rogaeva, E., Majounie, E., Cruchaga, C., Sassi, C., Kauwe, J.S.K., Younkin, S., Hazrati, L., Collinge, J., Pocock, J., Lashley, T., Williams, J., Lambert, J.-C., Amouyel, P., Goate, A., Rademakers, R., Morgan, K., Powell, J., St. George-Hyslop, P., Singleton, A.,

- Hardy, J., 2013. *TREM2* Variants in Alzheimer's Disease. *N. Engl. J. Med.* 368, 117–127. <https://doi.org/10.1056/NEJMoa1211851>
- Gyure, K.A., Durham, R., Stewart, W.F., Smialek, J.E., Troncoso, J.C., 2001. Intraneuronal A β -amyloid precedes development of amyloid plaques in Down syndrome. *Arch. Pathol. Lab. Med.* 125, 489–492. [https://doi.org/10.1043/0003-9985\(2001\)125<0489:IAAPDO>2.0.CO;2](https://doi.org/10.1043/0003-9985(2001)125<0489:IAAPDO>2.0.CO;2)
- Hamaguchi, T., Ono, K., Murase, A., Yamada, M., 2009. Phenolic Compounds Prevent Alzheimer's Pathology through Different Effects on the Amyloid- β Aggregation Pathway. *Am. J. Pathol.* 175, 2557–2565. <https://doi.org/10.2353/ajpath.2009.090417>
- Haque, A., Banik, N.L., Ray, S.K., 2008. New insights into the roles of endolysosomal cathepsins in the pathogenesis of Alzheimer's disease: cathepsin inhibitors as potential therapeutics. *CNS Neurol. Disord. Drug Targets* 7, 270–7.
- Head, B.P., Patel, H.H., Insel, P.A., 2014. Interaction of membrane/lipid rafts with the cytoskeleton: impact on signaling and function: Membrane/Lipid Rafts, Mediators of Cytoskeletal Arrangement and Cell Signaling. *Biochim. Biophys. Acta* 1838, 532–45. <https://doi.org/10.1016/J.BBAMEM.2013.07.018>
- Hirohata, M., Hasegawa, K., Tsutsumi-Yasuhara, S., Ohhashi, Y., Ookoshi, T., Ono, K., Yamada, M., Naiki, H., 2007. The Anti-Amyloidogenic Effect Is Exerted against Alzheimer's β -Amyloid Fibrils in Vitro by Preferential and Reversible Binding of Flavonoids to the Amyloid Fibril Structure [†]. *Biochemistry* 46, 1888–1899. <https://doi.org/10.1021/bi061540x>
- Hu, X., Crick, S.L., Bu, G., Frieden, C., Pappu, R. V., Lee, J.-M., 2009. Amyloid seeds formed by cellular uptake, concentration, and aggregation of the amyloid- β peptide. *Proc. Natl. Acad. Sci.* 106, 20324–20329. <https://doi.org/10.1073/pnas.0911281106>
- Hwang, H., Cho, S.M., Kwon, H.J., 2017. Approaches for discovering novel bioactive small molecules targeting autophagy. *Expert Opin. Drug Discov.* 12, 909–923. <https://doi.org/10.1080/17460441.2017.1349751>
- Inbar, P., Bautista, M.R., Takayama, S.A., Yang, J., 2008. Assay To Screen for

- Molecules That Associate with Alzheimer's Related β -Amyloid Fibrils. *Anal. Chem.* 80, 3502–3506. <https://doi.org/10.1021/ac702592f>
- Jin, S., Kedia, N., Illes-Toth, E., Haralampiev, I., Prisner, S., Herrmann, A., Wanker, E.E., Bieschke, J., 2016. Amyloid- β (1-42) Aggregation Initiates Its Cellular Uptake and Cytotoxicity. *J. Biol. Chem.* 291, 19590–19606. <https://doi.org/10.1074/jbc.M115.691840>
- Kajiho, H., Saito, K., Tsujita, K., Kontani, K., Araki, Y., Kurosu, H., Katada, T., 2003. RIN3: a novel Rab5 GEF interacting with amphiphysin II involved in the early endocytic pathway. *J. Cell Sci.* 116, 4159–4168. <https://doi.org/10.1242/jcs.00718>
- Kaur, J., Debnath, J., 2015. Autophagy at the crossroads of catabolism and anabolism. *Nat. Rev. Mol. Cell Biol.* 16, 461–472. <https://doi.org/10.1038/nrm4024>
- Kishi-Itakura, C., Koyama-Honda, I., Itakura, E., Mizushima, N., 2014. Ultrastructural analysis of autophagosome organization using mammalian autophagy-deficient cells. *J. Cell Sci.* 127, 4089–102. <https://doi.org/10.1242/jcs.156034>
- Klionsky, D.J., 2007. Autophagy: from phenomenology to molecular understanding in less than a decade. *Nat Rev Mol Cell Biol.* 8(11):931-7
- Koffie, R.M., Hashimoto, T., Tai, H.-C., Kay, K.R., Serrano-Pozo, A., Joyner, D., Hou, S., Kopeikina, K.J., Frosch, M.P., Lee, V.M., Holtzman, D.M., Hyman, B.T., Spire-Jones, T.L., 2012. Apolipoprotein E4 effects in Alzheimer's disease are mediated by synaptotoxic oligomeric amyloid- β . *Brain* 135, 2155–2168. <https://doi.org/10.1093/brain/aws127>
- Koivusalo, M., Welch, C., Hayashi, H., Scott, C.C., Kim, M., Alexander, T., Touret, N., Hahn, K.M., Grinstein, S., 2010. Amiloride inhibits macropinocytosis by lowering submembranous pH and preventing Rac1 and Cdc42 signaling. *J. Cell Biol.* 188, 547–63. <https://doi.org/10.1083/jcb.200908086>
- Kolb, H.C., Finn, M.G., Sharpless, K.B., 2001. Click Chemistry: Diverse Chemical Function from a Few Good Reactions. *Angew. Chemie Int. Ed.* 40, 2004–2021. [https://doi.org/10.1002/1521-3773\(20010601\)40:11<2004::AID-ANIE2004>3.0.CO;2-5](https://doi.org/10.1002/1521-3773(20010601)40:11<2004::AID-ANIE2004>3.0.CO;2-5)

- Kovács, T., Billes, V., Komlós, M., Hotzi, B., Manzóger, A., Tarnóci, A., Papp, D., Szikszai, F., Szinyákovics, J., Rácz, Á., Noszál, B., Veszelka, S., Walter, F.R., Deli, M.A., Hackler, L., Alfoldi, R., Huzian, O., Puskas, L.G., Liliom, H., Tárnok, K., Schlett, K., Borsy, A., Welker, E., Kovács, A.L., Pádár, Z., Erdős, A., Legradi, A., Bjelik, A., Gulya, K., Gulyás, B., Vellai, T., 2017. The small molecule AUTEN-99 (autophagy enhancer-99) prevents the progression of neurodegenerative symptoms. *Sci. Rep.* 7, 42014. <https://doi.org/10.1038/srep42014>
- Krafft, A., Jo LaDu Blaine Stine, M.W., Dahlgren, K.N., Blaine Stine, W., Krafft, G.A., Jo LaDu †, M., 2003. In Vitro Characterization of Conditions for Amyloid- β Peptide Oligomerization and Fibrillogenesis*. *J. Biol. Chem* 278, 11612–11622. <https://doi.org/10.1074/jbc.M210207200>
- Kunkle, B.W., Vardarajan, B.N., Naj, A.C., 2017. Early-onset alzheimer disease and candidate risk genes involved in endolysosomal transport. *JAMA Neurol.* 74, 1113–1122.
- Kuszczyk, M.A., Sanchez, S., Pankiewicz, J., Kim, J., Duszczyk, M., Guridi, M., Asuni, A.A., Sullivan, P.M., Holtzman, D.M., Sadowski, M.J., 2013. Blocking the Interaction between Apolipoprotein E and A β Reduces Intraneuronal Accumulation of A β and Inhibits Synaptic Degeneration. *Am. J. Pathol.* 182, 1750–1768. <https://doi.org/10.1016/j.ajpath.2013.01.034>
- LaFerla, F.M., Green, K.N., Oddo, S., 2007. Intracellular amyloid- β in Alzheimer's disease. *Nat. Rev. Neurosci.* 8, 499–509. <https://doi.org/10.1038/nrn2168>
- Lai, A.Y., McLaurin, J., 2011. Mechanisms of Amyloid-Beta Peptide Uptake by Neurons: The Role of Lipid Rafts and Lipid Raft-Associated Proteins. *SAGE-Hindawi Access to Res. Int. J. Alzheimer's Dis. Artic. ID 548380*. <https://doi.org/10.4061/2011/548380>
- Lee, J.-H., Moon, J.-H., Kim, S.-W., Jeong, J.-K., Nazim, U.M., Lee, Y.-J., Seol, J.-W., Park, S.-Y., 2015. EGCG-mediated autophagy flux has a neuroprotection effect via a class III histone deacetylase in primary neuron cells. *Oncotarget* 6(12):9701-17
- Li, Q., Gordon, M., Tan, J., Morgan, D., 2006. Oral administration of green tea epigallocatechin-3-gallate (EGCG) reduces amyloid beta deposition in transgenic

- mouse model of Alzheimer's disease. *Exp. Neurol.* 198, 576.
<https://doi.org/10.1016/J.EXPNEUROL.2006.02.062>
- Lin, C.-L., Chen, T.-F., Chiu, M.-J., Way, T.-D., Lin, J.-K., 2009. Epigallocatechin gallate (EGCG) suppresses β -amyloid-induced neurotoxicity through inhibiting c-Abl/FE65 nuclear translocation and GSK3 β activation. *Neurobiol. Aging* 30, 81–92.
<https://doi.org/10.1016/j.neurobiolaging.2007.05.012>
- Liu, Y., Liu, X., Hao, W., Decker, Y., Schomburg, R., Fülöp, L., Pasparakis, M., Menger, M.D., Fassbender, K., n.d. Neurobiology of Disease IKK κ Deficiency in Myeloid Cells Ameliorates Alzheimer's Disease-Related Symptoms and Pathology and Cologne Excellence Cluster on Cellular Stress Responses in Aging-Associated Diseases. <https://doi.org/10.1523/JNEUROSCI.1348-14.2014>
- Liu, Y., Schubert, D., 2002. Cytotoxic Amyloid Peptides Inhibit Cellular 3-(4,5-Dimethylthiazol-2-yl)-2,5-Diphenyltetrazolium Bromide (MTT) Reduction by Enhancing MTT Formazan Exocytosis. *J. Neurochem.* 69, 2285–2293.
<https://doi.org/10.1046/j.1471-4159.1997.69062285.x>
- Lopez del Amo, J.M., Fink, U., Dasari, M., Grelle, G., Wanker, E.E., Bieschke, J., Reif, B., 2012. Structural Properties of EGCG-Induced, Nontoxic Alzheimer's Disease A β Oligomers, *Journal of Molecular Biology*. <https://doi.org/10.1016/j.jmb.2012.01.013>
- Luna-Muñoz, J., Peralta-Ramirez, J., Chávez-Macías, L., Harrington, C.R., Wischik, C.M., Mena, R., 2008. Thiazin red as a neuropathological tool for the rapid diagnosis of Alzheimer's disease in tissue imprints. *Acta Neuropathol.* 116, 507–515. <https://doi.org/10.1007/s00401-008-0431-x>
- Mandrekar, S., Jiang, Q., Lee, C.Y.D., Koenigsnecht-Talboo, J., Holtzman, D.M., Landreth, G.E., 2009. Microglia Mediate the Clearance of Soluble A β through Fluid Phase Macropinocytosis. *J. Neurosci.* 29, 4252–4262.
<https://doi.org/10.1523/JNEUROSCI.5572-08.2009>
- Martin, B.L., Schrader-Fischer, G., Busciglio, J., Duke, M., Paganetti, P., Yankner, B.A., 1995. Intracellular accumulation of β -amyloid in cells expressing the Swedish mutant amyloid precursor protein. *J. Biol. Chem.* 270, 26727–30.

- Masters, C.L., Bateman, R., Blennow, K., Rowe, C.C., Sperling, R.A., Cummings, J.L., 2015. Alzheimer's disease. *Nat. Rev. Dis. Prim.* 1, 15056.
<https://doi.org/10.1038/nrdp.2015.56>
- Masters, C.L., Selkoe, D.J., 2012. Biochemistry of amyloid β -protein and amyloid deposits in Alzheimer disease. *Cold Spring Harb. Perspect. Med.* 2, 1–24.
<https://doi.org/10.1101/cshperspect.a006262>
- Mauvezin, C., Neufeld, T.P., 2015. Bafilomycin A1 disrupts autophagic flux by inhibiting both V-ATPase-dependent acidification and Ca-P60A/SERCA-dependent autophagosome-lysosome fusion. *Autophagy* 11, 1437–1438.
<https://doi.org/10.1080/15548627.2015.1066957>
- McNaughton, D., Knight, W., Guerreiro, R., Ryan, N., Lowe, J., Poulter, M., Nicholl, D.J., Hardy, J., Revesz, T., Lowe, J., Rossor, M., Collinge, J., Mead, S., 2012. Duplication of amyloid precursor protein (APP), but not prion protein (PRNP) gene is a significant cause of early onset dementia in a large UK series. *Neurobiol. Aging* 33, 426.e13-426.e21. <https://doi.org/10.1016/J.NEUROBIOLAGING.2010.10.010>
- Menzies, F.M., Fleming, A., Rubinsztein, D.C., 2015. Compromised autophagy and neurodegenerative diseases. *Nat. Rev. Neurosci.* 16, 345–357.
<https://doi.org/10.1038/nrn3961>
- Mercy, L., Dawson, K., Brayne, C., 2008. Incidence of early-onset dementias in Cambridgeshire , United Kingdom.
- Michelini, E., Cevenini, L., Mezzanotte, L., Coppa, A., Roda, A., 2010. Cell-based assays: fuelling drug discovery. *Anal. Bioanal. Chem.* 398, 227–238.
<https://doi.org/10.1007/s00216-010-3933-z>
- Mueller-Stainer, S., Zhou, Y., Arai, H., Roberson, E.D., Sun, B., Chen, J., Wang, X., Yu, G., Esposito, L., Mucke, L., Gan, L., 2006. Anti-amyloidogenic and Neuroprotective Functions of Cathepsin B: Implications for Alzheimer's Disease. *Neuron* 51, 703–714. <https://doi.org/10.1016/j.neuron.2006.07.027>
- Mullard, A., 2017. BACE inhibitor bust in Alzheimer trial. *Nat. Rev. Drug Discov.* 16, 155–155. <https://doi.org/10.1038/nrd.2017.43>

- N., V.B., Yalun, Z., H., L.J., Rong, C., Christopher, B., Mahdi, G., Christiane, R., Dolly, R., Yufeng, S., Ekaterina, R., Peter, S.G., Richard, M., 2015. Coding mutations in SORL1 and Alzheimer disease. *Ann. Neurol.* 77, 215–227.
<https://doi.org/doi:10.1002/ana.24305>
- Nie, Q., Du, X., Geng, M., 2011. Small molecule inhibitors of amyloid β peptide aggregation as a potential therapeutic strategy for Alzheimer's disease. *Acta Pharmacol. Sin.* 32, 545–551. <https://doi.org/10.1038/aps.2011.14>
- Nikoletopoulou, V., Papandreou, M.E., Tavernarakis, N., 2015. Autophagy in the physiology and pathology of the central nervous system. *Cell Death Differ.* 22, 398–407. <https://doi.org/10.1038/cdd.2014.204>
- Nixon, R.A., 2013. The role of autophagy in neurodegenerative disease. *Nat. Med.* 19. <https://doi.org/10.1038/nm.3232>
- Nixon, R.A., Mathews, P.M., Cataldo, A.M., 2001. The neuronal endosomal-lysosomal system in Alzheimer's disease. *J. Alzheimer's Dis.* 3, 97–107.
<https://doi.org/10.3233/JAD-2001-3114>
- Noguchi, S., Murakami, K., Yamada, N., 1993. Apolipoprotein E genotype and Alzheimer's disease. *Lancet (London, England)* 342, 737.
- O'Brien, R.J., Wong, P.C., 2011. Amyloid Precursor Protein Processing and Alzheimer's Disease. *Annu. Rev. Neurosci.* 34, 185–204. <https://doi.org/10.1146/annurev-neuro-061010-113613.Amyloid>
- Orr, M.E., Oddo, S., 2013. Autophagic/lysosomal dysfunction in Alzheimer's disease. *Alzheimers. Res. Ther.* 5, 53. <https://doi.org/10.1186/alzrt217>
- Palhano, F.L., Lee, J., Grimster, N.P., Kelly, J.W., 2013. Toward the Molecular Mechanism(s) by Which EGCG Treatment Remodels Mature Amyloid Fibrils. *J. Am. Chem. Soc.* 135, 7503–7510. <https://doi.org/10.1021/ja3115696>
- Parsons, C.G., Rammes, G., 2017. Preclinical to phase II amyloid beta ($A\beta$) peptide modulators under investigation for Alzheimer's disease. *Expert Opin. Investig. Drugs* 26, 579–592. <https://doi.org/10.1080/13543784.2017.1313832>

- Pastor, P., Roe, C.M., Villegas, A., Bedoya, G., Chakraverty, S., García, G., Tirado, V., Norton, J., Ríos, S., Martínez, M., Kosik, K.S., Lopera, F., Goate, A.M., 2003. Apolipoprotein E ϵ 4 modifies Alzheimer's disease onset in an E280A PS1 kindred. *Ann. Neurol.* 54, 163–169. <https://doi.org/10.1002/ana.10636>
- Peric, A., Annaert, W., 2015. Early etiology of Alzheimer's disease: tipping the balance toward autophagy or endosomal dysfunction? *Acta Neuropathol* 129, 363–381. <https://doi.org/10.1007/s00401-014-1379-7>
- Perlenfein, T.J., Murphy, R.M., 2017. A mechanistic model to predict effects of cathepsin B and cystatin C on β -Amyloid aggregation and degradation. *J. Biol. Chem.* 292, 21071–21082. <https://doi.org/10.1074/jbc.M117.811448>
- Poskanzer, D.C., 1969. L-Dopa in Parkinson's Syndrome. *N. Engl. J. Med.* 280, 382–383. <https://doi.org/10.1056/NEJM196902132800708>
- Prince, M., Comas-Herrera, A., Knapp, M., Guerchet, M., Karagiannidou, M., 2016. World Alzheimer Report 2016 Improving healthcare for people living with dementia. Coverage, Quality and costs now and in the future. *Alzheimer's Dis. Int.* 1–140.
- Prins, N.D., Scheltens, P., 2013. Treating Alzheimer's disease with monoclonal antibodies: current status and outlook for the future. *Alzheimers. Res. Ther.* 5, 56. <https://doi.org/10.1186/alzrt220>
- Pungerčar, J.R., Caglič, D., Sajid, M., Dolinar, M., Vasiljeva, O., Požgan, U., Turk, D., Bogyo, M., Turk, V., Turk, B., 2009. Autocatalytic processing of procathepsin B is triggered by proenzyme activity. *FEBS J.* 276, 660–668. <https://doi.org/10.1111/j.1742-4658.2008.06815.x>
- Regitz, C., Dußling, L.M., Wenzel, U., 2014. Amyloid-beta (A β _{1–42})-induced paralysis in *Caenorhabditis elegans* is inhibited by the polyphenol quercetin through activation of protein degradation pathways. *Mol. Nutr. Food Res* 58(10):1931-40. <https://doi.org/10.1002/mnfr.201400014>
- Ripoli, C., Cocco, S., Li Puma, D.D., Piacentini, R., Mastrodonato, A., Scala, F., Puzzo, D., D'Ascenzo, M., Grassi, C., 2014. Intracellular accumulation of amyloid-beta (Abeta) protein plays a major role in Abeta-induced alterations of glutamatergic

- synaptic transmission and plasticity. *J Neurosci* 34, 12893–12903.
<https://doi.org/10.1523/jneurosci.1201-14.2014>
- Rovelet-Lecrux, A., Hannequin, D., Raux, G., Meur, N. Le, Laquerrière, A., Vital, A., Dumanchin, C., Feuillet, S., Brice, A., Vercelletto, M., Dubas, F., Frebourg, T., Campion, D., 2006. APP locus duplication causes autosomal dominant early-onset Alzheimer disease with cerebral amyloid angiopathy. *Nat. Genet.* 38, 24–26.
<https://doi.org/10.1038/ng1718>
- Salloway, S., Sperling, R., Fox, N.C., Blennow, K., Klunk, W., Raskind, M., Sabbagh, M., Honig, L.S., Porsteinsson, A.P., Ferris, S., Reichert, M., Ketter, N., Nejadnik, B., Guenzler, V., Miloslavsky, M., Wang, D., Lu, Y., Lull, J., Tudor, I.C., Liu, E., Grundman, M., Yuen, E., Black, R., Brashear, H.R., Bapineuzumab 301 and 302 Clinical Trial Investigators, 2014. Two Phase 3 Trials of Bapineuzumab in Mild-to-Moderate Alzheimer's Disease. *N. Engl. J. Med.* 370, 322–333.
<https://doi.org/10.1056/NEJMoa1304839>
- Scheltens, P., Blennow, K., Breteler, M.M.B., de Strooper, B., Frisoni, G.B., Salloway, S., Van der Flier, W.M., 2016. Alzheimer's disease. *Lancet* 388, 505–517.
[https://doi.org/10.1016/S0140-6736\(15\)01124-1](https://doi.org/10.1016/S0140-6736(15)01124-1)
- Sevigny, J., Chiao, P., Bussière, T., Weinreb, Paul H., Williams, L., Maier, M., Dunstan, R., Salloway, S., Che, T., Ling, Y., O'Gorman, John, Fang Qian, Mahin Arastu, Mingwei Li, S.C., Melanie S. Brennan, Omar Quintero-Monzon, Robert H. Scannevin, H. Moore Arnold, Thomas Engber, K.R., James Ferrero, Yaming Hang, Alvydas Mikulskis, Jan Grimm, Christoph Hock, Roger M. Nitsch, A.S., 2016. The antibody aducanumab reduces A β plaques in Alzheimer's disease. *Nature* 537, 50–56. <https://doi.org/10.1038/nature19323>
- Shi, X.-D., Sun, K., Hu, R., Liu, X.-Y., Hu, Q.-M., Sun, X.-Y., Yao, B., Sun, N., Hao, J.-R., Wei, P., Han, Y., Gao, C., 2016. Blocking the Interaction between EphB2 and ADDLs by a Small Peptide Rescues Impaired Synaptic Plasticity and Memory Deficits in a Mouse Model of Alzheimer's Disease. *J. Neurosci.* 36, 11959–11973.
<https://doi.org/10.1523/JNEUROSCI.1327-16.2016>
- Simeonov, A., Davis, M.I., 2004. Interference with Fluorescence and Absorbance, Assay Guidance Manual. Eli Lilly & Company and the National Center for

Advancing Translational Sciences.

- Singh, R., Cuervo, A.M., 2011. Autophagy in the Cellular Energetic Balance. *Cell Metab.* 13, 495–504. <https://doi.org/10.1016/j.cmet.2011.04.004>
- Sowade, R.F., Jahn, T.R., 2017. Seed-induced acceleration of amyloid β Mediated neurotoxicity in vivo. *Nat. Commun.* 8, 1–12. <https://doi.org/10.1038/s41467-017-00579-4>
- Stanton, M.G., Hubbs, J., Sloman, D., Hamblett, C., Andrade, P., Angagaw, M., Bi, G., Black, R.M., Crispino, J., Cruz, J.C., Fan, E., Farris, G., Hughes, B.L., Kenific, C.M., Middleton, R.E., Nikov, G., Sajonz, P., Shah, S., Shomer, N., Szewczak, A.A., Tanga, F., Tudge, M.T., Shearman, M., Munoz, B., 2010. Fluorinated piperidine acetic acids as gamma-secretase modulators. *Bioorg. Med. Chem. Lett.* 20, 755–8. <https://doi.org/10.1016/j.bmcl.2009.11.034>
- Stefani, M., Rigacci, S., 2013. Protein Folding and Aggregation into Amyloid: The Interference by Natural Phenolic Compounds. *Int. J. Mol. Sci.* 14, 12411–12457. <https://doi.org/10.3390/ijms140612411>
- Stenvang, M., Christiansen, G., Otzen, D.E., 2016. Epigallocatechin gallate remodels fibrils of Lattice Corneal Dystrophy protein, facilitating proteolytic degradation and preventing formation of membrane-permeabilizing species. *Biochemistry* 55(16):2344-57. <https://doi.org/10.1021/acs.biochem.6b00063>
- Strömberg, K., Eketjäll, S., Georgievska, B., Tunblad, K., Eliason, K., Olsson, F., Radesäter, A.-C., Klintonberg, R., Arvidsson, P.I., von Berg, S., Fälting, J., Cowburn, R.F., Dabrowski, M., 2015. Combining an amyloid- β ($A\beta$) cleaving enzyme inhibitor with a γ -secretase modulator results in an additive reduction of $A\beta$ production. *FEBS J.* 282, 65–73. <https://doi.org/10.1111/febs.13103>
- Sun-Wada, G.-H., Tabata, H., Kawamura, N., Aoyama, M., Wada, Y., 2009. Direct recruitment of H⁺-ATPase from lysosomes for phagosomal acidification. *J. Cell Sci.* 122, 2504–2513. <https://doi.org/10.1242/jcs.050443>
- Sun, A., Nguyen, X. V., Bing, G., 2002. Comparative Analysis of an Improved Thioflavin-S Stain, Gallyas Silver Stain, and Immunohistochemistry for

- Neurofibrillary Tangle Demonstration on the Same Sections. *J. Histochem. Cytochem.* 50, 463–472. <https://doi.org/10.1177/002215540205000403>
- Sun, B., Zhou, Y., Halabisky, B., Lo, I., Cho, S.-H., Mueller-Steiner, S., Devidze, N., Wang, X., Grubb, A., Gan, L., 2008. Cystatin C-Cathepsin B Axis Regulates Amyloid β Levels and Associated Neuronal Deficits in an Animal Model of Alzheimer's Disease. *Neuron* 60, 247–257. <https://doi.org/10.1016/J.NEURON.2008.10.001>
- Suzuki, K., Aimi, T., Ishihara, T., Mizushima, T., 2016. Identification of approved drugs that inhibit the binding of amyloid β oligomers to ephrin type-B receptor 2. *FEBS Open Bio* 6, 461–8. <https://doi.org/10.1002/2211-5463.12056>
- Tai, L.M., Bilousova, T., Jungbauer, L., Roeske, S.K., Youmans, K.L., Yu, C., Poon, W.W., Cornwell, L.B., Miller, C.A., Vinters, H. V., Van Eldik, L.J., Fardo, D.W., Estus, S., Bu, G., Gyls, K.H., LaDu, M.J., 2013. Levels of Soluble Apolipoprotein E/Amyloid- β ($A\beta$) Complex Are Reduced and Oligomeric $A\beta$ Increased with *APOE4* and Alzheimer Disease in a Transgenic Mouse Model and Human Samples. *J. Biol. Chem.* 288, 5914–5926. <https://doi.org/10.1074/jbc.M112.442103>
- Takahashi, R.H., Capetillo-Zarate, E., Lin, M.T., Milner, T.A., Gouras, G.K., 2013. Accumulation of Intraneuronal β -Amyloid 42 Peptides Is Associated with Early Changes in Microtubule-Associated Protein 2 in Neurites and Synapses. <https://doi.org/10.1371/journal.pone.0051965>
- Takahashi, R.H., Milner, T.A., Li, F., Nam, E.E., Edgar, M.A., Yamaguchi, H., Beal, M.F., Xu, H., Greengard, P., Gouras, G.K., 2002. Intraneuronal Alzheimer $A\beta$ 42 accumulates in multivesicular bodies and is associated with synaptic pathology. *Am. J. Pathol.* 161, 1869–1879. [https://doi.org/10.1016/S0002-9440\(10\)64463-X](https://doi.org/10.1016/S0002-9440(10)64463-X)
- Takahashi, R.H., Nagao, T., Gouras, G.K., 2017. Plaque formation and the intraneuronal accumulation of β -amyloid in Alzheimer's disease. *Pathol. Int.* 67, 185–193. <https://doi.org/10.1111/pin.12520>
- Tan, C.-C., Yu, J.-T., Tan, M.-S., Jiang, T., Zhu, X.-C., Tan, L., 2014. Autophagy in aging and neurodegenerative diseases: implications for pathogenesis and therapy. *Neurobiol. Aging* 35, 941–957.

<https://doi.org/10.1016/J.NEUROBIOLAGING.2013.11.019>

- Tian, Y., Bustos, V., Flajolet, M., Greengard, P., 2011. A small-molecule enhancer of autophagy decreases levels of Abeta and APP-CTF via Atg5-dependent autophagy pathway. *FASEB J.* 25, 1934–42. <https://doi.org/10.1096/fj.10-175158>
- Ulland, T.K., Song, W.M., Huang, S.C.C., Ulrich, J.D., Sergushichev, A., Beatty, W.L., Loboda, A.A., Zhou, Y., Cairns, N.J., Kambal, A., Loginicheva, E., Gilfillan, S., Cella, M., Virgin, H.W., Unanue, E.R., Wang, Y., Artyomov, M.N., Holtzman, D.M., Colonna, M., 2017. TREM2 Maintains Microglial Metabolic Fitness in Alzheimer's Disease. *Cell* 170, 649–663.e13. <https://doi.org/10.1016/j.cell.2017.07.023>
- van Dyck, C.H., 2017. Anti-Amyloid- β Monoclonal Antibodies for Alzheimer's Disease: Pitfalls and Promise. *Biol. Psychiatry* 83, 311–319. <https://doi.org/10.1016/j.biopsych.2017.08.010>
- Wang, J., Gu, B.J., Masters, C.L., Wang, Y.J., 2017. A systemic view of Alzheimer disease - Insights from amyloid- β metabolism beyond the brain. *Nat. Rev. Neurol.* 13, 612–623. <https://doi.org/10.1038/nrneurol.2017.111>
- Wang, Q., Yu, X., Li, L., Zheng, J., 2014. Inhibition of amyloid- β aggregation in Alzheimer's disease. *Curr. Pharm. Des.* 20, 1223–43.
- Wen, J., Fang, F., Guo, S.-H., Zhang, Y., Peng, X.-L., Sun, W.-M., Wei, X.-R., He, J.-S., Hung, T., 2018. Amyloid β -Derived Diffusible Ligands (ADDLs) Induce Abnormal Autophagy Associated with A β Aggregation Degree. *J. Mol. Neurosci.* 64, 162–174. <https://doi.org/10.1007/s12031-017-1015-9>
- West, M., Coleman, P., Flood, D., Troncoso, J., 1994. Differences in the pattern of hippocampal neuronal loss in normal ageing and Alzheimer's disease. *Lancet* 344, 769–772. [https://doi.org/10.1016/S0140-6736\(94\)92338-8](https://doi.org/10.1016/S0140-6736(94)92338-8)
- Winblad, B., Amouyel, P., Andrieu, S., Ballard, C., Brayne, C., Brodaty, H., Cedazo-Minguez, A., Dubois, B., Edvardsson, D., Feldman, H., Fratiglioni, L., Frisoni, G.B., Gauthier, S., Georges, J., Graff, C., Iqbal, K., Jessen, F., Johansson, G., Jönsson, L., Kivipelto, M., Knapp, M., Mangialasche, F., Melis, R., Nordberg, A., Rikkert, M.O., Qiu, C., Sakmar, T.P., Scheltens, P., Schneider, L.S., Sperling, R., Tjernberg,

- L.O., Waldemar, G., Wimo, A., Zetterberg, H., 2016. Defeating Alzheimer's disease and other dementias: a priority for European science and society. *Lancet Neurol.* 15, 455–532. [https://doi.org/10.1016/S1474-4422\(16\)00062-4](https://doi.org/10.1016/S1474-4422(16)00062-4)
- Wolfe, M.S., 2012. γ -Secretase inhibitors and modulators for Alzheimer's disease. *J. Neurochem.* 120, 89–98. <https://doi.org/10.1111/j.1471-4159.2011.07501.x>
- Wolfe, M.S., 2008. Selective amyloid- β lowering agents. *BMC Neurosci.* 9, S4. <https://doi.org/10.1186/1471-2202-9-S2-S4>
- Yang, H., Hu, H.-Y., 2016. Sequestration of cellular interacting partners by protein aggregates: implication in a loss-of-function pathology. *FEBS J.* 283, 3705–3717. <https://doi.org/10.1111/febs.13722>
- Yeh, F.L., Wang, Y., Tom, I., Gonzalez, L.C., Sheng, M., 2016. TREM2 Binds to Apolipoproteins, Including APOE and CLU/APOJ, and Thereby Facilitates Uptake of Amyloid- β by Microglia. *Neuron* 91, 328–340. <https://doi.org/10.1016/J.NEURON.2016.06.015>
- Youmans, K.L., Tai, L.M., Nwabuisi-Heath, E., Jungbauer, L., Kanekiyo, T., Gan, M., Kim, J., Eimer, W.A., Estus, S., Rebeck, G.W., Weeber, E.J., Bu, G., Yu, C., LaDu, M.J., 2012. APOE4-specific Changes in A β Accumulation in a New Transgenic Mouse Model of Alzheimer Disease. *J. Biol. Chem.* 287, 41774–41786. <https://doi.org/10.1074/jbc.M112.407957>
- Zeineddine, R., Yerbury, J.J., 2015. The role of macropinocytosis in the propagation of protein aggregation associated with neurodegenerative diseases. *Front. Physiol.* 6, 277. <https://doi.org/10.3389/fphys.2015.00277>
- Zhang, J.-H., Chung, T.D.Y., Oldenburg, K.R., 1999. A Simple Statistical Parameter for Use in Evaluation and Validation of High Throughput Screening Assays. *J. Biomol. Screen.* 4, 67–73. <https://doi.org/10.1177/108705719900400206>
- Zhang, Y., Thompson, R., Zhang, H., Xu, H., 2011. APP processing in Alzheimer's disease. *Mol. Brain* 4, 3. <https://doi.org/10.1186/1756-6606-4-3>
- Zhong, L., Hu, J., Shu, W., Gao, B., Xiong, S., 2015. Epigallocatechin-3-gallate opposes HBV-induced incomplete autophagy by enhancing lysosomal acidification, which is

- unfavorable for HBV replication. *Cell Death Dis.* 6, e1770.
<https://doi.org/10.1038/cddis.2015.136>
- Zhong, N., Weisgraber, K.H., 2009. Understanding the Association of Apolipoprotein E4 with Alzheimer Disease: Clues from Its Structure. *J. Biol. Chem.* 284, 6027–6031.
<https://doi.org/10.1074/jbc.R800009200>
- Zhou, J., Farah, B.L., Sinha, R.A., Wu, Y., Singh, B.K., Bay, B.H., Yang, C.S., Yen, P.M., 2014. Epigallocatechin-3-Gallate (EGCG), a green tea polyphenol, stimulates hepatic autophagy and lipid clearance. *PLoS One* 9(1):e87161.
<https://doi.org/10.1371/journal.pone.0087161>
- Zhou, J., Tan, S.-H., Nicolas, V., Bauvy, C., Yang, N.-D., Zhang, J., Xue, Y., Codogno, P., Shen, H.-M., 2013. Activation of lysosomal function in the course of autophagy via mTORC1 suppression and autophagosome-lysosome fusion. *Cell Res.* 23, 508–523. <https://doi.org/10.1038/cr.2013.11>
- Ziegler-Waldkirch, S., d’Errico, P., Sauer, J.-F., Erny, D., Savanthrapadian, S., Loreth, D., Katzmarski, N., Blank, T., Bartos, M., Prinz, M., Meyer-Luehmann, M., 2018. Seed-induced A β deposition is modulated by microglia under environmental enrichment in a mouse model of Alzheimer’s disease. *EMBO J.* 37, 167–182.
<https://doi.org/10.15252/emj.201797021>

7 Addendum

Eidesstattliche Versicherung

„Ich, Christopher Secker, versichere an Eides statt durch meine eigenhändige Unterschrift, dass ich die vorgelegte Dissertation mit dem Thema: „EGCG directly targets intracellular amyloid- β (1-42) aggregates and promotes their lysosomal degradation“ selbstständig und ohne nicht offengelegte Hilfe Dritter verfasst und keine anderen als die angegebenen Quellen und Hilfsmittel genutzt habe.

Alle Stellen, die wörtlich oder dem Sinne nach auf Publikationen oder Vorträgen anderer Autoren beruhen, sind als solche in korrekter Zitierung (siehe „Uniform Requirements for Manuscripts (URM)“ des ICMJE -www.icmje.org) kenntlich gemacht. Die Abschnitte zu Methodik (insbesondere praktische Arbeiten, Laborbestimmungen, statistische Aufarbeitung) und Resultaten (insbesondere Abbildungen, Graphiken und Tabellen) entsprechen den URM (s.o) und werden von mir verantwortet.

Meine Anteile an etwaigen Publikationen zu dieser Dissertation entsprechen denen, die in der untenstehenden gemeinsamen Erklärung mit dem/der Betreuer/in, angegeben sind. Sämtliche Publikationen, die aus dieser Dissertation hervorgegangen sind und bei denen ich Autor bin, entsprechen den URM (s.o) und werden von mir verantwortet.

Die Bedeutung dieser eidesstattlichen Versicherung und die strafrechtlichen Folgen einer unwahren eidesstattlichen Versicherung (§156,161 des Strafgesetzbuches) sind mir bekannt und bewusst.“

Berlin, den 18 Juni 2018.

Contributions

Experiments were performed, and data was analyzed by the doctoral candidate, Christopher Secker (CS), under supervision of Dr. Alexander Buntru (AB), Dr. Thomas Wiglenda (TW) and Prof. Dr. E. E. Wanker (EEW). Master student Simona Kostova (SK) and technician Lydia Brusendorf (LB) supported the establishment of the assays and conducted individual experiments. Primary neurons were prepared by Dr. Aline Schulz (AS) from AG Meyer at the MDC and electron microscopy imaging was performed with the help of Dr. Bettina Purfürst at the EM core facility of the MDC. Prof. Dr. Constantin Czekelius and Angelika Motzny from the Heinrich-Heine University Düsseldorf synthesized custom EGCG derivatives. All presented data was analyzed and interpreted by CS.

Contributions to this work in detail are as follows:

- EW, AB, TW and CS conceived the A β 42-TAMRA degradation assay. LB, SK and CS technically characterized and established the compound screening assay.
- LB, SK and CS performed uptake experiments. SK performed staining and imaging for aggregate localization and actin uptake inhibition. CS and LB performed macropinocytosis experiments.
- AB and CS conceived polyphenol library screen. LB conducted screen and performed titration experiments.
- CS and LB performed compound validation, seeding and toxicity experiments. LB conducted SH-EP cell and CS primary neuron toxicity assays.
- SK performed staining and imaging for lysosomal markers, CS performed co-localization analysis.
- CS performed lysosome inhibition, CatB induction and activity, EGCG derivative library screening, AFM, EM and QIAD remodeling, compound co-localization and *in vitro* cleavage experiments.

Curriculum Vitae

Mein Lebenslauf wird aus datenschutzrechtlichen Gründen in der elektronischen Version meiner Arbeit nicht veröffentlicht.

Mein Lebenslauf wird aus datenschutzrechtlichen Gründen in der elektronischen Version meiner Arbeit nicht veröffentlicht.

Mein Lebenslauf wird aus datenschutzrechtlichen Gründen in der elektronischen Version meiner Arbeit nicht veröffentlicht.

Mein Lebenslauf wird aus datenschutzrechtlichen Gründen in der elektronischen Version meiner Arbeit nicht veröffentlicht.

List of Publications

- 2 Trepte P, Kruse S, Kostova S, Hoffmann S, Buntru A, Tempelmeier A, **Secker C**, Diez L, Schulz A, Klockmeier K, Zenkner M, Golusik S, Rau K, Schnoegl S, Garner CC, Wanker EE et al., „ A luminescence-based two-hybrid technology for quantitative mapping of protein-protein interactions.” *Mol Syst Biol.* 2018 *14(7):e8071.*
- 1 Trepte P, Buntru A, Klockmeier K, Willmore L, Arumughan A, **Secker C**, Zenkner M, Brusendorf L, Rau K, Redel A, Wanker EE. “DULIP: A Dual Luminescence-Based Co-Immunoprecipitation Assay for Interactome Mapping in Mammalian Cells.” *J Mol Biol.* 2015 *427(21):3375-88.*

Acknowledgments

I want to thank S, my family, friends and amazing colleagues for always supporting me throughout science and life. Especially I want to thank Philipp, Philipp, Alex, Lydia, Thomas, Nancy, Lisa, Konrad, Simona, Anne, Hannah, Christian, Alessandro, Anup, Martina, Sigrid and Erich for great guidance, openness and support. Thank you!